Simulating floods

On the application of a 2D-hydraulic model for flood hazard and risk assessment

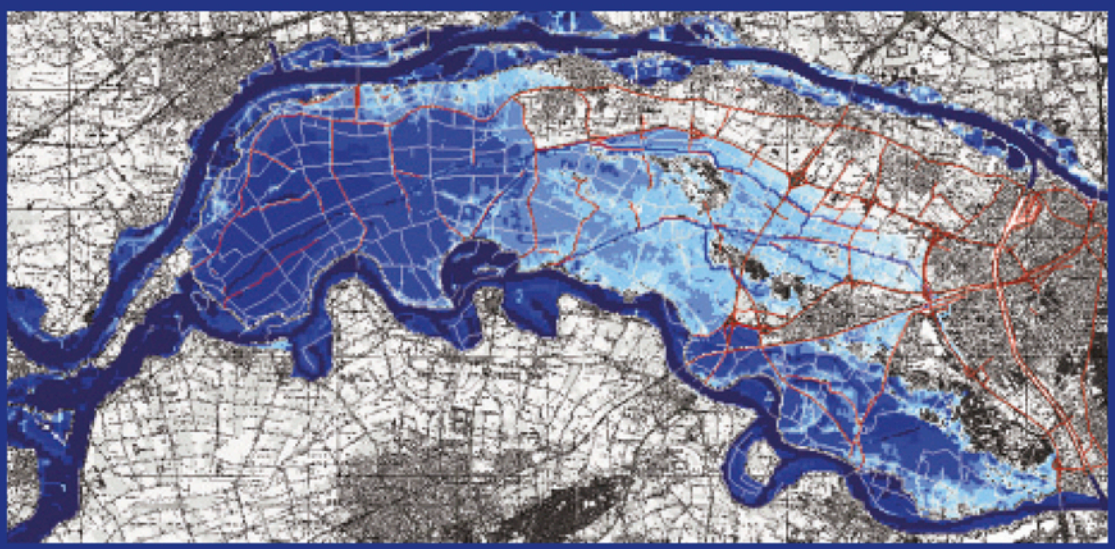

Dinand Alkema

Simulating floods

On the application of a 2D-hydraulic model for flood hazard and risk assessment

Dinand Alkema

International Institute for Geo-information Science and Earth Observation, Enschede, The Netherlands

ITC dissertation number 147
ITC, P.O. Box 6, 7500 AA Enschede, the Netherlands

ISBN 978 90 6164 263 3

Cover designed by Dinand Alkema
Printed by ITC Printing Department

Copyright © 2007 by Dinand Alkema

Simulating floods

On the application of a 2D-hydraulic model for flood hazard and risk assessment

Simulatie van overstromingen

Over het toepassen van een 2D-hydraulisch model voor het bepalen van overstromingsgevaar.

(met een samenvatting in het Nederlands)

Proefschrift
ter verkrijging van de graad van doctor aan de
Universiteit Utrecht
op gezag van de rector magnificus, prof. dr. W.H. Gispen,
ingevolge het besluit van het college van promoties in het openbaar te
verdedigen op vrijdag 7 september 2007 des ochtends te 10.30 uur

door

Dinand Alkema

geboren op 20 juni 1969 te Groningen

Promotoren:
Prof. dr. J.D. Nieuwenhuis
Prof. dr. S.M. de Jong

Co-promotor:
Dr. Th. van Asch

This doctoral dissertation was produced with the financial support of:

- The European Union (contract: ERBFMRX-CT97-0162) through the GETS project (Geomorphology and Environmental Impact Assessment to Transportation Systems).

- The Belvedere Bureau of the Dutch ministry of Housing, Spatial Planning and the Environment.

- SLARIM – Strengthening Local Authorities in Risk Management; Internal ITC research project.

Acknowledgements

After 7 years of research and working on three different case studies, in four institutes and in two different countries, it is obvious that this work would not have been possible without the help, input, suggestions, encouragements and collaboration of a great number of people. In fact it is almost impossible to list all of them, and therefore the following list is horribly incomplete. However it would be worse not to make an attempt to acknowledge those who have played a key part in the materialisation of this work. So at the risk that I forget someone – my apologies – I would like to express my sincere gratitude to the following persons:

To my promotors Prof. Dr. Jan Nieuwenhuis and Prof. Dr. Steven de Jong and to my co-promotor Dr. Theo van Asch, for supporting me in carrying out this work. I thank them for their encouragement and suggestions throughout these years and their trust in my abilities.

To Prof. Dr. Andrea Fabbri who, as coordinator of GETS project, offered me the possibility to return to the beautiful world of geomorphology and to Prof. Dr. Angelo Cavallin who was responsible for the case study Trento that formed the foundation of this work. Both showed faith in my approach to tackle the problems that needed to be solved, and allowed me to find my own way of doing research and to learn from my mistakes.

To Prof. Dr. Guus Stelling who gave me the opportunity to work with his dynamic 2D flood propagation model Delft-FLS. This turned out to be pivotal to my research, because this modelling approach became the central theme of this thesis. Without FLS this thesis would have been completely different – if it would have materialised at all. WL|Delft Hydraulics is gratefully acknowledged for their support with the software.

To Dr. Ad de Roo, who made it possible for me to test my ideas and the Delft-FLS on a real flood event and who invited me over to the Joint Research Center of the European Commission in Ispra, Northern Italy to work with him.

To Dr. Annika Hesselink and Dr. Hans Middelkoop who made it possible for me to continue working on flood modelling in the Netherlands with a study in "*het Land van Maas en Waal*".

To Prof. Dr. Freek van der Meer and Dr. Cees van Westen who, after I became employed at the ITC, stimulated me to continue with this thesis. Apart from my obligations to ITC, they allowed me to dedicate my research time to this work and it would not have been possible to finish it without their support and encouragement.

To my colleagues in the GETS project for the good cooperation and the great times we had together. I especially would like to thank Davide Geneletti – my "Trento-partner" – for the friendship, the good teamwork and the many discussions we had in Matarello and "Toronto". Another word of thanks goes to Karin Pfeffer for her assistance with the spatial multi-criteria evaluation and to Alfred Wagtendonk for the construction of the interactive internet site.

To my colleagues at the university of Milano-Bicocca, Mattia de Amicis, Andrea Zanchi, Simone Sterlacchini, Tulia Bonomi and all the others that made my stay in Milan a beautiful memory. A special word of thanks goes to Lucia Luzi for the perfect apartment that I was allowed to use during those three years.

To the staff at the various offices of the Autonomous Province of Trento and the Authority of the Adige Basin. Especially Gianluca Tommasi and Francesca de Francesch at the Geologic Survey and Alessandro Moltrer at the Office for Environmental Impact Assessment are thanked for their support in the Trento case study.

To my colleagues at the Joint Research Centre in Ispra, with whom it was great to cooperate. It was truly a wonderful experience to work in this international research institute. I also would like to thank the Landesumweltamt Brandenburg – especially Meike Gierk - for providing the data and for their constructive support.

To those who helped me during the "Belvedere" study, most notably to Ton Markus who helped me with the interactive CD-ROM. Nathalie Asselman

from WL|Delft Hydraulics and Dré van Marrewijk and Oswald Lagendijk from Belvedere are thanked for their useful suggestions and feedback. Gratefully acknowledged are the Province of Gelderland, the Water board "*Rivierenland*" and *Rijkswaterstaat* who, through their contacts Bas Overmars, Eef Janssen and Stephanie Holterman, provided data and support. Maarten Kleinhans is thanked for his help with the sedimentation estimation.

To my colleagues at the ITC who allowed me to continue with this work and offered many helpful suggestions. Nanette Kingma is thanked for the collaboration in flood hazard and risk research. Loes Colenbrander, Ronnie Geerding, en Job Duim are acknowledged for their support in the final stages of completing this thesis.

Seven years is a long time. In my personal live there have been many changes. I have lost several persons that were very dear to me: my cousin, my grandmother and a new-born niece. I also lost my mother-in-law, before we had the chance to get to know each other well. In 2002 my own mother passed away. And just before finishing this book, my father-in-law died unexpectedly. It is needless to say that I miss them all very much. But in that same period, also beautiful events happened. I married the woman that I love and we got a wonderful son Jorden. I want to thank those that are close to me and have been with me through these ups and downs, to my family, my family-in-law and to my friends who have stayed with me through all these years.

I dedicate this work to those that have passed away and to Evelijne who has been at my side during these seven long years.

Zwolle
July 2007

Table of Contents

List of Figures

List of Tables

Chapter 1 Introduction

1.1 Problem definition

River floods are a major problem all over the world and there is a growing concern about their relationship with climate change, engineering works and floodplain land use. At the same time development of floodplains continues at an accelerating pace. They are attractive areas to settle in, because of the availability of water (for house-hold use, irrigation, fishing and transport), fertile soils, and because it is easier to construct buildings and transportation lines on relatively flat terrain. Nowadays there is an unprecedented accumulation of valuable property on land that once was the domain of the river.
To avoid that these developed areas are regularly flooded, most rivers are constrained in their activities through a multitude of protective measures like the construction of dikes that confine the water to its allocated space, the riverbed. These protection works have made people feel safer and thus encouraged even more to live and work in potentially dangerous areas. Nowadays people have so much faith in the protection works that alluvial plains are among the most densely populated areas in the world with a large accumulation of valuable property. Abbott (1996) stated:

"Still, those who decide to build on a flood plain are gamblers. They may win their gamble for many years, but the stream still rules the floodplain, and every so often it comes back to collect all bets".

This has been demonstrated by the numerous riverine floods in the world that resulted in loss of life and in enormous material damage. To mention a few: the 1993 Mississippi flood (USA), the 1993 and 1995 Rhine and Meuse floods (the Netherlands and Germany), the 1994 Po River flood (Italy), the 1997 Oder flood (Central Europe), the 1998 Yangtze flood (China), the 2001 Orissa flood (India) and the 2002 Elbe flood (Germany). These floods not only resulted in loss of lives, directly and indirectly, but have disrupted entire societies and have caused billions of Euros in damages. For instance the estimated total losses of the 1993 and 1995 Rhine floods reached 4 billion Euros, the 1994 Po flood 9 billion Euros and the

1997 Oder flood 5 billion Euros (Conway, 2000). Figure 1.1 shows an estimate of the yearly inflation adjusted flood losses in the US (NOAA/NWS, 2000) in million dollars (adjusted to 1997 dollar value). These are direct damages due to flooding that results from rainfall and/or snowmelt. It does not include flooding due to winds, such as coastal flooding (e.g. hurricane storm surges). Despite the complexity of the problems and the limited resources available for extensive evaluation of the quality of the data, some conclusions are clear: there are large fluctuations in yearly flood-losses, ranging from nearly zero to almost 20 billion dollars (1993 Mississippi flood) and there is a steadily increasing trend of average annual flood losses to approximately 5 billion dollars per year in 2000 in the US alone.

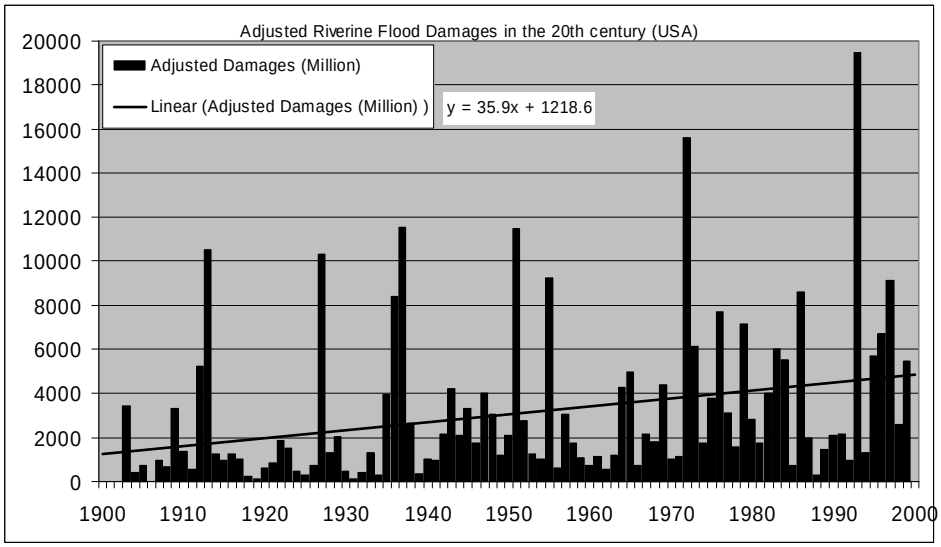

Figure 1.1. US Flood Losses 1900 – 2000 (1997 dollar values) - Compilation of Flood Loss Statistics.

1.2 Research question

In recent years two important developments have occurred that have facilitated the application of numerical flood modelling: the availability of faster and cheaper computers have made it possible to apply advanced flood modelling tools using numerical solutions of the flow equations for water. Simultaneous to this

development, modern survey techniques have become available that allow the rapid and relatively cheap collection of high quality input data for these models, such as the accurate representation of surface topography (Digital Elevation Models) with LIDAR techniques and detailed land-cover maps derived from high-resolution satellite images. These developments have made it possible to simulate flood behaviour and to study the characteristics of future (hypothetical) floods. This is a major leap forward, because it offers opportunities to prepare for the next flood event, but it also triggers the following question:

How to apply flood propagation models for hazard and risk assessment?

This general question can be subdivided into two parts: one part deals with the flood propagation model itself - what are its data requirements, what are the results (output) it generates and how do these compare with a real flood event? The second part of the question deals with the transformation of these model results into flood hazard and flood-risk maps – how to define multi-parameter flood hazard and flood-risk and how can scenario studies be used in a decision-making process?

1.3 Research objectives

The objectives of this study are 1) to demonstrate that the application of an advanced 2D hydraulic flood model for flood simulation can contribute to a better understanding and quantification of floods in areas with complex topography and 2) to show that scenario studies can help decision makers and planners in making more balanced decisions regarding developments in flood-prone areas.

To achieve these objectives and to answer the research questions this thesis is divided into four parts (see Figure 1.2): part 1 contains, apart from this introduction, a conceptual overview of the interaction between geomorphologic processes and the socio-economic environment in Chapter 2, and it describes the general requirements of flood modelling in Chapter 3. Part 2 is dedicated to testing the model by reconstructing an inundation event in Chapter 4, and by evaluating scenario floods in Chapter 5. Part 3 shows two case studies in Chapters 6 and 7,

where the model is used to assess the effects of surface topography and changes in surface topography on the flood characteristics. Part 4 discusses GIS-based multi-criteria evaluation as a procedure for multi-parameter flood-risk assessment in Chapter 8. Chapter 9 gives the overall conclusions.

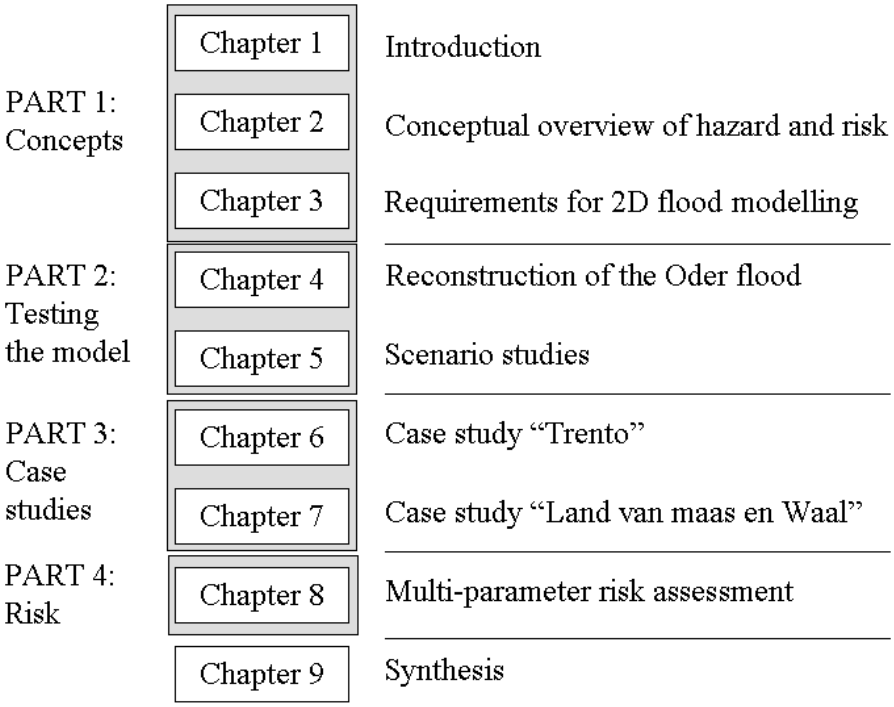

Figure 1.2. Structure of this thesis.

1.4 Approaches in p*redictive flood modelling*

The application of predictive models in flood inundation assessment is already widespread and has been so for many years and is a well-accepted decision support tool. The approach can be very simple, like intersecting a plane that represents the water surface with a digital elevation model, to very sophisticated like the three dimensional solutions of the Navier-Stokes equations (Hesselink et al. 2003).

However, two main approaches in fluvial hydraulic modelling happen to be the most popular: 1D modelling and 2D modelling.

1D modelling

This approach is based on the one-dimensional solution of the Saint-Venant equations (see e.g. Fread, 1992), like the models MIKE11 and HEC-RAS (Brunner, 2002). These models require characterization of the terrain through a series of cross-sections perpendicular to the direction of flow for which the average water depth and flow velocity are calculated. For the area between the cross-sections and the spatial extent of the flooded surface these values are interpolated. This type of modelling is often applied to catchment analysis and the underlying assumption is that the river flow is in the direction of a predefined flow path (the river or canal). This assumption is true in areas with well-defined valleys where the direction of the flow is clearly one-directional: downstream. Any flow perpendicular to the main flow-direction is neglected and lateral spread happens instantaneously as the water level in the river rises. For narrow valley floors this simplification does not lead to major problems, but in wide valleys with a relatively flat alluvial plain, or on alluvial fans and in the large delta areas in the world, these assumptions are not valid anymore.

2D modelling

In near-flat terrain with complex topography it cannot be assumed that all flow will be parallel to the main river. Also in urban environments and in areas with a dominant presence of man-made structures, models are required that calculate flow in both spatial dimensions, in X- and Y-direction, Such models, like Delft-FLS (Stelling, et al. 1998 and Hesselink et al. 2003), Telemac 2D (Hervouet and Van Haren, 1996) and MIKE21 (Abbott and Price, 1994) are based on the two-dimensional solution of the De Saint Venant equations. They require a continuous representation of the terrain topography in the form of a digital surface model. These models can also be applied in the case of a diverging flow at a dike breach.

This study focuses on the application of 2 dimensional hydraulic models for four reasons:

- It is a relatively new tool. The application of 2D flood propagation models have been made possible by the rise of cheaper and faster computers and the availability of accurate terrain models (e.g. Laser

Altimetric Techniques), and land-cover data (e.g. high resolution satellite imagery).

- Most flood disasters with severe economic and social consequences occur in the near-flat alluvial plains and delta areas. These areas are often highly urbanised and are characterised by complex topography.
- 2D flood propagation modelling gives additional information on the flow characteristics of the flood, like flow velocity and propagation characteristics. It is hypothesised that this will be beneficial for a more comprehensive flood hazard and flood-risk assessment.
- To study the applicability of such models for scenario studies as support tool for decision-making.

1.5 Context

The work presented in this thesis is the result of three research projects: the "Trento" case study, the "Oder" case study and the "*Land van Maas en Waal*" case study. The "Trento" case study started in 1998 in the GETS project that was funded by the European Union (contract ERBFMRX-CT97-0162). GETS is the acronym for Geomorphology and Environmental Impact Assessment to Transportation Systems, and it ran from 1998 to 2001.
The "Oder" case study was carried out in 2001 at the Joint Research Centre of the European Commission in Ispra, Italy.
The "*Land van Maas en Waal*" case study was carried out in 2002 and 2003 in collaboration with Utrecht University in a research project funded by the "*Projectbureau Belvedere*" of the Dutch ministry of Housing, Spatial Planning and the Environment.

Chapter 2 A conceptual overview of geo-hazard risk assessment

This chapter is a modified version of a paper by Alkema, D. and Cavallin, A. (2003): *Geomorphologic risk assessment for EIA. Acta Geologica, Studi Trentini di Scienze Naturali. Museo Tridentino di Scienze Natural – Trento. Vol. 78. pp 139-146*

This chapter gives a conceptual overview of how geo-hazards (floods and landslides) can interact with the socio-economic environment. It introduces the terms hazards, vulnerability and risk and gives the basic requirements for hazard and risk assessment and how these can be used for decision-making, e.g. for Environmental Impact Assessment.

Abstract

When geomorphologic processes become hazardous, they can have negative consequences like causing damage, disturbing socio-economic activities and even cause deaths and injuries. To assess these consequences the following information is needed: 1) the characteristics of the hazards, 2) the vulnerability of the exposed elements to these hazards and 3) the importance we give to the elements exposed to the hazards. In our increasingly complex society, it is not sufficient anymore to analyse a singular problem and find a problem-related solution. An integrated approach is required that considers risk as the interference of natural geomorphologic systems with the socio-economic systems. The introduction of a new element into the systems – like the construction of new infrastructures – may have unforeseen and unwanted consequences. An environmental impact study is the proper instrument to analyse how direct and induced hazards may affect the risk in the area surrounding the new project.

2.1 Introduction

Man's interaction with the natural environment is complex. On one hand, we try to isolate ourselves from the dynamics of the natural environment and create safe-havens where we can live and work without too much disturbance. On the other hand, we need the natural environment for its resources, for food, for recreation, etc. We appreciate the aesthetical beauty of the landscape but we loath the extremes in the natural processes that may harm our life, health or living conditions. The problem is that the socio-economic and the natural environment compete for space and interfere. In those areas where the dynamics of both environments are high and space is scarce, this interference may have disastrous consequences. New projects, like the construction of new infrastructures, expanding residential areas or industrial zones, may have unforeseen negative consequences. The development of Environmental Impact Assessment (EIA) procedures for new large projects, now mandatory in many countries, reflects the awareness of this problem (see e.g. Wathern, 1988 and Wood, 1995). An environmental impact can be described as the change in an environmental parameter, over a specific period and within a defined area, resulting from the development compared with the situation which would have occurred had the development not been initiated (Wathern, 1988). The change can be direct through a cause-effect relation, or indirect through a complex system of relationships. EIA permits to identify, to predict and to assess the environmental impacts of a development. It has become an accepted management tool for considering a set of alternatives and activities in the decision-making process in many countries. The main reason for this is that an EIA provides decision-makers with a systematic analysis of the environmental consequences of a development, so that they can include environmental considerations in the decision process to select alternatives (Beinat et al. 1999). Traditional EIAs tend to focus on ecology and pollution but have as shortcoming that they tend to focus on the static elements of the environment and on a limited area surrounding a new project. They often disregard broader range or indirect effects. In most EIA studies, geomorphology has been analysed to evaluate the consequences for geomorphologic assets rather than the interaction between geomorphologic processes and the new project.

Cavallin et al. (1994) stated that in studying environmental consequences in an EIA, the analysis of the physical and geomorphologic conditions is very important, because many of the characteristics are defined by the geomorphologic setting. This observation is not new, as can be seen by the numerous publications on the incorporation of geomorphology in EIA (e.g. Van Asch and Van Dijck, 1994; Rivas et al. 1994). Few examples exist where geomorphology plays a central role and most of these tend to focus geomorphologic forms. Studies on processes, like landslides, floods and erosion are more complex and difficult (Cavallin and Marchetti, 1995).

2.2 Geo-hazard and risk

Geomorphology is the science of landforms (the Earth's surface) and of the processes that have formed or reshaped them (Selby, 1989). There are two complementary approaches to the cause-effect relationship between landforms and processes like weathering, erosion, deposition etc. The first approach studies existing landforms from which the evolutionary processes are inferred. The second approach studies the current operating geomorphologic processes to assess their influence on the landforms upon which they are acting. If these processes operate at a rate above a certain threshold, they may become hazardous for the surrounding area, for instance they may result in instability and erosion on slopes, floodings in river- or coastal areas or earthquakes and volcanism in the Earth's crust. A geomorphologic hazard can be described as the probability that a certain potentially harmful geomorphologic process will occur in a certain territory with a certain intensity in a given period of time. Geomorphologic hazards are natural events that can cause loss of life or damage to property.

The US-EPA (1998) states that risk is dually composed of hazard and exposure. Geomorphologic risk (R) is the expected number of lives lost, injured persons, damage to properties, or disruption of economic activities due to a geomorphologic hazard. It depends on the magnitude of the hazard (H), on the vulnerability (Vu) of the exposed element to that particular hazard and the value (Va) of the element (Varnes, 1984):

$$R = H \times Vu \times Va$$

Vulnerability is the inability of an element or system to maintain its structure and pattern of behaviour in the presence of a geomorphologic hazard. It is often expressed as a function of the hazard with a value range between 0 and 1, where 0 means no damage and 1 means total loss (see also Figure 2.4). Value in this context, represents the degree to which we care about something; this can sometimes be expressed as economic (monetary) value but can it can also stand for e.g. intrinsic-, social-, scientific-, sentimental-, or ecological- value.
This definition shows that geomorphologic hazards themselves are not so much the problem – they simply happen – but it is their interaction with things we care about that creates a disaster. Risk can increase due to an increase of the geomorphologic hazard (change in the geomorphologic systems) or due to an increase of the vulnerability or value of the exposed elements (change in the socio-economic environment) – see Figure 2.1.

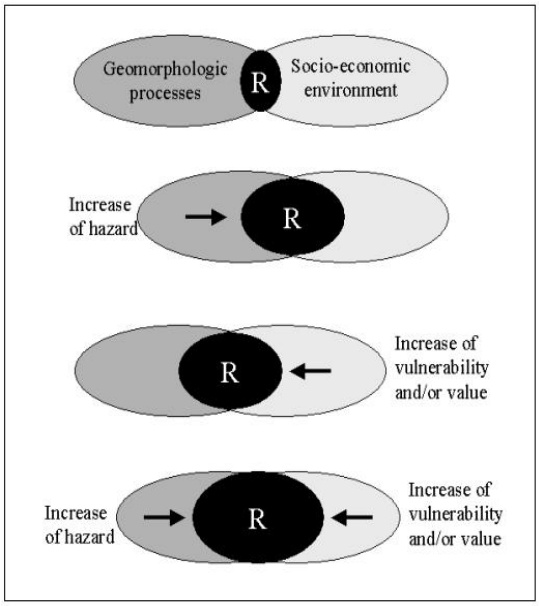

Figure 2.1. Risk (R) exists where geomorphologic processes overlap with the socio-economic environment. Risk can increase due to an (spatial and/or temporal) increase of geomorphologic hazards, an increase of the vulnerability and/or value or both.

When there are no vulnerable or valuable elements exposed to the geomorphologic hazard, the risk is negligible. This implies that the study of geomorphologic risk has to be set in a wider context. Information on the vulnerability and the value of

the elements has to come from experts outside the field of geomorphology, most notably from those working in the socio-economic environment. White et al. (1992) noted:

> *"Traditionally natural sciences are concerned with the natural environment; social sciences and applied sciences with the socio-economic environment. In reality these two components of our environment are inseparable; the natural environment cannot be fully understood in isolation from us and our interactions with it."*

One of the challenges of today is to bridge the gap between geomorphology and socio-economic sciences. This calls for a multi-disciplinary and integrated assessment where the owners of the problem get together to structure the problem in order to reach a better understanding of the interference of geomorphologic processes and things we care about. Values are fundamental to all that we do; and thus, values should be the driving force for our decision-making (Keeney, 1996). These values need to be identified and defined by all stakeholders involved in the design, realisation and supervision of the new project but also by those that could be affected by it or by its consequences. Values can be related to "*human*" issues (life, health, well-being,...), "*economic*" issues (destruction, damage, loss of profit) and "*environmental*" issues (destruction, loss or degradation of habitats, aesthetic value). In general, we want to avoid that geomorphologic hazards affect our *values* in a negative way.

2.3 Response to hazards

The response to geomorphologic hazards has evolved through time. The first and most practical response is the *avoidance* of geomorphologic hazards. Areas with dynamic geomorphologic processes are less suitable for settlement. But hazards cannot always be avoided because other – often-conflicting – considerations are part of the decision that resulted in the choice for a particular location.
The second stage of response can be characterised as *solution-oriented*. The hazard is recognised as a problem that needs to be solved. Dikes are constructed, hill slopes are drained, rock-faces are braced, etc. For centuries, engineers identified the problem and constructed protection works. For each specific problem a specific solution.

The third stage started in the 1980's when it became apparent that problems could not always be solved without considering external factors. The *integrated assessmen*t (IA) considers the various aspects of the problem, not only on the hazard side but also on the socio-economic side (see e.g. Harris, 2002). In general IA can be characterised as the structured process of dealing with complex issues, using knowledge from various disciplines and/or stakeholders, such that integrated insights are made available to decision-makers (Rotmans, 1998). Hazards are considered as part of geomorphologic systems that interfere with the socio-economic systems. It is not a coincidence that in the same period the first Environmental Impact Assessment regulations were issued.
Some researchers (e.g. Van Leussen, 2002) identify a fourth development that they call *collaborative assessment*. Hazards are no longer identified as singular problems, but as part of a wider range of problems, all related to environmental issues. No single party is able to formulate the problem, let alone find solutions. Problem identification and solving has become a collaborative process. The challenge according to them is to mobilise all parties that are affected by geomorphologic hazards and to move them towards collective actions and solutions.

2.4 Linking geomorphologic processes and the socio-economic environment

Geomorphologic processes, such as fluvial river processes, erosion and mass movements (slope processes) etc. are the dynamic actors that help to shape the landscape. Their rate of activity can vary greatly and when certain thresholds are surpassed these processes manifest themselves as geomorphologic hazards. Geomorphologists can identify which elements control these hazards (hazard assessment) and collaboration with socio-economic scientists can reveal how these hazards eventually affect our values (risk assessment). This multi-disciplinary discussion will show the complexity of the geomorphologic and socio-economic systems. It can also result in a preliminary, qualitative assessment of how a change may cascade though both systems and aggravate the risk. When a new project is planned in an area with active geomorphologic processes it is clear that these can affect the new project and disrupt its functioning, cause damage or even its destruction. These hazards are called *direct hazards*. How much the project is affected by a *direct hazard* depends on the magnitude of the hazard and on the

robustness of project's design (or its vulnerability to that particular hazard). On the other hand, the presence of the project may also trigger or activate dormant or non-active geomorphologic processes, which – in turn - may become geomorphologic hazards. These hazards are called *induced hazards* because they are the result of interference between geomorphologic processes and a new project. Cavallin et al. (1994) identified three different types of risk or hypothetical damage, associated with *direct hazards* and *induced hazards* (Figure 2.2):

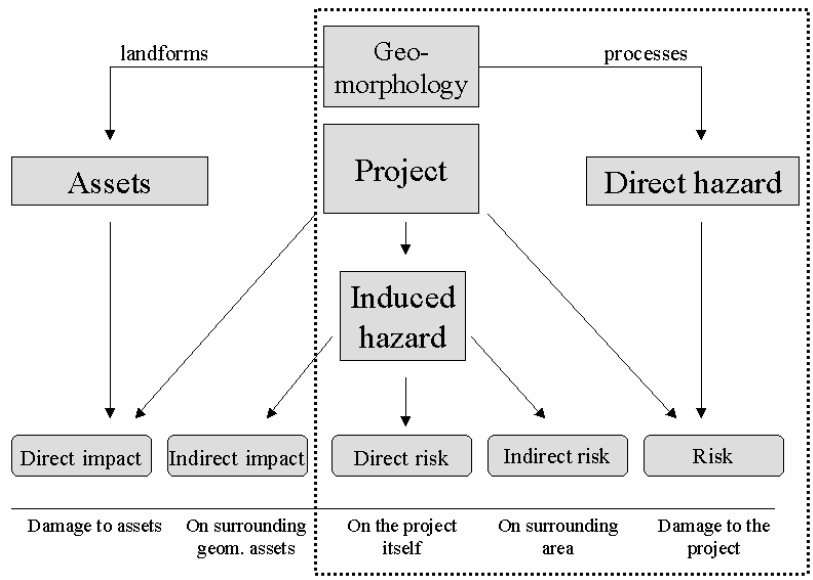

Figure 2.2. The interaction between geomorphology and a project (Cavallin et al. 1994). This chapter focuses on the part of the diagram indicated by the dashed box.

risk: the probability that the project is damaged due to a geomorphologic process (*direct hazard*);

direct risk: the probability that the project changes the characteristics of a geomorphologic process (*induced hazard*) which in turn may damage the project;

indirect risk: the probability of damage to the surrounding environment due to changes in the characteristics of a geomorphologic process, caused by the project (*induced hazard*).

Traditional EIAs often fail to foresee the effects of these induced hazards that may have consequences for the project itself or the surrounding area. Figure 2.3 illustrates this for floods and mass-movements:

Floods

Risk:	a flood occurs and inundates the proposed new motorway (left).
Direct Risk:	to avoid inundation during a flood the motorway is built on an embankment that deviates the flood so that it inundates the motorway at an unforeseen location.
Indirect Risk:	the motorway deviates the floodwater in such a way that previously unaffected areas are now inundated.

Mass movements

Risk:	a mass movement occurs and affects the new motorway.
Direct Risk:	the presence of the new motorway causes a mass movement that affects the motorway
Indirect Risk:	the presence of the new motorway causes a mass movement that affects the surrounding area.

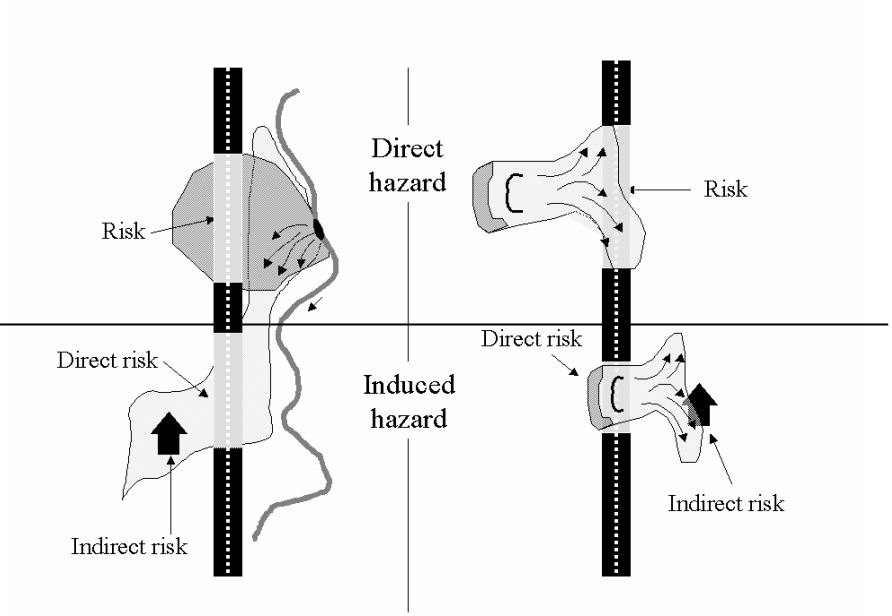

Figure 2.3. The effects of direct and induced hazards for floods (left) and landslides (right).

2.5 Hazard and risk assessment for EIA; A three-step approach

A geomorphologic risk assessment for Environmental Impact Assessment consists of three parts:

- Hazard and risk identification
- Hazard assessment
- Risk assessment

Hazard and risk identification

Hazard and risk identification means that potential geomorphologic hazards need to be identified and that a preliminary assessment has to be made on their potential interference with the socio-economic environment; in other words, could there be a problem? There are various ways to identify the potential geomorphologic hazards, e.g. through geomorphologic mapping by experts or (statistical) analysis of historic events. If hazardous processes are identified, then a preliminary risk

assessment should indicate whether they can interfere with things we care about - our *values*

Hazard assessment

Once a potential hazard is identified, it is important to know its characteristics. What is the extent of the inundated area of the 50-year flood or what is the potential run-out area of landslides? What are the controls of the characteristics of these geomorphologic hazards? In the last decades, a lot of knowledge has been accumulated to characterise *direct hazards*: what are the likely locations of slope instability, or what could be the peak discharge of the river after prolonged precipitation? The use of statistical modelling for slope stability analysis is exemplified by e.g. van Westen (1993), Chung and Fabbri (1999). Van Westen (2004) gives a good overview of developments in the field of landslide hazard zonation. For flood prediction 1-D catchments models are often used, e.g. HEC-HMS and HEC-RAS (US-ACE, 1997). *Induced hazards* are more difficult to foresee and qualitative assessments are usually not sufficient. The assessment of *induced hazards* requires more detailed and quantitative analyses that are able to forecast how much the processes are disturbed, what components within the various systems are affected and how the new project changes the characteristics of a geomorphologic hazard. Tools are needed to estimate where a change within the boundary conditions and the input data determine the outcome of the computations. Deterministic models fulfil this requirement and allow the evaluation of the consequences of a new project on the characteristics of the geomorphologic processes through scenario-studies. If the characteristics are changed, this could have consequences for the project itself (*direct risk*) or for its surroundings (*indirect risk*).

An important consideration for the choice of models is the model output. The output parameters should give a correct characterisation of the processes. For instance, in the case of floods, it is not sufficient to know the extent of the flooded area. Other parameters like inundation depth, flow velocity, warning time, duration, sedimentation, etc. are equally important to properly assess the hazard. The parameters should be transparent and meaningful so that experts from other disciplines can also perceive their meaning during the risk assessment. Lorenz (1999) calls these parameters *indicators*:

"Indicators describe the system or process in such a way that they have significance beyond their face value; they aim to communicate information of the system or process; the dominant criterion behind an indicator's specification is scientific knowledge and judgement".

Indicators have a dual function, on one hand they quantify the dynamics of the underlying geomorphologic process and on the other hand they can be related directly to human concerns (life, well-being, environment, etc.). Indicators are the key elements to evaluate and forecast the changes in the natural environment and the distribution of risk and impact (Cavallin et al. 1994).

Risk assessment

For a geomorphologic risk assessment additional information is required regarding the vulnerability of the elements exposed to a particular geomorphologic hazard and on their value. The critical part of the risk assessment is to find relationships that transform the hazard indicators into a degree of dysfunction, for instance to find at what intensity or magnitude of the hazard do the elements start to loose their ability to function as normal (lower threshold) and at what levels of intensity or magnitude are the elements completely destroyed (upper threshold), see Figure 2.4.

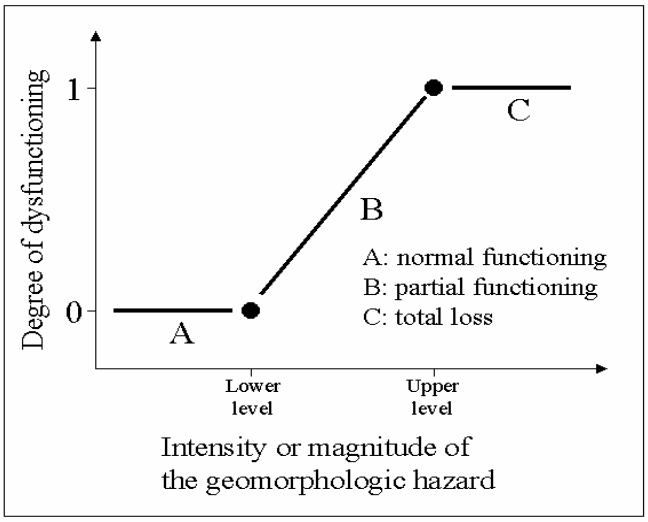

Figure 2.4. Vulnerability functions describe at what level of hazard the (partial) dysfunction of the exposed element starts and at what level the element is completely destroyed.

2.6 Flood hazard and risk assessment

Flood-risk assessment requires knowledge of the hydrological and hydraulic processes that form the source of the flood hazard and of the valuation of the socio-economic consequences. A flood hazard and risk assessment contains the parts that follow:

One-dimensional catchment modelling *(Hazard and Risk identification)*:
The first step is to transform catchment characteristics like topography, relief and land-cover, complemented with hydrological boundary conditions into estimates of the discharge at various locations along the river downstream. This can be done with (distributed) 1-dimensional models. The underlying assumption is that all flow is parallel to the direction of the main channel (hence 1D-modelling). These kinds of models are very useful to assess the response of the river to climatic events and to changes in the topography and land-cover. Typical models to do this are: HEC-HMS and HEC-RAS of the US Army Corps of Engineers (e.g. US-ACE, 1997), MIKE-SHE (Refsgaard and Storm, 1995), IHDM (Beven et al. 1987), THALES (Grayson et al. 1992) and LISFLOOD (De Roo et al. 2000).

Two-dimensional flood propagation modelling *(Hazard assessment)*:
The second step is usually carried out at a local to regional scale, at a selected stretch of the river. The aim of this step is to obtain the characteristics of a flood as it enters and propagates through complex topography where the assumption of parallel flow is not valid, e.g. after a dike breach or on an alluvial fan. These models provide information on how fast the water will flow and how it propagates through the area. This type of modelling is therefore very suitable to assess the effects of the surface topography, like embanked roads and different land-cover types on the flood behaviour (see e.g. Stelling et al. 1998).

Flood-risk valuation *(Risk assessment)*:
The third step requires knowledge of the vulnerability and value of the elements exposed to the floodwater. What are the consequences of a flood for the people living and working in a specific area? Is there time for evacuation, are critical buildings in danger (schools, hospitals,...) and what is the economic and non-economic damage? Agricultural activities suffer damage in a different way than for instance an urban area. Furthermore it should be noted that not all damage can be

quantified in monetary terms, like health and psychological consequences. Therefore an analysis is required that transforms the results of the flood propagation characteristics into a valuation of the risk. See e.g. Moser (1994). Experience from past floods, economic analyses, agricultural expertise, emergency practice and knowledge from other disciplines need to be combined to arrive at an integrated risk assessment, see e.g. Pielke et al. (2002).

2.7 Transformation of flood hazard into flood-risk

Several studies have been made to transform flood hazard indicators into flood-risk. In general, two types of risk assessment can be distinguished: those that try to express the flood-risk in monetary units (damage) and those that aim to evaluate the flood-risks in terms of human life, well-being and degree of disturbance. The most well known are the so-called stage-damage curves (US ACE, 1996; ANUFLOOD; Smith, 1994; Kok et al. 2002) that relate inundation depth to degree of dysfunction for an element exposed to the floodwater. So far this is the only method that is based on factual information where historic water depth information is linked with actual damage estimates. A major drawback of this method, identified by many authors, is that using only water depth as indicator is an oversimplification of the flood hazard. Gendreau (1998) combines water depth, duration and maximum acceptable return period. Abt et al. (1989), Témez (1992) and Penning-Rowsell and Tunstall (1996) propose combinations of flow velocity and water depth to distinguish between hazardous and non-hazardous floods. This is also recommended by the RIPARIUS final report (Blyth et al. 2001) that suggest that a limited set of risk categories should be defined, e.g. risk of structural damage, risk to adults, risk to children, low risk. Borrows (1999) proposes a hazard and risk matrix in which hazard categories are defined by flow velocity, water depth, flood warning time and annual probability of flooding. Smith (2004) presents critical curves (from different sources) based on flow velocity and water depth for risk to pedestrians, cars, light structures and concrete buildings. However, there hardly exists any historic data on the relation of these additional indicators and the degree of dysfunction of the exposed elements. The wide variety of methods and approaches of flood-risk assessment show that transforming flood hazard indicators into a risk assessment is still awkward.

2.8 Conclusion

Geomorphologic risk arises when elements with a certain vulnerability and value are exposed to geomorphologic hazards. When thresholds are surpassed, geomorphologic processes may become geo-hazards. This implies that for a risk assessment, good knowledge of both geomorphologic and socio-economic systems is required which makes risk assessment a multi-disciplinary endeavour. It is important to identify the controls of geomorphologic processes (geo-sciences) as well as the elements exposed to geomorphologic hazards (social and engineering sciences).

The first step towards a risk assessment is to identify potential geomorphologic hazards that could interfere with the socio-economic environment (*risk identification*). The second step, the *hazard assessment*, is to characterise and quantify the hazards and to predict how the geomorphologic systems and socio-economic systems will interfere. The third step, the *risk assessment*, is to transform the hazard assessment into risk. This requires additional information on the vulnerability of all exposed elements and their value. This last step is the most difficult, because it goes beyond the boundaries of traditional scientific disciplines and thus requires interdisciplinary cooperation.

Risk assessment has to be included in Environmental Impact Assessment procedures for new large projects, like the construction of new infrastructure. Important is that not only the direct consequences of the new project are assessed, but also its indirect and broader range effects. When a new project induces new hazards, or changes their characteristics it may result in an increase of geomorphologic risk.

The next chapters of this thesis will deal further with the second and third step: Chapters 4, 5 and 6 are dedicated to quantifying the flood hazard. A 2D flood model will be used to characterize the dynamics of a flood in terms of water depth and flow velocities. It will be shown that in certain areas it is not useful to define flood hazard simply as the probability of occurrence of a flood (as defined by Varnes) and that a refinement is required. In these areas, flood hazard can be better represented by a set of flood hazard parameter maps. In Chapter 6, 7 and 8 the focus will shift towards risk assessment and the difficulties that exist in creating a multi-parameter flood-risk map. However, this last step is essential because flood considerations will not be included in the decision-making process if the consequences for the socio-economic environment are not somehow quantified.

Chapter 3 2D flood modelling with Delft-FLS

The previous chapter presented the conceptual framework for hazard and risk assessment. This chapter will deal with an important tool for simulating flood events in complex terrain: a 2D flood propagation model. Such a model offers possibilities to quantify the dynamics of a flood event and to run different scenarios to evaluate the consequences of certain actions (or in-actions). These analysis may then be used as basis for decision-making and flood-risk assessment.

Abstract

This chapter presents the theoretical and practical basis for the application of 2D hydraulic models for flood hazard assessment. It first deals with the specific needs of flood hazard assessment, and what this implies for the choice of modelling approach. The second section describes the selected model – Delft-FLS - in more detail. Finally the general data management environment is described in which the modelling is embedded. The model needs spatial and temporal input data and it generates a large amount of spatial-temporal output data in the form of map-series with the spatial and temporal changes in water depth and flow velocity. For the management of these input and output data a GIS is required for storage, processing and analysis.

3.1 The need for 2D-models

In section 2.2 a geomorphologic hazard was defined as the probability that a certain geomorphologic process will occur in a certain area with a certain intensity within a given period of time. To translate this to floods, one can define flood hazard as the probability that a certain area will be inundated within a given period of time. Thus, traditional flood hazard maps delineate the annual chance of inundation, as shown in the top part of Figure 3.1. In this situation there is an inverse relationship between water level and chance of occurrence: the higher the water level the smaller the chance that it happens. In Figure 3.1 location A is more hazardous than location D.

In the lower part of Figure 3.1 the "Polder" situation is depicted, a situation that can be found in all major river delta areas, coastal plains and alluvial plains in the world where the river is flanked by widespread near-flat terrain. In some cases the surrounding terrain lies below the level of the river as a result of different subsidence characteristics between the more sandy deposits in and along the riverbed and the clayey, peaty deposits in the back-swamp areas. Often this difference in height is enhanced by artificial drainage of the back-swamps that leads to further subsidence.

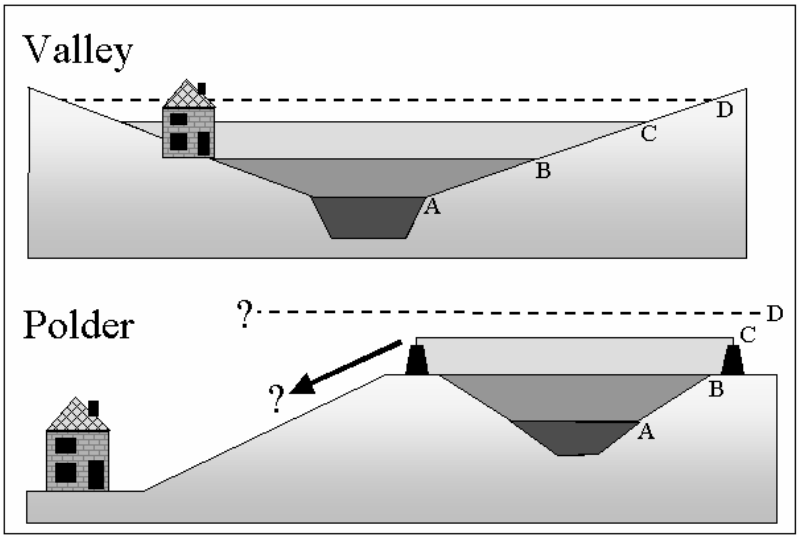

Figure 3.1 Morphological differences between upstream and downstream surface topography and its consequences for flood hazard zonation.

In the "polder" situation there is only a relation between the water level and return period of the flood as long as the river water does not overtop or breach the natural levees (B) or the dikes (C). A traditional hazard map equals the hazard in the whole polder area as the chance that the dikes are. This approach does not allow the differentiation in degrees of hazard within the alluvial plain (or polder) because it does not consider the propagation of the inundation flow. Clearly, the water level D in the lower part of Figure 3.1 is not instantly achieved in the whole flooded alluvial plain or polder. It takes time to fill the bathtub. How much time depends on the flux of water into the area and the characteristics of the terrain, like resistance to overland flow and the presence of obstacles like buildings,

embankments, etc. This temporal component is essential for decision-makers because people living in areas that are inundated within hours are more "at risk" than people living further on that have still days to respond to the hazard. Authorities need to know in advance which people to evacuate first and which roads are still accessible. Traditional flood hazard maps do not provide the right information to develop such evacuation plans. Furthermore they offer no help to planners to analyse the impact of new developments within these areas on possible future inundations. Simulating scenario floods with a 2D flood propagation model can help in these cases.

3.2 Numerical flood simulation

To quantify the flow of water as function of the topography, physically based hydrodynamic or hydraulic models are needed. Such models are based on the principle of conservation of mass, momentum and energy. Even though the theory was developed in the 17th to 19th century by Isaac Newton (1643-1727), Claude-Louis Navier (1785-1836), Adhémar Jean Claude Barré De Saint Venant (1797-1886) and George Gabriel Stokes (1819-1903), the modelling of the flow of water over initially dry areas is still extremely complicated (Alcrudo and Garcia Navarro, 1994), not in the least because no analytical solutions have been found yet for the full 3D unsteady Navier-Stokes non-linear partial differential equations. This set of equations relate the motion of fluids and gasses to viscosity, pressure, gravity and other internal and external forces. The equations are rather generic as they apply to all kinds of fluid-like substances that can range from the flow of air to the motion of stars in a galaxy. For applications in flood studies certain assumptions can be made to derive a new set of equations that are specifically applicable to the flow of inviscid water, like shallow depth of the flow compared to its width and that the bottom slope is relatively small. In these cases flood modelling can be done using the 3D shallow water flow equations of De Saint Venant (1871).
Furthermore, for flood applications it is often not needed to have information on the vertical velocity profile and on water flow in the vertical direction. This simplification allows the omission of the vertical (z-) component from the equations. For channel flow modelling one may then further reduce the number of dimensions by assuming that there is no flow perpendicular to the main direction of the river, so that flow is calculated in only one direction.

One-dimensional flow

When considering channel flow, it is assumed that the flow behaviour can be satisfactorily described as unsteady flow (flow characteristics may change over time) in one spatial dimension by 2 state variables: velocity (u) and water depth (h) as function of time (t) and space (x), while taking into account the following additional assumptions (Stelling and Verwey, 2005):

- Discharge is the integral of the velocities through a cross-section, perpendicular to the axis of flow (x-direction);
- The water level is constant along the cross-section: all water movement up and down happens at the same rate. There is no flow calculated perpendicular to the axis of flow;
- The pressure distribution in the vertical is hydrostatic;
- Water density is considered constant;
- The resistance relationship for steady flow is also applicable for unsteady flow;
- The bed slope is not too step (cosine of the slope is approximately 1).

The Saint-Venant equations

To solve u and h, two independent equations are required and usually the continuity equation (based on the conservation of mass principle) and the momentum equation (based on the conservation of momentum principle) are used. These two equations derived by De Saint Venant in 1871 are shown below in their Eulerian form per unit width of channel with no lateral inflow:

$$\frac{\partial(h+z_b)}{\partial t}+\frac{\partial(uh)}{\partial x}=0 \qquad 3.1$$

$$\frac{\partial u}{\partial t}+u\frac{\partial u}{\partial x}+g\frac{\partial(h+z_b)}{\partial x}+c_f\frac{u|u|}{h}=0 \qquad 3.2$$

Where:

x is the position along the channel axis (m); **t** is time (s), **u** is the velocity vector in the x-direction (m/s), **h** is the water depth (m), $\mathbf{z_b}$ is the local bottom level above the reference datum, $\mathbf{c_f}$ is the dimensionless bottom friction coefficient and **g** is the constant of gravity (9.81 m^2/s).

Stelling and Verwey (2005) give the following meaning to the terms in the equations: the first term in formula 3.1 represents the rate of volume stored over a unit length of channel. The second term accounts for the rate at which the discharge changes along the channel per unit of time. In formula 3.2 the first term represents the change of momentum in a control volume of unit length of channel and reflects the inertia of the water mass present in that control volume. The second term is called the convective momentum term and reflects the balance of momentum flowing through the control volumes' upstream and downstream cross-section. The third term combines the effect of impulses generated by differences in upstream and downstream hydrostatic forces (hydrostatic pressure term) and the gravity acting on the mass in the control volume (gravity term) and the last term is the so-called friction term that represents the effect of channel friction. Solutions based on the full set of equations (3.1 and 3.2) are defined as the full dynamic wave description (Stelling and Verwey, 2005).

Numerical solutions of the full dynamic wave description

Modern 1D hydraulic models are based upon numerical solutions of the full dynamic wave description. This is largely a result of the rise of fast and cheap computation power in the 1990s. The search for robust numerical solutions follows many paths as can be demonstrated by the enormous amount of publications in this field (e.g. Alcrudo and Garcia Navarro, 1994; Hervouet and Janin, 1994; Benkhaldoun and Monthe, 1994; Di Giammarco and Todini 1994; Bates and De Roo, 2000; Horritt and Bates, 2002; Dresback et al. 2005, Stelling and Verwey (2005), Kamrath et al. 2006). Along the path the modellers make choices regarding:

a) The discretization form of the problem;
b) The computation of the derivatives, using implicit or explicit difference methods;
c) The use of staggered or non-staggered schemes solutions;
d) Approximation of the convective momentum term in equation 3.2;
e) Estimation of the computational time step (dt).

Ad a). The most widely used forms of discretization are finite difference methods, finite element methods and the finite volume methods. Finite difference methods can be used in a grid environment whereas finite element and finite volume methods require a mesh representation. All have in common that infinitesimal small increments in space and time are replaced by discrete finite increments that

give an approximate of the differential equation (finite difference method) or its solution (finite elements and finite volume methods). The applicability of either method depends on the problem. Finite difference methods are simpler to apply and work well in cases the problem can be represented well by a simple geometry (like a grid). Finite elements methods can handle more complex geometries.

Ad b). There are several ways to compute the derivatives in the equations. Explicit methods use a so-called forward difference in time and compute the state of the system as a function of the previous state. Implicit methods use a so-called backward difference at each computational time step to find the solution involving both the current state and the future state. Although the explicit solution is easier to implement, the implicit method is more frequently applied because it offers robust solutions with larger time steps than the explicit methods. The extra computations that the implicit method needs balance the smaller time-steps required by the explicit method to achieve the same accuracy. Stelling and Verwey (2005) state that implicit methods offer advantages regarding unconditional numerical stability and that it solves satisfactorily the robustness problems related to non-linear effects and flooding and drying of channels and floodplains.

Ad c). Staggered and non-staggered grids relate to the spatial and temporal representation of the two state variables v and h. When these two are computed at the same grid points (cells), the grid is so-called non-staggered. In contrast the grid is called staggered when the state variables are computed on alternating grid points. It has been shown by e.g. Stelling et al. (1998) that the staggered grid offers advantages by guaranteeing the convergence of the numerical solutions and the better ability to handle flooding and drying of grid cells (see also Stelling and Verwey, 2005).

Ad d). The non-linear convective momentum term in equation 3.2 requires a transformation. Stelling and Duinmeijer (2003) state that the correct formulation depends on the way in which the convective speed of momentum is interpolated on the grid. This results in an approximation that is only first order accurate whereas the numerical discretization is other terms in the Saint Venant equations are second order accurate. For most practical applications this lower accuracy is quite acceptable, although locally the convective momentum term can become dominant. Most advanced models have specific solutions for these local conditions.

Ad e). The incremental time-step dt has to be defined to compute the state of the system at the next time step. The incremental time-step can be *a priori* user-defined like the incremental spatial step dx. However more robust ways of estimating dt are based on the state of the system at a previous time-step. In these cases the time-step is estimated using the Courant number condition where dt <= dx/Vmax. According to Stelling and Verwey (2005) this approach has as the advantage that newly computed water levels can never fall below the bottom of the channel, thus avoiding negative water depths.

Two-dimensional flow

The basic assumptions discussed in the previous section also apply to the 2D shallow water equations. In their 2D Eulerian form, per unit width of the channel and neglecting lateral flow, the continuity equation (formula 3.3) and the momentum equations (3.4 and 3.5) read:

$$\frac{\partial h}{\partial t} + \frac{\partial (uh)}{\partial x} + \frac{\partial (vh)}{\partial y} = 0 \qquad 3.3$$

$$\frac{\partial u}{\partial t} + u\frac{\partial u}{\partial x} + v\frac{\partial u}{\partial y} + g\frac{\partial (h + z_b)}{\partial x} + c_f \frac{u\sqrt{u^2 + v^2}}{h} = 0 \qquad 3.4$$

$$\frac{\partial v}{\partial t} + u\frac{\partial v}{\partial x} + v\frac{\partial v}{\partial y} + g\frac{\partial (h + z_b)}{\partial y} + c_f \frac{v\sqrt{u^2 + v^2}}{h} = 0 \qquad 3.5$$

Where

x and **y** represent the orthogonal axis and **u** and **v** the velocity vectors along these axis respectively. The staggered grid shown in Figure 3.2, shows that water level (h) and flow velocity vectors (u and v) are computed at alternating grid points. The flow velocity (V) can easily be computed as the vector sum of the vector velocities u and v:

$$V = (u^2+v^2)^{1/2} \qquad 3.6$$

It should be noted that this schematisation of the problem computes water flow only towards the 4-connected cells and that no flow is calculated to the diagonals (8-connected cells). In the input data preparation this requires attention. Stelling and Duinmeijer (2003) and Stelling and Verwey (2005) give a thorough description of the way the numerical solutions of the 2D Saint Venant equations are implemented in Delft-FLS.

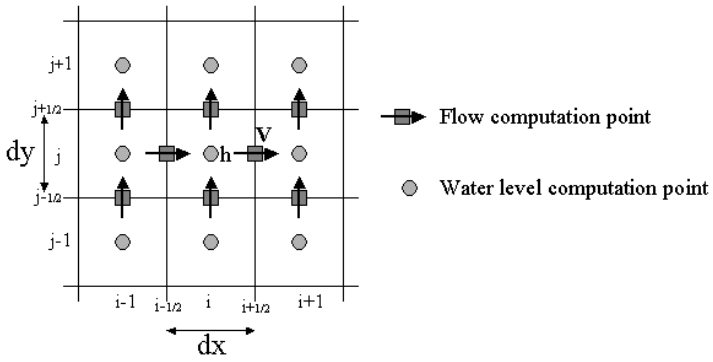

Figure 3.2. Staggered grid schematisation for 2D flow simulations

3.3 Delft-FLS

Delft-FLS - developed at WL|Delft Hydraulics - is a 2D hydrodynamic simulation package based on the full 2D shallow water equations that are solved using the finite difference method on a rectangular staggered grid. A description of the applied numerical solutions is given in Stelling et al. (1998) and Hesselink et al. (2003). In Stelling et al. (1998) is described how problems regarding water fronts or bores and hydraulics jumps are solved efficiently, which is especially relevant for inundations as a result of dam breaches. The scheme used in Delft-FLS is based upon the following characteristics (Hesselink et al. 2003):

- The continuity equation is approximated in such a way that (a) mass is conserved not only globally but also locally and (b) the total water depth is guaranteed to be always positive which excludes the necessity of "flooding and drying" procedures.
- The momentum equation is approximated in such a way that a proper momentum balance is fulfilled near large gradients.

The combination of positive water depths and mass conservation assures a stable numerical solution that converges thanks to the momentum balance. Given the approximations, Delft-FLS has a wide range of applications (Stelling et al. 1998), including practical problems such as overland flow, dam breaches, hydraulic jumps, flooding and drying of tidal flats, tidal bores etc. It adheres to the velocity Courant number as an automated time-step estimator, which reduces or enlarges the computational time step according to the flow characteristics at any moment during the simulation. Therefore it is efficient for most free surface flows, including flows in complex networks (Stelling et al. 1998). Because Delft-FLS computes on a rectangular grid, geometrical input data can be specified in a number of ways and land layout features such as dikes, roads, railroads, waterways, viaducts etc. can easily be included in the analysis. The user can force dike failures so that "what-if" scenarios can be investigated.

3.4 Input data

The implementation of 2D propagation models for flood hazard assessment is a complex process because of the handling of large amounts of spatial and non-spatial data. In this study a Geographical Information System (GIS) is used in parallel with the flood model to pre-process the data required as input for the model, as well as to post-process the model results and transform them into flood parameter maps – see Figure 3.3. This section describes the generation of the input data required for the model, using a flood study in Trento, Italy as example.

The Trento example

The city of Trento was severely flooded in 1966. Based on information and data provided by the Local and Regional Authorities in Trento, this event was reconstructed, using the 1966 surface topography and boundary conditions. In a second model run the 1966 event was simulated using the present (2000) topography where the city of Trento has expanded into the floodplain and major infrastructures have been constructed (Brenner highway and the Trento-Bypass road). Differences in the flood characteristics between the two scenarios can be attributed to these constructions on the floodplain. Figure 3.4 shows the location of the study area.

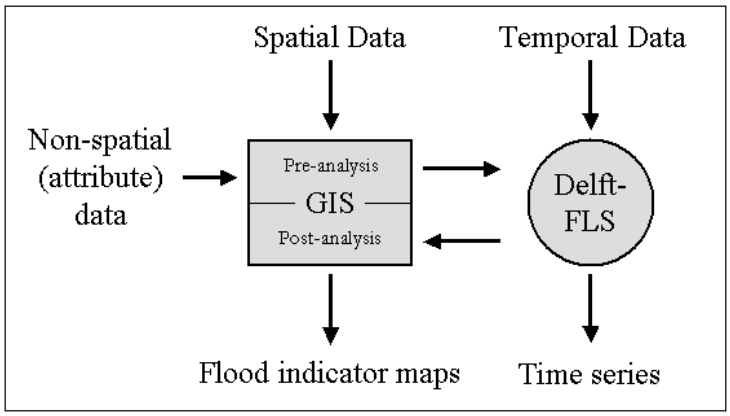

Figure 3.3. The use of a GIS in parallel with the flood model to process input and output data.

The model needs the following input data (see e.g. Stelling et al. 1998 and Stelling, 2000):

Spatial data
- Elevation;
- Surface roughness.

Temporal data
- Initial water levels;
- Upstream and downstream boundary conditions (water levels, fluxes, ..);
- User-defined dike breach evolution and final breach geometry (if applicable).

A scenario is defined in the so-called Master Definition File (mdf), which is a text-file that contains all instructions required by the program to run the simulation – see Stelling (2000). It also contains options for the output generation.

Spatial data

The elevation map has to contain all surface elements that can affect the flow of water, even features that are not included in regular digital terrain models (DTM) like dikes, embanked infrastructure, large buildings or riverbed morphology.

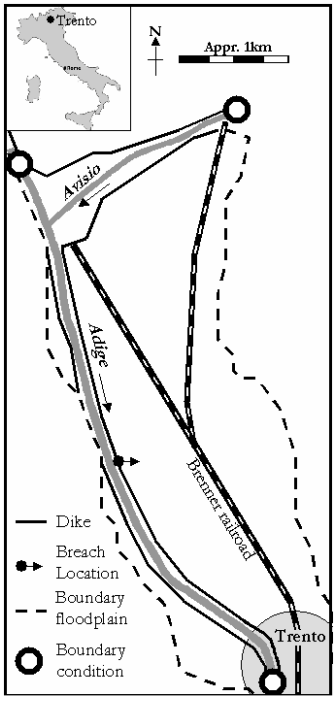

Figure 3.4. Location of the study area.

Many of these features have to be extracted from topographical maps, building footprints maps, field surveys, river cross-sections or bathymetry data and other sources. All these data layers need to be integrated to create the final Digital Surface Map (DSM) that contains all flow influencing objects, like terrain elevation, height and location of dikes and embankments and location of tunnels and bridges. Delft-FLS reads this DSM in standard ArcInfo asci (.asc) format with regularly spaced cells (grid) that contain the elevation values. The computation time largely depends on the number of cells in the grid, so for a given area it is advisable to generate the DSM at several resolutions to find a balance between resolution, number of grid cells and computation time. Another aspect that has to be considered in the choice of the grid-size is the fact that the model only computes flow in the direction of the 4-connected cells and not to the diagonally (8-) connected cells. For the representation of street networks and channel systems this may impose restrictions on the grid-size, especially in urban areas. In the procedure to generate the DSM, the connectivity of the street network should be checked. A different problem arises when the DSM is derived from a Laser Altimetric Survey (or LIDAR). This kind of DSM contains all surface features at very high resolution

(often in the range of 1m) with a very high accuracy (in the range of centimetres). So in principle it is a very suitable basis for flood modelling. However, its high resolution, and consequently large number of grid-cells for larger areas, makes it impossible to feed it directly into the flood model, because the calculation time would become enormous. In this case a procedure has to be developed in the GIS to decrease the resolution without loosing the exact height information of critical flow-influencing objects (like dikes, embankments, etcetera). An example of such a procedure is given in Chapter 4.
Similarly, the surface roughness map has to be generated at the same resolution as the DSM to ensure that for each cell both elevation information and roughness values are available. Often the surface roughness map is derived from a land-cover or land use map. If these are not available, interpretation and classification of remotely sensed imagery (airborne or satellite based) can assist. In literature tabulated data exist that give values of roughness coefficients (usually Manning's coefficient) as a function of the land-cover, which can then be linked to the land-cover maps as attribute data, to generate a spatial representation of the roughness coefficients (see e.g. Chow, 1957; Barnes, 1967; Arcement and Schneider 1990).

The Provincial authorities of Trento (*Servicio Urbanistica*) provided the DTM, as well as the footprints of current buildings and the location of infrastructures. The elevation data was provided in grid-format with a grid size of 10 metres. During a field survey this data was complemented with information regarding the height of embankments and dikes. The bathymetry of the Adige River and its tributary the Avisio River was derived from cross-sections provided by the Authority of the Adige Basin. All data were integrated into two final Digital Surface Models, one with the 1966 topography and one representing the 2000 situation - see Figure 3.5. Comparison between the 1966 and 2000 topography reveals that large parts of the alluvial plain of the Adige and the alluvial fan of the Avisio have undergone significant transformations. Many new buildings and some major infrastructure were constructed in that time period, like a large industrial area North of Trento, a transit zone "*Interporto*" near the confluence of the Avisio and Adige, the Brenner highway and the Trento by-pass road.
The land-cover map made by Geneletti (2001) was used to obtain the spatial distribution of surface roughness coefficients, using the values of Manning's coefficient for the various land-cover types. These were obtained from Chow (1959) and Selby (1989) – see also section 6.2.

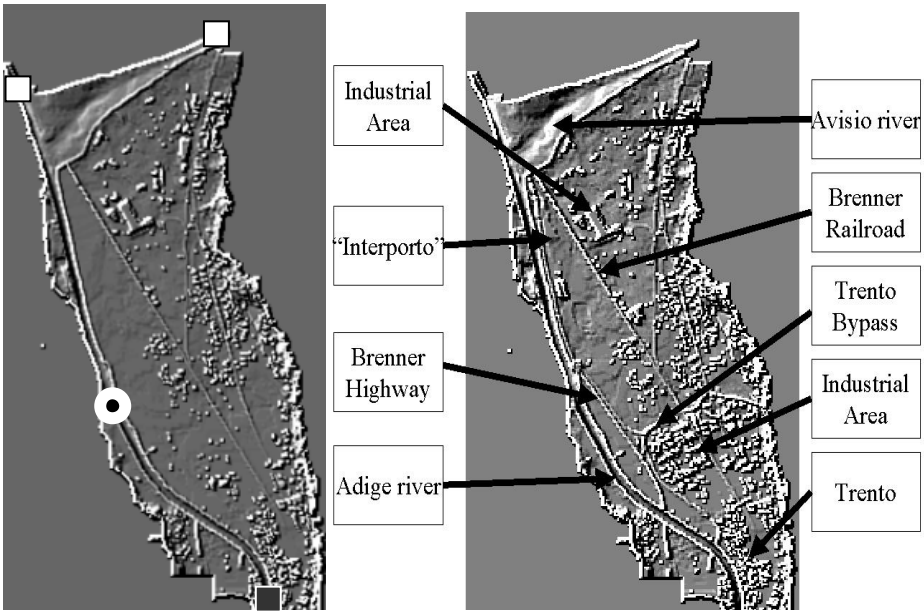

Figure 3.5. *(left) The surface topography in 1966. The dot indicates the location of the dike breach. (right), The white squares indicate the two upstream (discharge) boundaries (define the flow into the area) and the black square indicates the downstream (Q-h) boundary. (right) The detailed Digital Terrain Model representing the 2000 topography with some important topographical features. "Interporto" indicates a newly developed transit zone for cargo transfer from road to rail and v.v.*

Temporal data

There are to sets of temporal data required for a model run: 1) The initial conditions and 2) the boundary conditions.

Ad 1) Initial conditions.

The initial conditions describe the state of the system (water levels and fluxes) at the start of the computation. They can be defined in two different ways: 1) imposed by the modeller, and 2) calculated by Delft-FLS during a pre-modelling run, which creates a so-called restart file. In the second option the pre-simulation run starts at dry conditions and slowly water is added to reach a hydraulically stable starting point for the flood simulations. In this study for all scenarios restart files were constructed.

Ad 2) The boundary conditions

The boundary conditions describe the exchange of water mass between the study area and the rest of the universe during the model run. At these points (see Figures 3.4 and 3.5) is defined how much water enters the area and how much is leaving downstream. The upstream boundaries usually consist of time-series with water levels (m) or with discharges (m^3/s). The downstream boundaries are usually water levels (in the case of a lake or the sea) or a rating curve. This last option is the site-specific relationship between water levels and discharge (also known as Q-h relationship). In the case where the river continues beyond the downstream the rating curve is the preferred lower boundary condition, although it increases the computation time. The boundary conditions are in the form time-series tables of discharge (or water levels) or in a table with the relationship between water level (h) and the discharge (Q).

In the case of a dike breach, the modeller must define the location and development of the breach. Each raster cell that is part of the breach must be identified and linked to a file that contains the information on how much that raster cell is "lowered" as a function of time. For large breaches that cover multiple cells, the breach evolution can thus be reconstructed in detail.

The Basin Authority of the Adige River provided the discharge information of the Adige River (station San Michele) and the Avisio River (station Lavis) that are shown in Figure 3.6 as well as the rating curve of the Adige River at Trento (Figure 3.7). According to information from the Basin Authority (Mr. Bordato, oral communication) the estimated design discharge of the Adige protection works in the stretch between Avisio and Trento is approximately 1200 m^3/s. According to the graphs in Figure 3.6 this maximum discharge was reached at t = 10 hours, just before the peak discharges of both the Adige and Avisio. In the simulations, the breaching of the dike coincided with the moment of peak discharge (t = 10 hours) and based on information from past dike breaches (Adige Basin Authority; Mr. Bordato - oral communication) the maximum width of the breach was set to 50 meters wide (5 grid cells). In absence of reliable breach geometry information the maximum depth of the breach as assumed to be 4 meters (below the original height) which it reached at t = 12 hours.

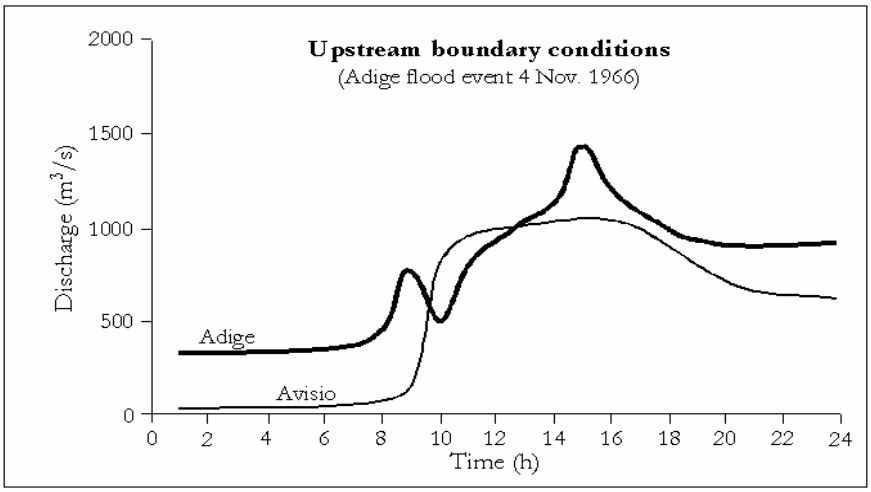

Figure 3.6. Discharges of the Adige and the Avisio during the 1966 flood.

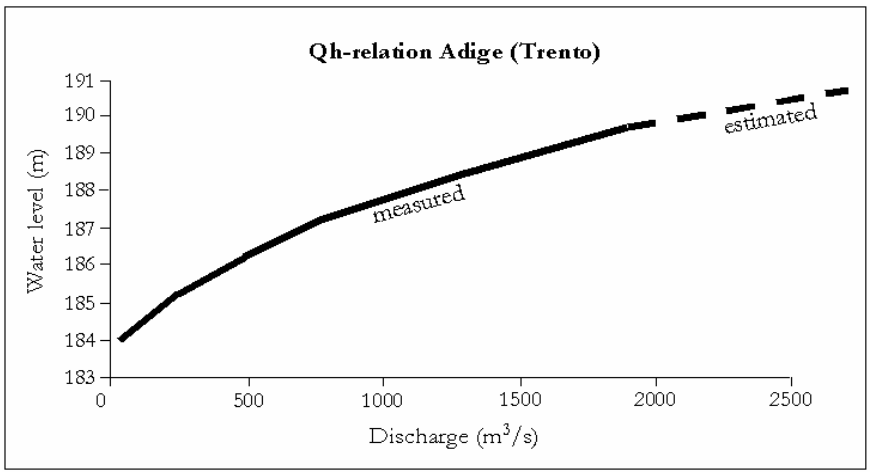

Figure 3.7. Q-h relationship – or rating curve – of the Adige at Trento.

3.5 Output data and generation of parameter maps

Delft-FLS generates three types of output: 1) dynamic output, 2) temporal output and 3) spatial-temporal output.

Ad 1) The dynamic output is in the form of an incremental flood animation file that can be visualised with a special software, Quickin, also developed by WL|Delft Hydraulic. This software is provided together with Delft-FLS and show the flood propagation as a video-animation.

Ad 2) The temporal output consists of tables with time-series of water depth at predefined locations and of discharge at predefined cross-sections.

Ad 3) At predefined time intervals maps are generated that show the spatial distribution of water depth and flow velocity. At the end of the simulation additional maps are created that contain the maximum water depth and flow velocity that occurred at each cell during the simulation.

Parameter maps
Although the dynamic and temporal outputs are very instructive and useful for various purposes (see e.g. Chapter 4), the most import information for hazard and risk assessment is contained within the map-series with water depth and flow velocity. These stacks of maps are saved in asci-format and must therefore be imported into a GIS for further analysis and visualization (see Figure 3.3). For a lengthy flood simulation these stacks can contain over a hundred files. To analyse this data an aggregation procedure has been developed to create 6 parameter maps that describe the different aspects of the flood event. Apart from the maps with the maximum water depth and flow velocity these parameter maps are (see Figure 3.8):

- Maximum impulse
- Maximum rising of the water level
- Flood propagation characteristics (also Warning time)
- Duration

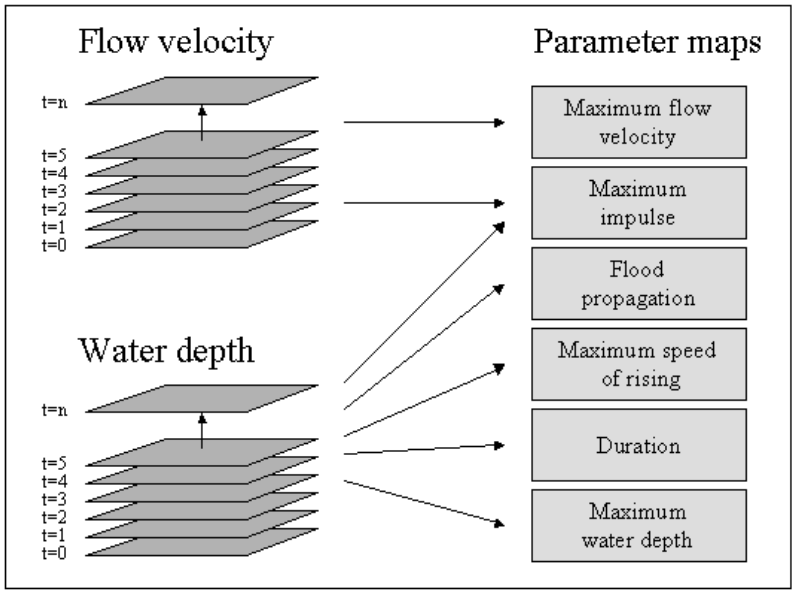

Figure 3.8. Transformation of the model output maps into flood hazard parameter maps. The colour coding shows how these parameter maps were used for the risk / damage assessment.

1 Maximum water depth (unit: m);

This map shows the maximum depth that occurred during the inundation. The rationale behind this parameter map is that areas with deep water are more dangerous to people and potentially more damaging to objects like houses and cars. It identifies areas where the second floor of houses, or even the third or fourth floor, is not a safe refuge. The maximum water depth map also serves as a possible means for model calibration. Maximum water depth is one of the few flood parameters that can easily be retrieved after a flood event because of wetting marks in and on houses.

2 Maximum flow velocity (unit: m/s);

This map shows the maximum flow velocity that occurred during the inundation. The rationale behind this parameter is that velocity is a component of the floodwater that can sweep people off their feet and make cars float away. This map shows where preferential flow paths may develop that could be dangerous for children, adults and cars.

3 Maximum impulse (unit: m^2/s);
This map shows the maximum impulse that occurred during the inundation. The impulse is calculated at each time step by multiplying water depth and flow velocity. For each pixel this value represents the amount of movement of the water mass (per pixel the mass only depends on the water depth, since the surface area of the pixel and volume weight of water are constant). The rationale behind this parameter is that flow velocity alone does not suffice to estimate the amount of potential damage or danger to humans and cars to be swept away. Shallow water with a high flow velocity does not have a lot of kinetic energy or momentum and neither has deep, but practically still-standing water. Deep, fast flowing water however is potentially dangerous for people and vehicles and is potentially damaging to objects like houses and crops.

4 Maximum rising of the water level (unit: m/h);
This map shows the maximum speed at which the water level rose at some point during the inundation. It is calculated by taking the difference between two successive water depth maps, divided by the time interval between the two maps. The result is an increase in water depth per hour. The rationale behind this parameter map is that a quick rising of the water level is potentially dangerous for people who may not have sufficient time to seek higher ground or elevated structures.

5 Flood propagation characteristics (unit: h);
This map shows how the flood propagates through the area. After each time interval the flooded area is identified and compared with the situation at the previous time interval. It records the time at which a cell is inundated for the first time. The rationale behind this parameter map is that it shows how much time it takes for the first floodwater to reach a certain location and thus how much warning time people have to prepare themselves. Areas that are flooded quickly are potentially more dangerous than areas further away.

6 Duration (unit: h).
This map estimates the time the floodwater remains at a certain location. It is based on several assumptions regarding the drainage of the floodwater from the flooded area. For instance in the studies presented in this book it is assumed that there is free drainage at the lowest point of the inundated area through a "canal" of

a certain width (1 or more pixels wide). It also requires a sufficiently long simulation run that includes the descending limb of the flood wave. The rate of water level change is calculated as dh/dt, where dh is the difference between the maximum water depth and the water depth at the end of the simulation and dt is the difference between the time at the end of the simulation and the time the maximum water depth is reached. The duration is estimated by extrapolating this rate of change until the moment of a water depth of zero is reached - see Figure 3.9.

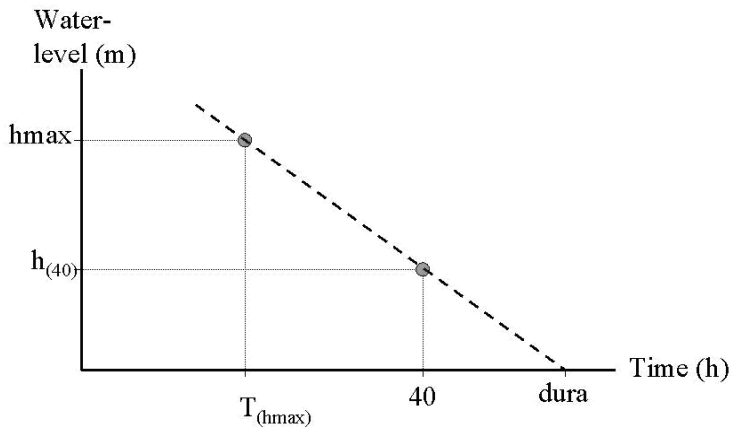

Figure 3.9. Estimation of the parameter "duration".

The rationale behind this parameter is that it gives a first, rough impression of how long the floodwater will stay in the area. This is the minimum time period that people have to be relocated, that businesses and industries are closed and that transportation in and through the area might be impossible or hindered. It is a strong parameter to assess the economic and social impact of the flood on the people living and working in the area. It is also an important parameter to estimate agricultural damage because many crops, like fruit bearing trees and vineyards can withstand inundation of their stems for a short time (usually some days), but if the period becomes too long the roots will starve from oxygen depletion and the trees will die.

Note: because of the longer simulation period required to compute the recession of the water level in the area, the duration was not calculated for this example.

3.6 Analysis of the results

For the example study of Trento, the first five parameter maps have been computed for the 1966 as well as for the 2000 topography. Figure 3.10a-c shows the results for both scenarios. The third map for each parameter shows the difference between the two scenarios (the 2000 results are subtracted from the 1966 results). Because all other parameters remained unchanged, the differences can be attributed to the topographical changes on the alluvial plain. The results show that these developments have a significant effect on all parameter maps. In some places maximum water depth was reduced, in other places it increased. The same holds for flow velocity, impulse, speed of rising of the water level and propagation of the inundation. To make things more complicated, the changes do not show the same spatial pattern. Where one parameter gives an improvement (less hazard) the other parameter shows a worsening of the situation (more hazard). Looking carefully at Figure 3.10 the following observations can be made:

- The Brenner Highway (see Figure 3.5) creates a sub-compartment directly behind the breach which results in an increase of water depth, impulse and rising of the water level;
- Also elsewhere, sub-compartments were created by embanked infra-structures which has significant consequences, especially for the speed with which the water level rises;
- Tunnels, bridges and other "connections" between compartments, create locally higher flow velocities and impulse;
- The obstruction to flow by elevated infrastructure and by buildings on the plain has decreased the flow over the plain downstream (South), thereby increasing the water depth and decreasing the warning time (flood propagation time) in the Northern part.

It is concluded that man-made objects like roads and railroads compartmentalise the floodplain and that the propagation of the flood follows these compartments as can be seen in Figure 3.10 that shows the flood propagation map. Another general conclusion is that tunnels, bridges, buildings and other man-made topographical elements funnel the floodwater through narrow passages, resulting in high flow-velocities and high impulse at these locations. The issue of how to continue with this multi-parameter flood hazard and risk assessment is discussed further in Chapters 6 and 8.

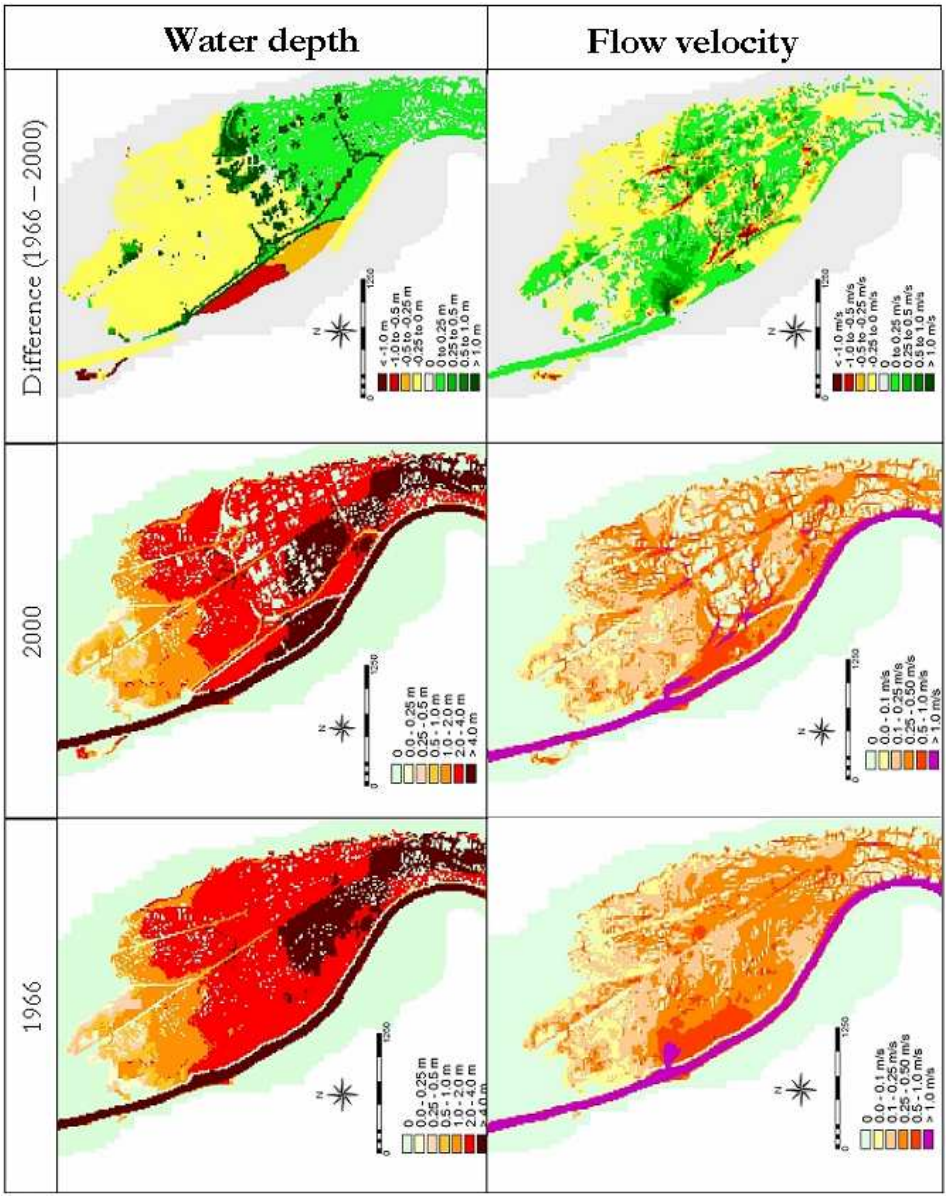

Figure 3.10a. Parameter maps water depth and flow velocity.

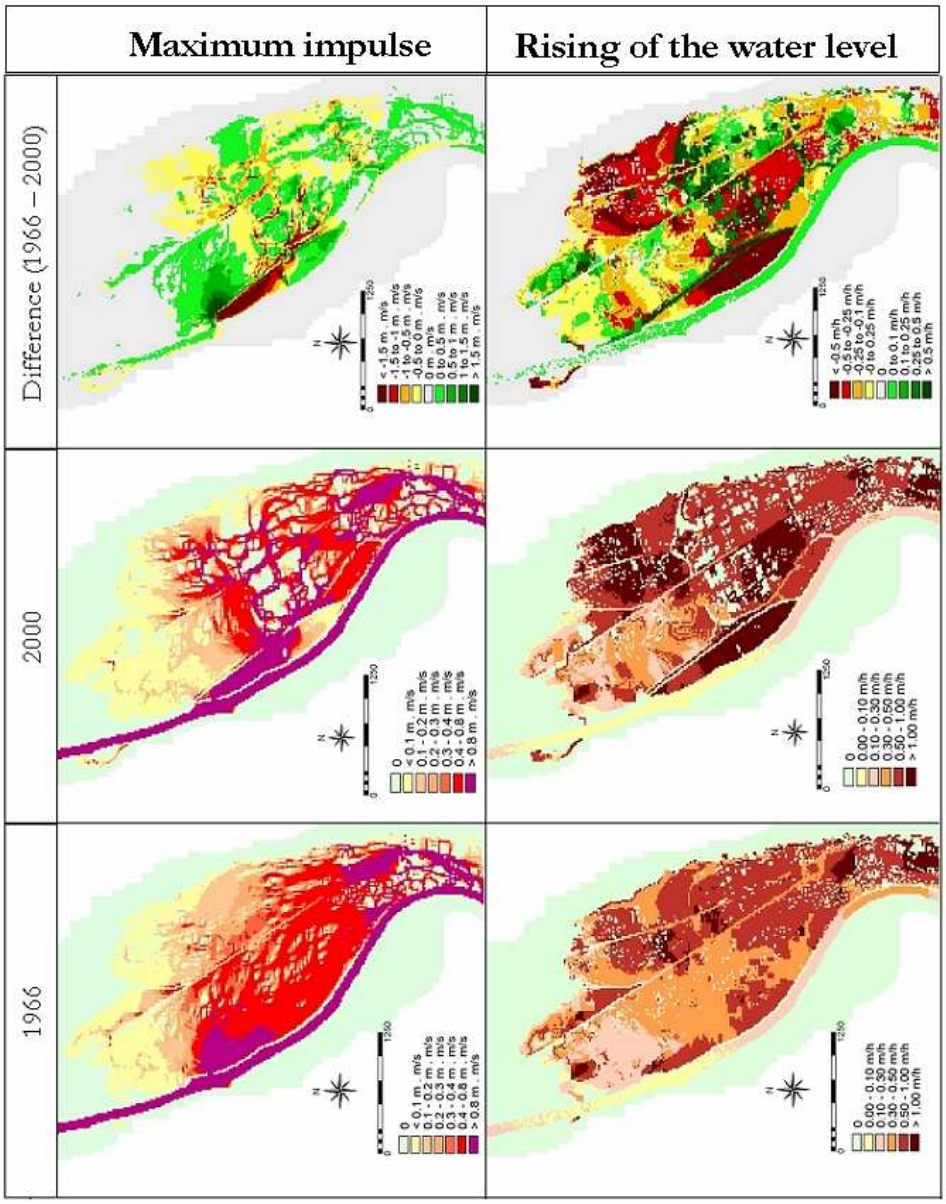

Figure 3.10b. Parameter maps impulse and rising of the water level.

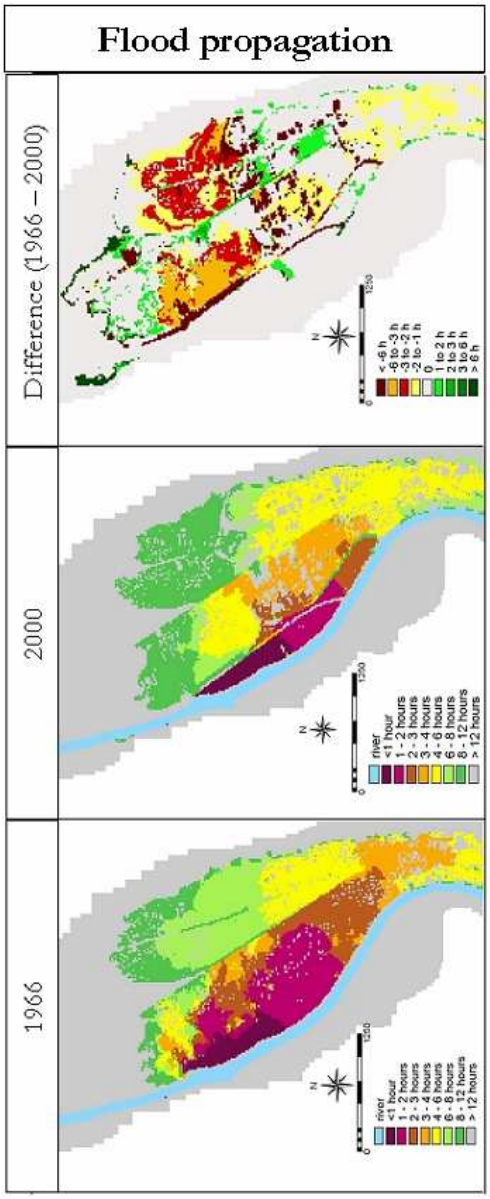

Figure 3.10c. Parameter map flood propagation

3.7 Model testing

There are three ways of testing a flood inundation model (see e.g. Hesselink et al. 2003):

- to test the numerical scheme of the model by comparison with analytical solutions and theoretical analyses of consistency, stability and convergence;
- by comparing the model simulation results with tightly controlled laboratory inundation experiments, (see e.g. Stelling and Verwey, 2005);
- by comparing the model simulation results with real-world flood events (Hesselink et al, 2003).

Until now, very few studies have been made to evaluate the performance of inundation models with real-world flood events. This is mainly due to model complexity and lack of real-world measurements. The information that is available after a flood is usually in the form a water level marks – or wetting marks, that give the local flood depth. Although these are important for model testing, they are not sufficient to test a 2D flood propagation model properly. To do this additional measurements are needed regarding the 'dynamic' characteristics of the flood like arrival time of the flood water, flow velocity and speed of rising of the water level. These are usually not available after a flood event. Hesselink at al. (2003) give an example of a real-world test with Delft-FLS which was used to simulate the 1805 inundation of a Dutch river polder and to compare the results with historic water level data. Among their conclusions was that such studies can be used to evaluate the model performance for real inundations, even for events with long return periods. In Chapter 4 another real-world event is reconstructed to test Delft-FLS.

3.8 Conclusion

This chapter presents the theoretical and practical basis for flood modelling in (nearly) flat terrain with complex topography. It is argued that in "polder" situation no linear relationship exists between water levels and probability of occurrence (return period) of a flood. For these areas traditional hazard maps are not very informative if the hazard is defined as the probability that an area is flooded. This

will result in large uniform areas with a probability of flooding (hazard) that is equal to probability of bank-full discharge of the river or the design characteristics of the protection works. In order to differentiate the hazards within the polder additional information is needed regarding the flood propagation, maximum water depths, flow velocities etc. To obtain this information 2D flood models can be applied to simulate the flow of water over (nearly) flat terrain and complex topography. The example of the Adige river near Trento demonstrates the application of Delft-FLS and shows what data is required to run the model and how the model results can be transformed into a set of flood parameter maps: 1) the maximum inundation depth, 2) the maximum flow velocity, 3) maximum impulse, 4) maximum speed of rising of the water level, 5) estimated duration of the inundation and 6) the propagation of the flood water (or warning time).
In the Trento example it is made clear that Delft-FLS can be used to assess the effects of terrain modifications on the characteristics of the flow. Differences between the 1966 and 2000 simulation can be attributed to the construction of new infrastructures, industrial sites and other major changes in topography. Unfortunately no historic data was available to test the model results regarding its prediction performance. This issue will be addressed in the next chapter.

Chapter 4 Reconstruction of the *Ziltendorfer Niederung* flood

In the previous chapter the 2D flood propagation model Delft-FLS used to simulate floods on the alluvial plain of the Adige River near Trento, Italy. This example served to demonstrate the input data requirements of the model, as well as the transformation of its output into a set of parameter maps, but it also demonstrated that man-made constructions on the alluvial plain can have a significant effect on the flood characteristics. In that example, however, it was not possible to test the performance of the model because no measurements were available to see to what extent Delft-FLS computed the flood parameters correctly. This chapter is dedicated to testing the performance of Delft-FLS by reconstructing a flood event of 1997 in Germany and by comparing the model results with observations made during and directly after the flood event.

Abstract

This chapter presents the results of the reconstruction of the inundation of the *Ziltendorfer Niederung* in Germany during the 1997 Oder floods with a two-dimensional flood propagation model. This model - Delft-FLS, developed at WL|Delft Hydraulics - was used to simulate the flow of river water into the low-lying area after a series of dike breaches. The availability of nearby upstream and downstream hydrographs made it possible to make a detailed reconstruction of the flood event. A series of high water marks and monitoring stations within the inundated area provided a good and independent dataset to validate the performance of the model. The conclusion is that Delft-FLS is capable to reconstruct the flood event accurately, and that the underestimation of the maximum water level of approximately 30 cm can be largely attributed to errors in the input data.

4.1 Introduction

This chapter deals with the application of Delft-FLS to reconstruct the inundation of the *Ziltendorfer Niederung* (Germany) during the 1997 Oder flood after the dikes

had failed at several locations. The *Landesumweltamt* Brandenburg (the Regional Authority) had collected a unique dataset, including a digital terrain model and up- and downstream hydrographs. In addition to these, also time series of water levels and maximum water levels at several locations in the inundated area were available. With this dataset it was possible to reconstruct the flood, using breach growth and surface roughness coefficients as calibration parameters. The time-series of water level readings provided an independent dataset to validate the results. The aim of this study is to investigate to what extent Delft-FLS is capable of accurately reconstructing the 1997 Ziltendorfer flood event.

4.2 The 1997 Oder flood

The *Ziltendorfer Niederung* is part of the natural floodplain of the Oder River, protected by dikes. The main land use is arable land with sparse settlements and isolated farms. The town of Eissenhüttenstadt is located a few kilometres upstream, the town of Frankfurt an der Oder a few kilometres downstream (see Figure 4.1). The distance between Eissenhüttenstadt and Frankfurt a/d Oder along the river is approximately 30 kilometres.

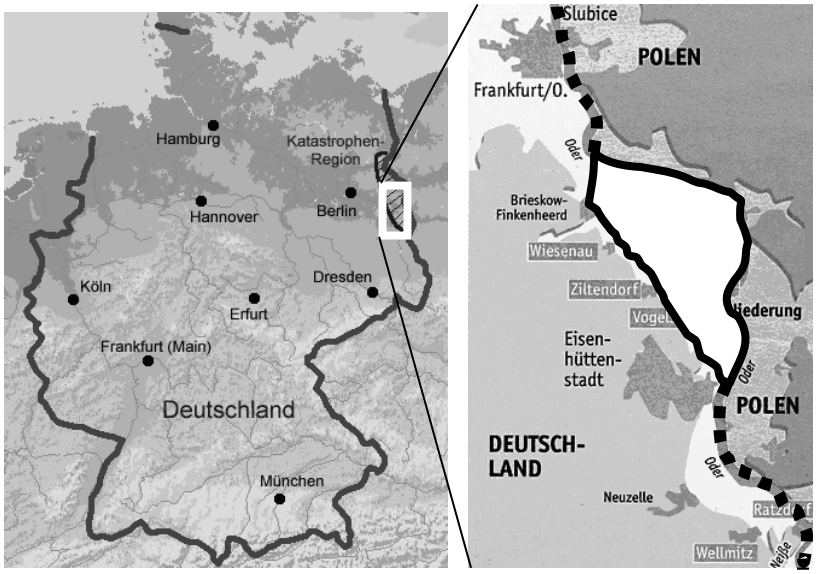

Figure 4.1. Location of the Ziltendorfer Niederung (scale app. 1: 500,000).

In July 1997 Central Europe experienced heavy and intensive rainfall. Some stations in the upper reaches of the Oder catchment, in the Czech Republic and in Poland, recorded more than 500 mm in 24 hours. This resulted in severe flooding of the Oder River in the Czech Republic, Poland and Germany and caused considerable material damage and over one hundred casualties (Grünewald, 1998). After several days the floodwater reached the German-Polish border and threatened the rural districts of the Brandenburg region. Emergency workers could not prevent the failure of the dikes protecting the low-lying *Ziltendorfer Niederung*, and in the morning of July 23rd the river water rushed into the area. The next day, in the afternoon of July the 24th, the dikes failed at a second location. Timely evacuation of the inhabitants ensured that no lives were lost, but extensive material damage could not be avoided. In the evening of July 26th, the water level in the *Ziltendorfer Niederung* had risen higher than the water level in the Oder river – that was already receding – and three consecutive dike breaches caused a surge of water from the area back into the Oder, aggravating the already tense situation downstream. For the location of the dike breaches, see Figure 4.2. For more information, see e.g. Grünewald (1998).

4.3 Available data

Digital Terrain Model (DTM)

A detailed DTM of the area was made directly after the flood, combining the results of a Laser Altimetric survey (LIDAR LIght Detection And Ranging of Laser Imaging Detection And Ranging) for the dry surface and echo soundings for the riverbed. The merging of these two separate surveys into one single highly accurate DTM as well as filtering out non-surface elements like trees, houses and cars was done at the Technical University of Vienna (Mandleburger, 2001). However, with a spatial resolution of 2.5 meters, this DTM was "too heavy" to be used in a flood inundation model. The computation time of a single run would be enormous. Therefore the DTM was resampled to a grid size of 30 meters. To ensure that the 'vertical' accuracy was not affected, the DTM was split-up in parts using a mask to produce three separate maps at a resolution of 2.5 meters: 1) a map containing all elements of which the exact maximum height information was required, like dikes and embankments; 2) a map containing all elements that required the exact local minimum heights, like the riverbed and canals and 3) a

map containing the rest of the elevation values. The maps with exact maximum and minimum heights were resampled to a grid with a resolution of 30 meters in the ILWIS Geographical Information System (GIS) using a maximum and minimum filtering operation respectively, to ensure that the correct height information was preserved on the 30 meter grid. The rest of the area was resampled to the same 30 meter grid by averaging the elevation values of the 12x12 corresponding 2.5 meter pixels. After these operations, the three parts were combined into a single DTM with a grid size of 30 meters. Figure 4.2 shows the original DTM and the resampled DTM that was used for the simulations.

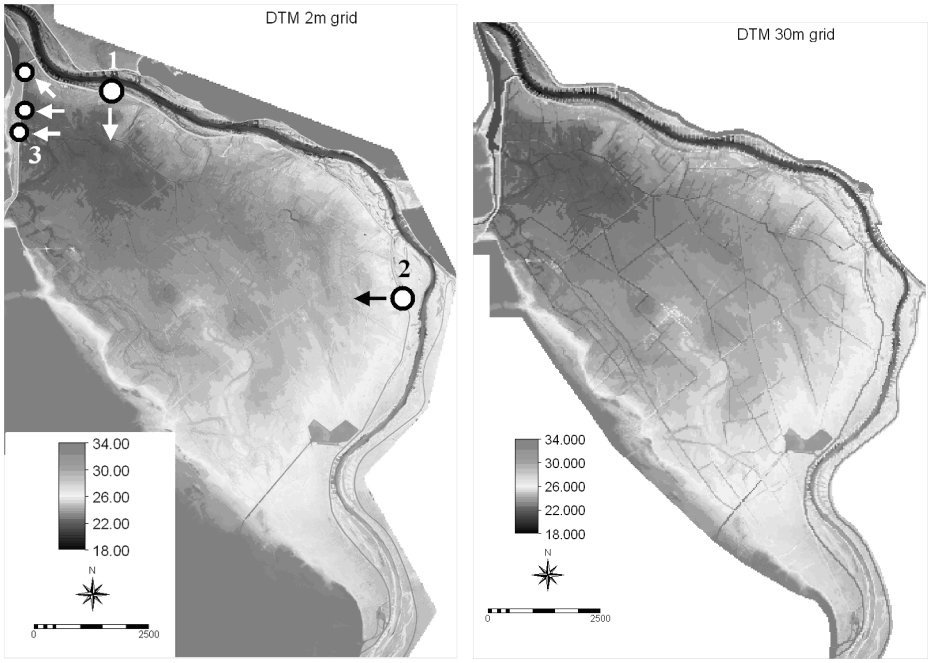

Figure 4.2. *The high-resolution DTM of the Ziltendorfer Niederung with a grid-size of 2.5 meters (left) compared with the resampled 30 meter grid version. Due to the combined mask- and filtering techniques canals and dikes show much more pronounced on the coarser DTM. The location of the breaches are indicated on the left–hand DTM in order of occurrence. The elevation values are in meters above the reference level (DHHN92).*

Hydrographical data

The *Ziltendorfer Niederung* is located directly in between the hydrographical stations of Eissenhüttenstadt (upstream) and Frankfurt an der Oder (downstream) – see Figure 4.1. Of both stations quarterly hours water level readings were transformed to discharge estimates using the empirical Q-h relationship, or rating curve, of these stations. The relationship reached up to a water level of 25.3 meters, so for higher water levels, the discharge was estimated – see Figure 4.3. Figure 4.4 shows the discharge curves of both Eissenhüttenstadt and Frankfurt an der Oder. The effect of two dike breaches and the following inundation of the *Ziltendorfer Niederung* is clearly visible in the downstream hydrograph. The breaches result in a sharp decrease of downstream discharge. The back-bursts that occurred on July 26th caused the discharge at Frankfurt to peak above 2,500 m^3/s. After that, the draining of the Niederung was responsible for higher downstream discharges for nearly the whole month of August.

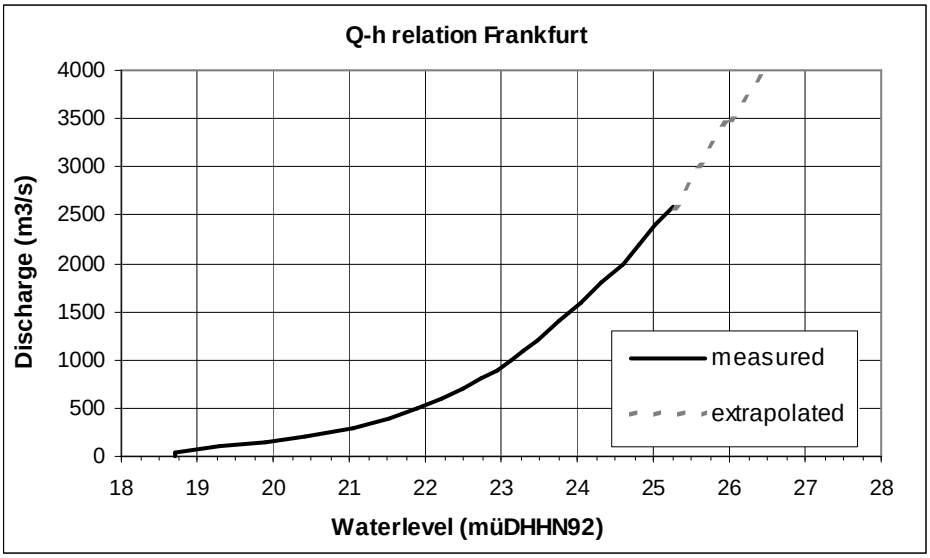

Figure 4.3. The Q-h relation for Frankfurt a/d Oder as used in Delft-FLS (Source: Landesumweltamt Brandenburg)

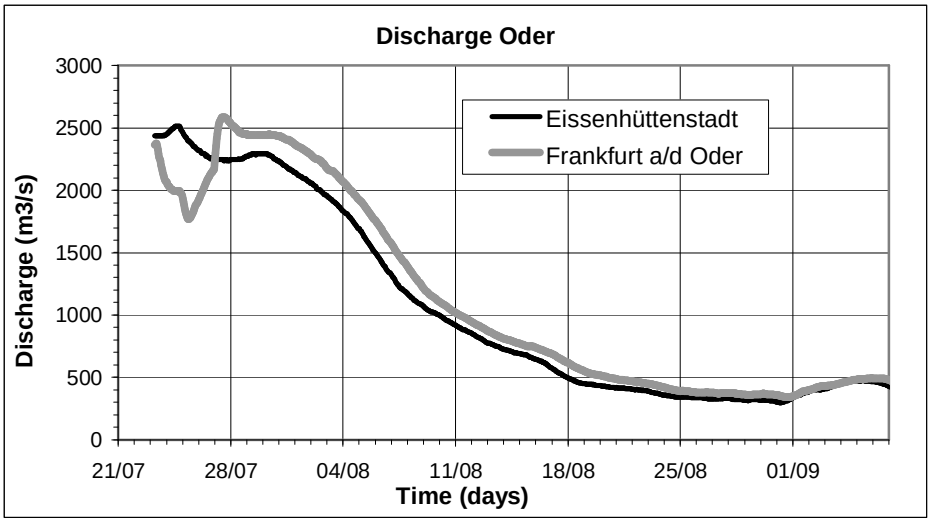

Figure 4.4. Hydrographs of Eissenhüttenstadt (upstream) and Frankfurt a/d Oder (30 kilometres further downstream); Year: 1997.

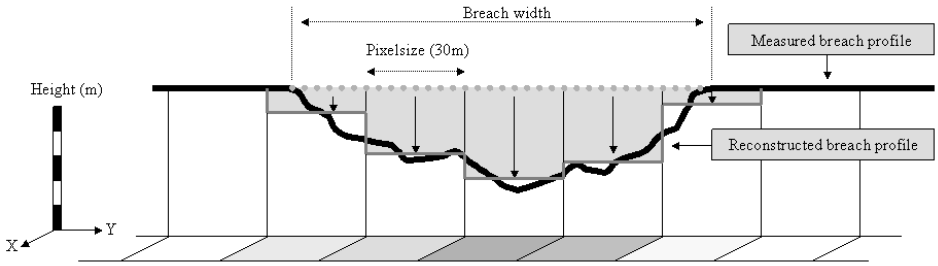

Figure 4.5. Reconstruction of the measured breach profile for the modelling

Breach geometry information

The first breach occurred in the Northern part of the Ziltendorfer Niederung on the 23rd of July 1997, at 9.05 am. The second breach was located on the Eastern side of the area and happened on the 24th, at 17:00 hours. In the evening of the 26th, after 21:30 hours three consecutive dike breaches in the Northern part, released water from the Niederung through the Briekower See, back into the Oder River. The Brandenburg authorities provided the location and time of each of the

breaches as well as their final geometry. In Delft-FLS the evolution of the breach-growth can be modelled as a step-wise lowering in time of the dike pixels until the final breach profile is reached. To see how much the "breach pixels" must be lowered, the final breach profile data was transferred to the resolution of the topography, which is 30 meters – see Figure 4.5. The rate at which the breaches evolved was determined during the calibration procedure that is explained in detail in section 4.4.

Dike profile and material

Cross-sections derived from the detailed DTM (Figure 4.6) show that the dikes have no uniform profile along the *Ziltendorfer Niederung*. This indicates that they were not constructed at once, but are the result of a gradual evolution. Through time the dikes were constructed, repaired, reinforced, and heightened. It is very likely that only local, mainly sandy material, was used for the construction. There is no information available on whether or not the dikes contain a clay core or a clay external cover.

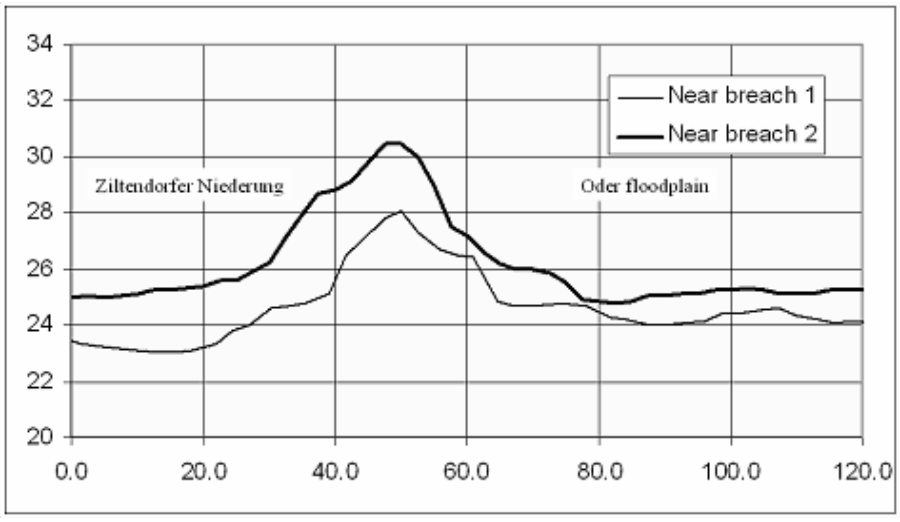

Figure 4.6. Cross-sections of the dikes near breaches 1 and 2 derived from the LIDAR survey. Height in meters above sea-level (DHHN92). Units are in meters.

Surface roughness

The surface roughness is an indication of the resistance that the water experiences while flowing over the topography. In this study, the surface roughness map was

derived from the land-cover map, which, in turn, was obtained from the Corine land-cover survey (Figure 4.7). The roughness values (Manning's coefficients) for the riverbed and floodplain were set to 0.027 and 0.032 respectively. Determining the values for the friction coefficients within the *Ziltendorfer Niederung* was part of the calibration procedure that is described in the next section (results are shown in Table 4.1).

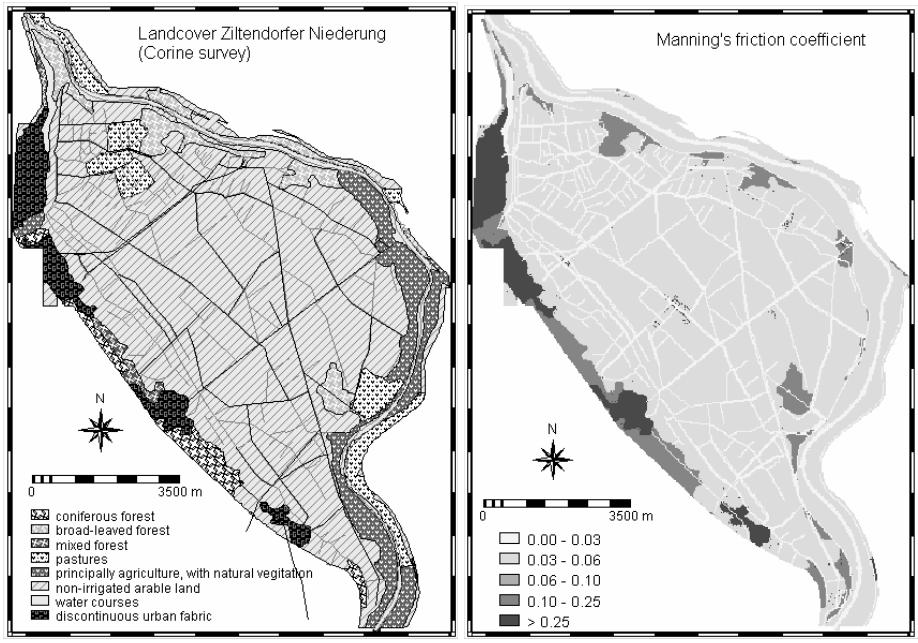

Figure 4.7. Corine land-cover map (left) and the derived surface roughness map (right)

4.5 Calibration

The downstream hydrograph at Frankfurt a/d Oder in Figure 4.4 clearly shows the effects of the dike breaches. In Figure 4.8 is demonstrated how this information, in combination with the upstream hydrograph of Eissenhüttenstadt, can be used to reconstruct the fluxes through each of the dike breaches into and out of the *Ziltendorfer Niederung*. It is assumed that lateral fluxes into the Oder River in the stretch between Eissenhüttenstadt and Frankfurt a/d Oder is negligible.

Two unknown variables determine the flow through the breaches: 1) the surface roughness coefficients and 2) the development of the breaches. Because the final breach profiles are known, the remaining question is how the breaches grew vertically and horizontally, the so-called breach evolution. It was observed that both variables had distinctive effects on the shape of the downstream hydrograph. This will be explained in the following two sections.

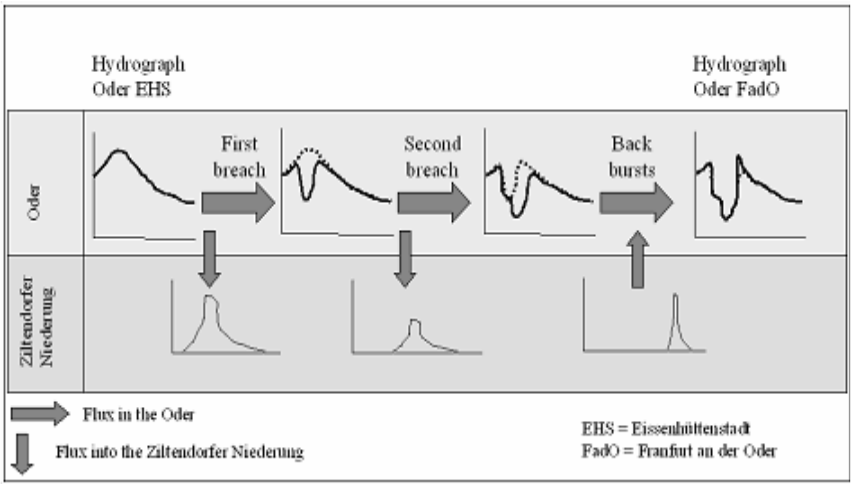

Figure 4.8. The effect of the consecutive dike breaches in the Ziltendorfer Niederung on the downstream hydrograph

Calibrating the friction coefficients

Figure 4.9 shows the reduction of the downstream discharge just after the first breach occurred and the water was diverted into the *Ziltendorfer Niederung*. In the same figure the results of three trial simulations are plotted where the friction coefficients are varied. Higher friction coefficients result in a higher discharge at Frankfurt a/d Oder, lower friction coefficients the downstream discharge decreased. This can be explained because higher friction within the Niederung hinders the flow into the area, and consequently more water remains in the river. Lower friction coefficients – easier flow into the *Niederung* - move the modelled downstream hydrograph downwards. It can thus be concluded that the surface friction controls the amount of water flowing through the breaches. Change of friction coefficients does not significantly affect the timing of the flow reduction.

Breach evolution

A similar analysis was carried out to assess the effect of the breach evolution on the downstream discharge. This is shown in Figure 4.10. Rapid breach growth results in a quick drop in downstream discharge, while a slower breach growth results in a much slower reduction of the downstream discharge. It was observed, however, that all evolution scenarios reach more or less the same minimum downstream discharge, and that only the timing when this minimum discharge is reached differs. It was thus concluded that the breach evolution determines the "steepness" of the graph and much less the flux through the breach.

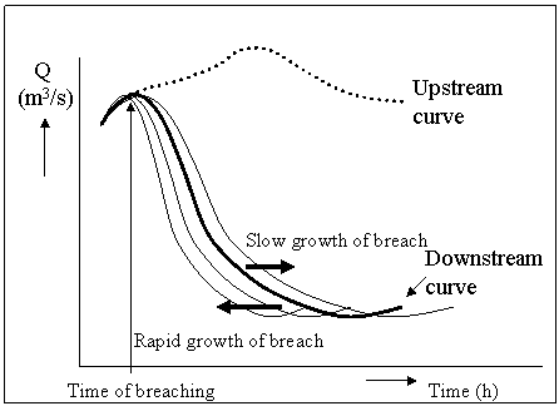

Figure 4.9. Examples of the effect of friction coefficients (Manning's n) on the downstream hydrograph.

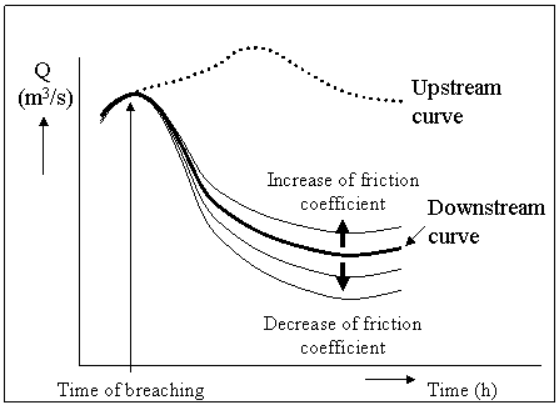

Figure 4.10. Different breach growth scenarios and their effect on the downstream hydrograph.

Calibrating on the downstream hydrograph

During the calibration the computed downstream curve was fitted as accurately as possible onto the measured downstream curve, by adjusting the surface roughness coefficients and the breach evolution. After several simulations a combination of these two control factors (see Table 4.1 and Figures 4.7, 4.11 and 4.12) was found that yielded a good fit as shown in Figure 4.13. The curve "measured south" is the upstream hydrograph of Eissenhüttenstadt and was used as the upstream boundary condition in the model. "Measured north" is the measured downstream hydrograph of Frankfurt an der Oder and Z0 is the computed curve. The failure of fitting the graphs accurately after the 3rd breaches is discussed further in section 4.8. The evolution of the first 2 breaches is discussed in the next section.

Table 4.1. Manning´s roughness coefficients after the calibration.

Land-cover / unit	Manning´s coefficient
River bed	0.027
Flood plain	0.032
Arable Land	0.03
Pasture	0.05
Forest	0.20
Roads and canals	0.02
Built-up	0.25

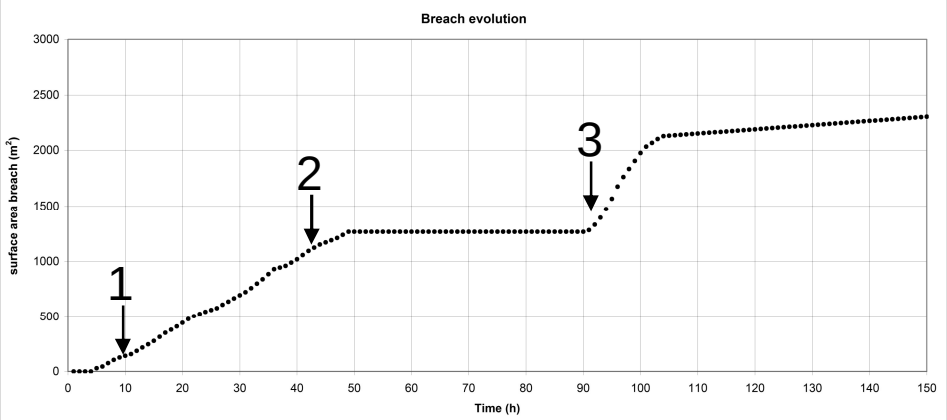

Figure 4.11. The calibrated breach evolution (cumulative surface area of the breaches) for all breaches (indicated by 1, 2 and 3)

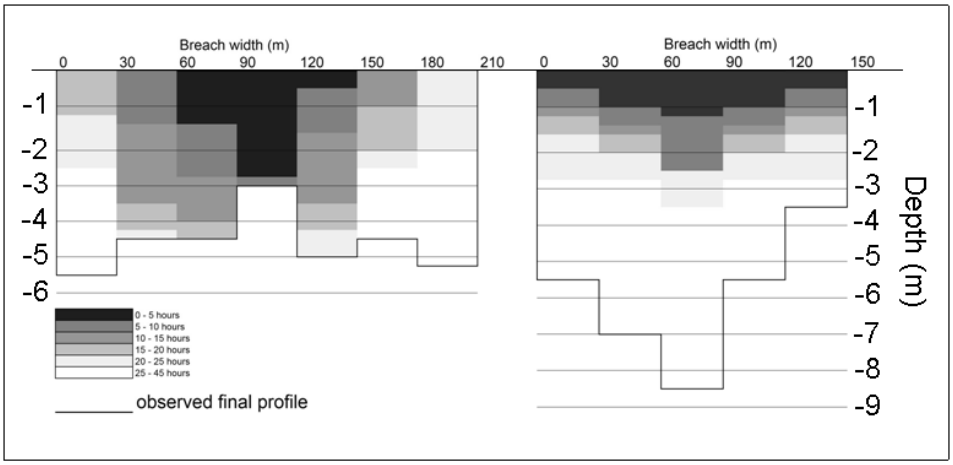

Figure 4.12. The evolution of breach 1 (left) and breach 2 (right) in hours after the first moment of failure (depth in meters).

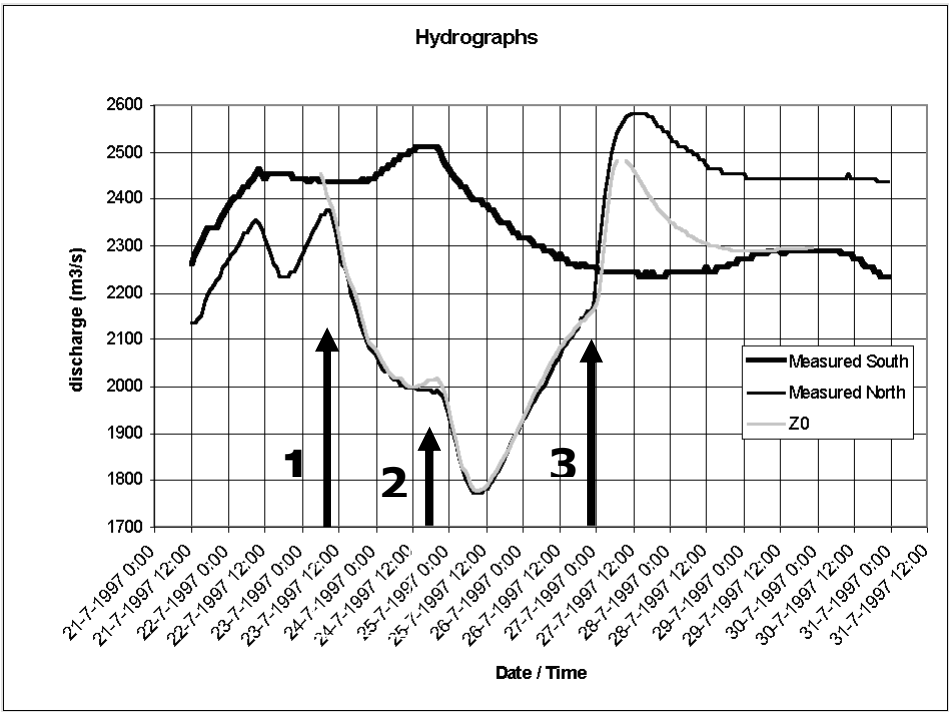

Figure 4.13. Calibrated downstream hydrograph compared with the measured (the arrows indicate the timing of the consecutive breaches).

Breach profiles

The first breach developed quickly in the first 24 hours (see Figure 4.11) and grew deeper and wider at the same time, giving it a general V-shaped breach profile (Figure 4.12). After 24 hours it grew deeper at the sides until it reached it's final profile at 40 hours after the start. The second breach developed much slower. It remained rather shallow at the start but grew quickly wider. Then, for almost 48 hours the gap hardly grew further (Figure 4.11). When the back-bursts occurred on the other side of the Niederung the breach was reactivated and grew slowly deeper until it reached a maximum depth of almost 9 meters (Figure 4.12). The evolution reconstruction of both breaches corresponds well with the fact that the first breach did not develop a scouring hole (maximum depth was 'only' 5 meters below the original height of the dike) whereas the second breach did, as can be clearly seen in Figure 4.14. The three back-bursts occurred within the time span of a few hours and all developed very quickly. The maximum width and depth was reached within a few hours.

Figure 4.14. Location of the first dike breach with no scouring hole (left) and the location of the second dike breach with scouring hole – now lake (right). Source Google Earth.

4.6 Inundation of the Ziltendorfer Niederung

Maximum flood extent

The model showed that the maximum flood extent was reached in the night of July 26th to 27th around midnight. The water in the *Ziltendorfer Niederung* reached a maximum level of 26.70 meter above sea level (DNNH92). The area of 4879 ha in the *Ziltendorfer Niederung* was flooded. When the maximum water level was reached, a total of 127 x 10^6 m^3 of water were stored in the flooded area. The average

inundation depth was 2.6 meters but at some places a maximum depth of over 4.5 meters was reached.

Flood parameter maps

Figure 4.15 shows the six flood parameter maps for the *Ziltendorfer Niederung* that are based on the hourly output maps of water depth and flow velocity, generated by Delft-FLS.

Maximum water depth. The highest inundation depths are found in the Northern part of the *Ziltendorfer Niederung*, east of Brieskow-Finkenheerd. Near the Brieskower See dike the inundation was at its deepest: 5.73 meters.

Maximum flow velocity. The highest flow velocities in the *Ziltendorfer Niederung* are found near the breaches of the Oder dikes. The maximum flow velocity simulated by Delft-FLS is 3,1 m/s. This is a depth-averaged value for a pixel of 30 x 30 meters. The map shows that the higher flow velocities are near the canal system. Apparently these play an important role in the advancement of the floodwater front at the onset of the inundation because they are the lowest points in the area and have a relative low friction coefficient. Higher flow velocities are also seen along the flow-paths between the dike breaches.

Maximum impulse. Impulse is defined as the product of water depth and flow velocity. Water depth is representative here for the mass of water per pixel. It describes the quantity of movement. In general it shows the same characteristics as the flow velocity map. The maximum impulse is found behind the breaches. More profound in the impulse map is the diagonal flow path between breach 2 (south of Aurith) and the breaches in the north.

Maximum speed of rising of the water level. The highest values for the speed of water level rising were found near and in the canals in the *Ziltendorfer Niederung*. Apparently the canals were used as preferential flow paths by the advancing water resulting in a rapid increase of the water depth.

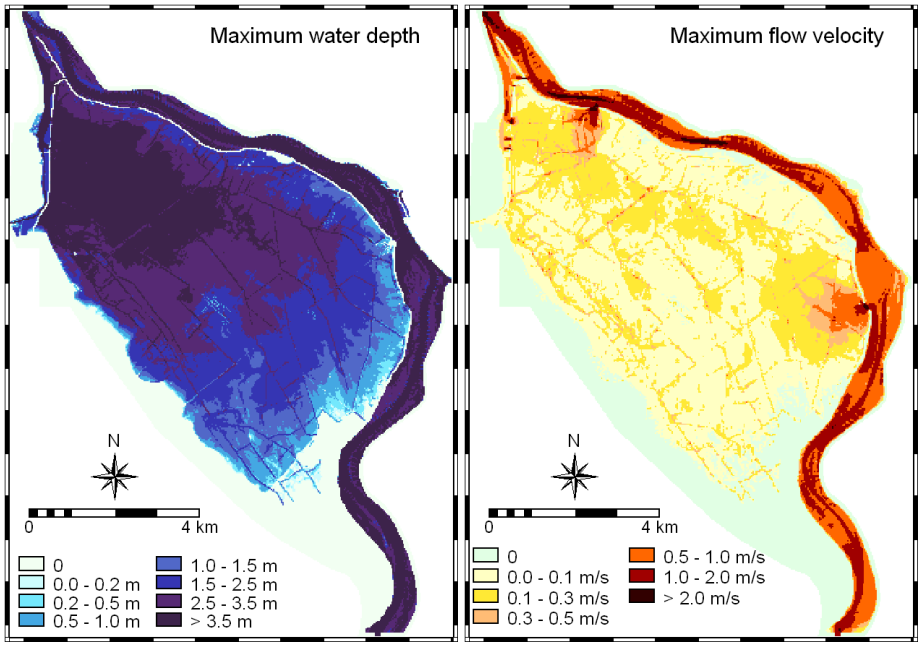

Figure 4.15. Parameter maps of the reconstructed Ziltendorfer Niederung inundation

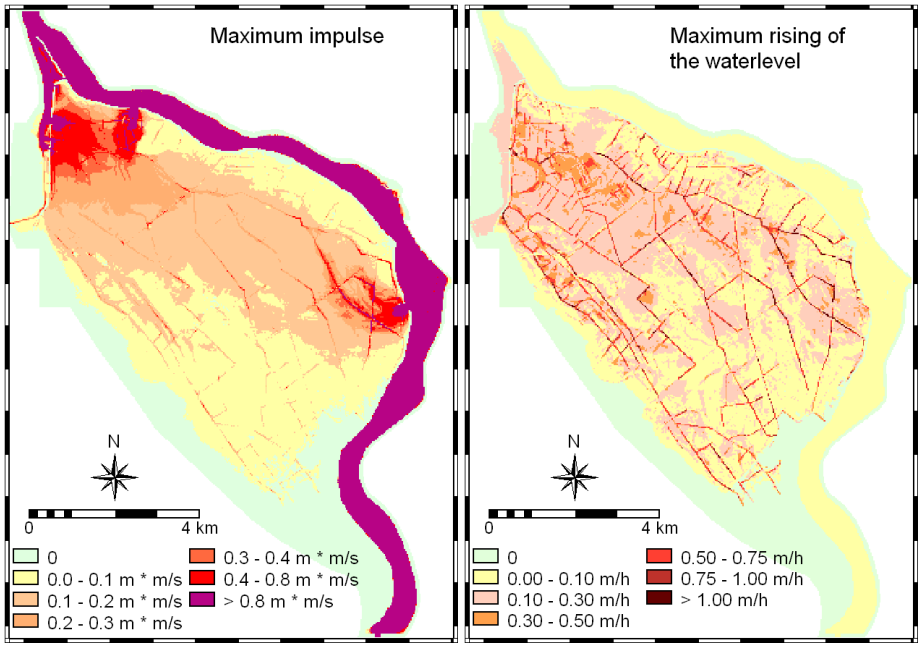

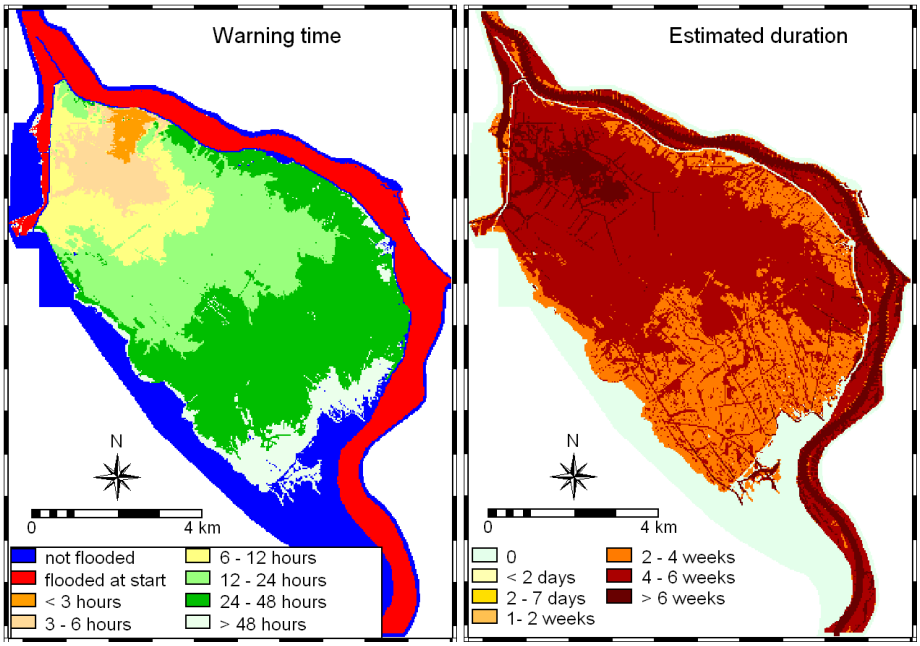

Figure 4.15 (continued). Parameter maps of the reconstructed Ziltendorfer Niederung inundation

Arrival time of the floodwater. This maps shows the propagation of the floodwater through the *Ziltendorfer Niederung*: it shows how long it took before a point was flooded in hours after the first breach. It can been seen clearly, that the propagation is from North to South. At the moment of the 2nd breach – 32 hours after the 1st breach – a large part of the *Ziltendorfer Niederung* is already flooded. Within 48 hours almost the whole area is inundated. The maximum flood extent is reached in the night of 26 to 27 July, 90 hours after the first breach.

Duration. This map shows how much time it would take if the water would drain naturally through the breaches. No additional pumping was simulated. It is estimated that the draining of most of the area would take between 2 to 6 weeks.

4.7 Validation of the modelling results

During and directly after the inundation water level measurements were recorded. Two types of data were measured: high-water marks and time series. High-water

marks give information on the maximum water level (maximum water depth) that was reached during the inundation, while the time-series give information on the movement of the water level in time. Figure 4.16 shows the locations of these measurements in the *Ziltendorfer Niederung*. Most monitoring information only show the water levels during the draining of the Niederung. These locations were defined in Delft-FLS in order to generate simulated time series for comparison with the measured levels. Table 4.2 shows the measured high-water marks and the simulated levels. Figures 4.17a to 4.17c show the measured graphs at some stations where the water level was monitored together with the simulated water levels. Table 4.3 shows the average differences between measured and simulated water levels for all the monitoring stations in the *Ziltendorfer Niederung*.

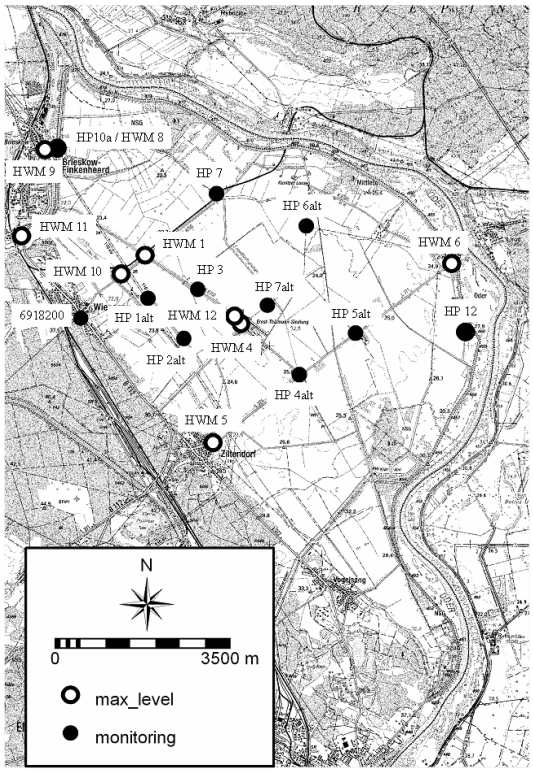

Figure 4.16. Map with the location of maximum water level marks (HWM) and water level monitoring stations (HP).

Table 4.2. High-water marks of measured and simulated water levels in meters above sea level (DHHN92). The simulated values underestimated the measured water levels with an average of 0.21 m.

Station	Measured	Simulated	Difference
HWM 1	27.11	26.70	-0.41
HWM 4	26.92	26.70	-0.22
HWM 5	26.75	26.70	-0.05
HWM 6	27.19	26.70	-0.49
HWM 7	27.63	27.04	-0.59
HWM 8	26.92	26.70	-0.22
HWM 9	26.29	26.49	0.20
HWM 10	26.98	26.70	-0.28
HWM 11	26.28	26.50	0.22
HWM 12	26.91	26.70	-0.21

Table 4.3. Overview of the average differences between measured and simulated results of the hydrograph time series at all monitoring stations in the inundated area (see also Figure 4.17a-c).

Station	Difference	Station	Difference
HP 1 alt	-0.35 m	HP 7 alt	-0.34 m
HP 2 alt	-0.39 m	HP 7	-0.49 m
HP 3	-0.30 m	HP 10a	-0.34 m
HP 4 alt	-0.28 m	HP 12	0.10 m
HP 5 alt	-0.36 m	W6918200	-0.16 m
HP 6 alt	-0.36 m		
Average (all monitoring stations)		-0.30 m	

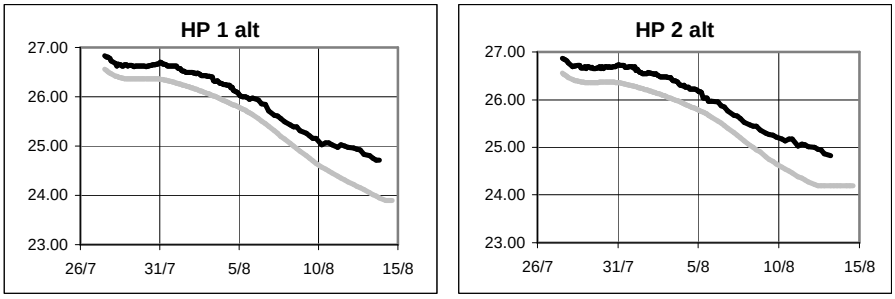

Figure 4.17a. Comparison between the measured (black line) and simulated water level (grey line) at station HP 1 alt (left) and at station HP 2 Alt (right). The Average differences are respectively 0.35 m and 0.39 m.

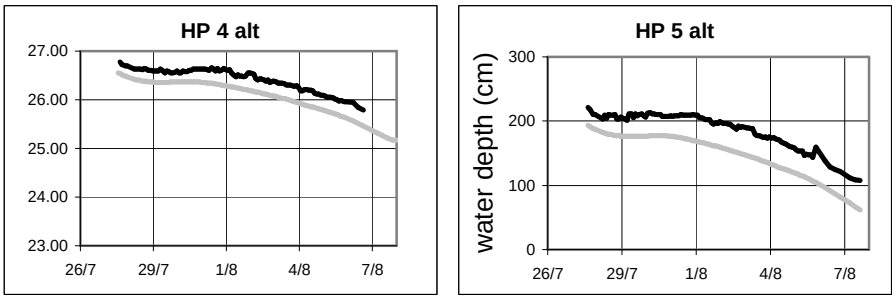

Figure 4.17b. Comparison between the measured (black line) and simulated water level (grey line) at station HP 4 alt (left) and at station HP 5 Alt (right). The Average differences are respectively 0.28 m and 0.36 m.

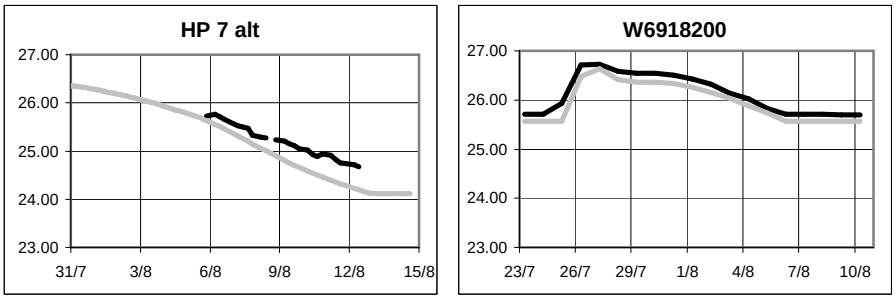

Figure 4.17c. Comparison between the measured (black line) and simulated water level (grey line) at station HP 7 alt (left) and at station W6918200 (right). The Average differences are respectively 0.34 m and 0.16 m.

4.8 Discussion

In general the model results correspond well with the observed data. This proves the capability of the Delft-FLS to simulate floods accurately, although there are some differences between observed and simulated values that need further attention:

- After July the 26th the simulated downstream hydrograph under-estimated significantly the measured downstream hydrograph. Further calibration could not improve this fact – see Figure 4.13.
- For most validation stations the simulated levels are lower than the observed levels with an average difference of 21 centimetres for the high-water marks and 30 centimetres for the time-series. The greatest average difference is almost half a meter for the time series at station HP 7.

The possible reasons for these differences will be discussed next.

Water balance

Figure 4.18 shows the measured upstream- and downstream discharges of the Oder, as well as the computed downstream discharge. It shows that at the moment at which the draining of the *Ziltendorfer Niederung* starts (in the night of the back-burst in the Brieskower See dikes), the simulated curve underestimates the measured curve. This difference reaches almost 150 m^3/s at its maximum. If the draining of the *Ziltendorfer Niederung* is simulated too slowly, then it is expected that the initial underestimation would gradually change into an overestimation. Figure 4.18 shows that this does not happen. Around August 9th the two curves coincide, but from there on the simulated hydrograph does not give higher discharges than the measured hydrograph to compensate for its earlier underestimation.

Figure 4.19 shows that in the time period of the simulation a total (cumulative) volume of 4.00 10^9 m^3 water has come into the study area from upstream at the Southern (upstream) boundary. In the simulations 4.08 10^9 m^3 water has flown out of the area at the Northern, downstream boundary. The fact that more water (a volume of 0.08 10^9 m^3) has left the area is due to change in storage in the Oder: at the start of the simulations the water level was high (discharge approximately 2000 m^3/s) – and was lower at the end (discharge approximately 400 m^3/s). Based on an analysis of the DTM, this change of storage is estimated to be 0.06 10^9 m^3 which corresponds well with the observed difference. According to the "measured" cumulative graph a total amount of 4.28 10^9 m^3 water has left the area at the downstream boundary equals. The difference of 0.28 10^9 m^3 is too big to be

explained by the change in storage in the Oder riverbed. More water has flown out of the area than can be accommodated for by the inflow or by storage change. In the following sections several possible sources of errors are further examined.

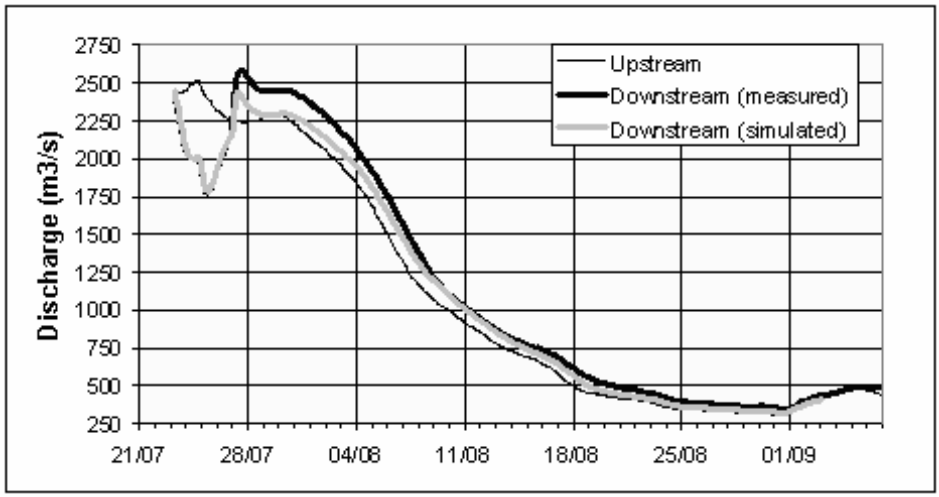

Figure 4.18. The measured and simulated discharges of the Oder

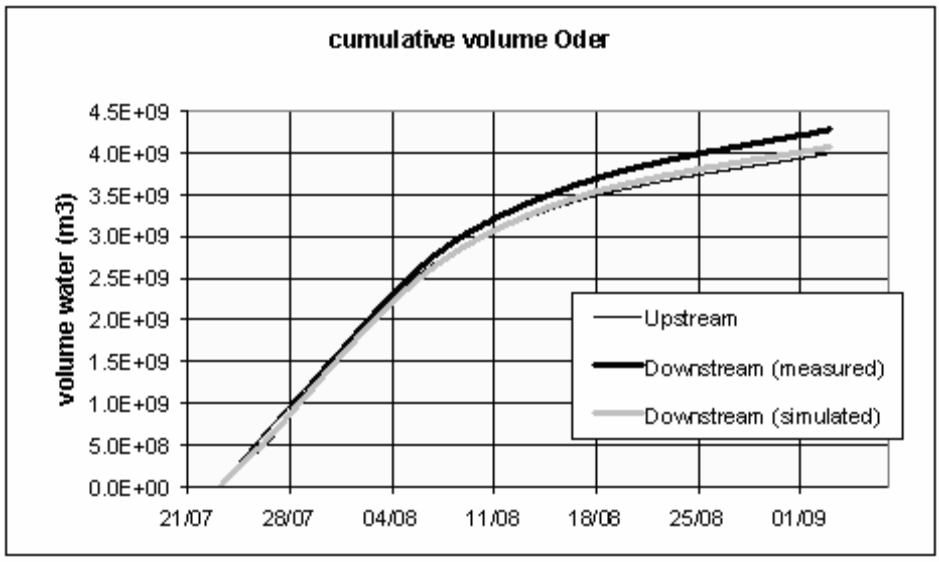

Figure 4.19. Cumulative volume entering the study area (upstream) and leaving (downstream)

Sources of error

The Q-h relation. Further inquiries at the authorities revealed that the downstream Q-h relation was not the site specific relation for Frankfurt an der Oder, but the transposed relation of Eissenhüttenstadt. As a consequence this false Q-h relationship "forces" to model to discharge 0.28 10^9 m^3 too much downstream (about 7 % too much). This will mean that for the model, there is less water available to be stored in the *Ziltendorfer Niederung*, which will result in an underestimation of the maximum water levels. If the error in the rating curve is linear over all discharges, the volume of water stored the Niederung would also be 7% higher. The maximum stored volume in the *Ziltendorfer Niederung* was 127 10^6 m^3. 7% of this value is 8.9 10^6 m^3 over a surface area of 49 10^6 m^2 (4879 ha) would add 18 centimetres to the water level.

Resampling the DTM. Assuming that the LIDAR DTM with a grid resolution of 2.5 meters, contains no errors, it can be calculated that at the moment of maximum inundation extent, 183 $\cdot 10^6$ m^3 water was stored in the *Ziltendorfer Niederung* and in the Oder. The same analysis with the 30 meter DTM gives a maximum stored volume of 186 $\cdot 10^6$ m^3. Thus, resampling the DTM to a coarser grid resulted in a overestimation of the retention capacity of the *Ziltendorfer Niederung* of 3.2 $\cdot 10^6$ m^3. Because the total area of the water surface (*Ziltendorfer Niederung* + Oder) is 62 $\cdot 10^6$ m^2, this error accounts for an underestimation of the water level of 5 cm.

Water already in the *Ziltendorfer Niederung*. Before the inundation of the *Ziltendorfer Niederung* there was already some water stored in canals and ponds. This water was not considered in this study. The *Landesumweltamt* Brandenburg estimated that this storage would add up to about 1.0 $\cdot 10^6$ m^3. This would account for an underestimation of the maximum water level of approximately 2 cm.

Wind. Wind pushes the water up to a higher level by its drag-force. A wind-speed of 20 m/s over a stretch of water of 10 km and 1 m deep, with a Cd coefficient at the air-water interface of 0.002 can cause a wind set-up of 1 m (Stelling 2000). A value of 20 m/s is equivalent to wind force 8 on the Beaufort scale. However, the weather was not particularly windy in the study area at the time of the flooding (*Landesumweltamt* Brandenburg – Mrs. M. Gierk, oral communication). The estimated wind-force Beaufort 3 – an average wind-speed of approximately 5 m/s – would result in a set-up of maximum several centimetres. Furthermore, wind

push-up would show a spatial trend (higher water levels in one part and lower water levels in anther part), due to the wind direction. This trend was not observed.

Waves. The high-water marks are registered as the line between the wetted (dirty) and dry (clean) surface on particular objects – and are recorded after the floodwater has receded. Waves may result wetting lines that are several centimetres above the average water surface. It is unknown if this type of error also applies to the monitoring stations.

Vertical fluxes. The analysis did not include vertical input of water due to rain or loss due to infiltration and evaporation. If there would have been a lot of precipitation, this might have added several centimetres to the measured water level. But during the inundation of the *Ziltendorfer Niederung* the weather was warm and summer-like with no significant rainfall. In fact, if evapotranspiration and infiltration were dominant the model should have over-estimated the water levels.

Volume of objects, trees, crops etc. In the DTM that was used, objects like trees, cars, walls of houses, crops etc. were not included. It was calculated that for an increase of 1 cm, a volume of 600.000 m^3 of solid objects is required. Because it seems unlikely that a volume of this magnitude was present in area, this source does not seem like a serious candidate to explain the difference.

Reading errors. For the reading of the high-water marks there could be two sub-sources for error: 1) The reading itself and 2) the transformation of these readings to absolute levels in the DHHN92 reference system. For the high-water marks, both types of errors can easily be made, however it unknown how the reading was done at the monitoring stations.

4.9 Conclusion

This study shows that the 2D-model Delft-FLS is a useful and accurate tool. Even though the model results do not fully coincide with the validation dataset, it is shown that a significant part of the differences can be attributed to error sources within the dataset. It was also possible to reconstruct the evolution of the dike

breaches and to obtain realistic values for the surface roughness during the calibration process. Especially the reconstruction of the breach evolution is important, because little information on this topic is known.

It is concluded from the water balance that the discharge at the downstream boundary is overestimated, resulting in a water balance error of 0.28 10^9 m^3 water, or 7% of the total water volume. This explains why it was not possible to make the simulated downstream hydrograph completely coincide with the measured discharge curve of Frankfurt a/d Oder. The model had "released" too much water during the first part of the simulation and had not enough water in storage to supply the peak and the receding limb of the graph. The fact that the two curves coincide neatly in the first part of the graph is due to over-calibration of the evolution of the first two breaches.

The overestimation of the downstream discharge is due to an inaccurate rating curve. This inaccuracy partly explains the observed underestimation of the water levels compared to the validation dataset. Other significant sources of errors are: the resampling of the DTM (error ca. 5 cm), water already in present in the *Ziltendorfer Niederung* before the inundation (error ca. 2 cm), wind and wave action and reading errors.

Chapter 5 Scenario-studies for the *Ziltendorfer Niederung* flood

The successful reconstruction of the Ziltendorfer Niederung flood described in the previous chapter, triggered several questions. The regional authorities showed interested on what would have happened if the sequence of events would have been different. This chapter is dedicated in answering their questions.

Abstract

The reconstruction of the *Ziltendorfer Niederung* flood with Delft-FLS, demonstrated how a series of dike breaches resulted in the inundation of the area. This triggered several questions at the Brandenburg Authorities to gain a better understanding of the flood event. This chapter seeks answers to their "what-if" questions to investigate what would have happened under different circumstances. It is concluded that the dikes would not have been overtopped and that the *Ziltendorfer Niederung* would not have been flooded had the dikes not failed. It is also concluded that for the maximum water depth and flood extent, it did not really matter if there was one or two dike breaches. Also the timing of the breaching did not have a big effect on the flood characteristics in the *Ziltendorfer Niederung*. It did however, have significant impact on the downstream discharge and water levels in the Oder River.

Increasing the surface roughness in the river bed in the stretch along the *Ziltendorfer Niederung* will not decrease water levels in the river downstream, but will result in higher water levels in this river stretch, increasing the probability that the dikes will be overtopped. If the back-bursts that caused a sudden release of water back into the Oder could have been prevented, there would have been no surge of water downstream and this would have had a positive effect on the flood consequences downstream.

5.1 Introduction

In the previous chapter Delft-FLS was used to reconstruct the 1997 Oder flood in the *Ziltendorfer Niederung*, Germany. This reconstruction of the flood event improved the understanding of the dynamics of the inundation. The flood model generated information on the spatial distribution of flow velocities and energy distribution in the flowing water. It also showed how the floodwater propagated through the area and how surface elements like embankments, canals and tunnels directed the water flow. Based on the reconstruction in the previous chapter, this chapter will look deeper into several "what-if"-scenarios, to answer questions like, what would have happened if the dikes wouldn't have failed, or what if the surface roughness coefficients are changed? Answering these questions is not only relevant for areas that have experienced a flood, but is relevant for any area that is exposed to flood hazard. The "what-if" -scenarios in this chapter were developed in close collaboration with the *Landesumweltamt* Brandenburg.

5.2 Definition and evaluation of the different flood scenarios

In this study, the following four scenarios are defined in close collaboration with the Brandenburg Authorities. The scenarios are simulated with Delft-FLS, using the same model settings as described in the previous chapter. The results of the scenarios are compared with the results of the 1997 flood reconstruction

Z0 Reconstruction of the 1997 inundation

The Z0 scenario is the detailed reconstruction of the 1997 inundation of the *Ziltendorfer Niederung* based on the extensive calibration and validation dataset that was provided by the Brandenburg authorities. This reconstruction is described in detail in the previous chapter.

Z1 No dike breaches

This scenario is similar to Z0, with the exception that there are no dike breaches. The aim of tis scenario is to see what would have happened then. Would they have been overtopped and if so, where? What would have been the consequences for the downstream hydrograph?

Z2 Only the first dike breach

This scenario examines the consequences in case only the first dike breach would have occurred. The evolution of the 1st dike breach is the same as described in Chapter 4. The aim is to see if there would have been significant differences if the 2nd and 3rd breaches could have been prevented. What would the consequences be for the filling in of the *Ziltendorfer Niederung* in terms of speed and rising of the water level? And what would the downstream curve look like?

Z3 Different timing of the first dike breach

This scenario examines the consequences of a different timing of the first dike breach. The aim is to see the consequences for the downstream water levels and for the filling in of the *Ziltendorfer Niederung*. The new 1st breaching was simulated at 21/07/1997 at 15:00, 42 hours before the actual breach when the discharge at Eissenhüttenstadt reached 2300 m^3/s. The second breach and the three consecutive back-bursts are not simulated.

Z4 No dike breaches but increased roughness of the winter bed

This scenario looks deeper into the effects of increasing the surface roughness in the Oder river bed. The aim is to see if this will delay the flood wave and reduce the water levels downstream and to see what will be the consequences for the *Ziltendorfer Niederung*. In this scenario there are no dike breaches.
The surface roughness coefficient of the Oder winter bed (the frequently flooded part of the Oder floodplain between the dikes) was increased with 50% from 0.032 to 0.048 (Manning's coefficients).

To evaluate the different scenarios, the model results were compared. This was done for: 1) the effects for the Oder River hydrograph downstream and 2) for the inundation of the *Ziltendorfer Niederung*. The river characteristics that were evaluated are: 1) downstream discharge, 2) water levels at various locations along the Oder, and 3) margin between maximum water level in the Oder and the dike heights. The effect of the different inundation scenarios for the *Ziltendorfer Niederung* were assessed by comparing: 1) maximum inundation depth, 2) maximum flow velocity, 3) maximum impulse, 4) maximum speed of rising of the water level, 5) flood propagation / warning time, and 6) estimated duration.

5.4 Comparison of the effects on the Oder River.

Downstream discharges

Figure 5.1 shows the simulated curves of the downstream discharges. The curve Z0 is the calibrated curve of the 1997 reconstruction. Table 5.1 gives the maximum peak discharge for each scenario.

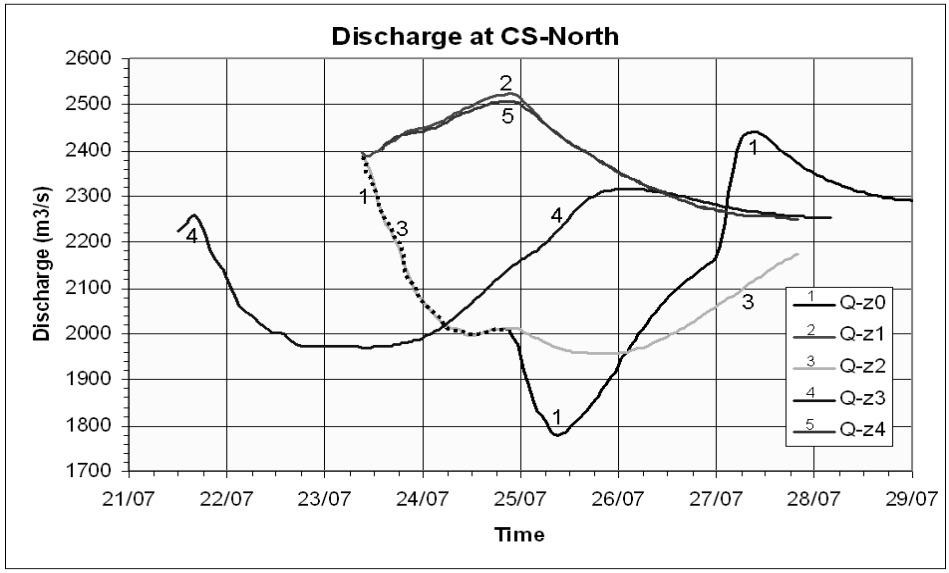

Figure 5.1. The downstream discharges of the four scenarios compared with the calibration scenario (Z0).

Table 5.1. Peak downstream discharge.("real" gives the measured peak discharge at the station of Frankfurt a/d Oder)

	Peak Discharge	Time	
Real	**2584 m³/s**	**27/07/1997**	**11:00**
Z0	2482 m³/s	27/07/1997	10:00
Z1	2523 m³/s	24/07/1997	22:00
Z2	2454 m³/s	23/07/1997	09:00
Z3	2317 m³/s	26/07/1997	01:00
Z4	2508 m³/s	24/07/1997	20:00

Z1 No dike breaches

The simulation started on the 23rd of July at 9 am, at the time the first dike breach started. The results of this scenario showed that had there been no dike breaches, the dikes would not have been overtopped: the *Ziltendorfer Niederung* would not have been flooded. The shape of the downstream curve is thus similar to that of the upstream curve with a delay of approximately 12 hours.

Z2 Only the first dike breach

The downstream discharge calculated in this scenario is identical to the discharge in the Z0 scenario, until the moment of the second breach in Z0. Instead of a rapid decrease of discharge and water levels (as in Z0), the discharge in this scenario reduces slowly another 50 m3/s. The minimum discharge is reached in the night of the 25th to the 26th of July. The simulation was stopped on the evening of the 27th of July, while the discharge was rising again. It can be assumed that the discharge after the 28th would decrease again, with a higher discharge than the Oder discharge at CS-South (Frankfurt a/d Oder) due to the draining of the *Ziltendorfer Niederung*. The absence of back-bursts in this scenario prevents a surge of water into Oder.

Z3 Different timing of the first dike breach

Scenario Z3 has the lowest peak discharge – about 10 % less than all other scenarios. This is due to the timing of the first breach. By opening the *Ziltendorfer Niederung* before the Oder reaches its maximum discharge at Eissenhüttenstadt, the hydrograph is cut off. The breach evolution in this scenario is the same as the one found during the calibration for the first breach. It might even be possible (not checked in this study) that a different opening procedure would result in a further reduction of the downstream peak discharge. Also in this scenario the absence of the back-bursts prevents the surge of water into the Oder.

Z4 No dike breaches but increased roughness of the floodplain

In scenario Z4 the increased surface roughness does not affect the discharge of the Oder – the hydrograph nearly coincides with scenario Z1, but not completely because in the southern part of the *Ziltendorfer Niederung* the dikes are overtopped and a (relatively) small amount of water enters the Niederung (see also next section). The peak discharge of scenario Z4 is 15 m^3/s less than that of scenario Z1. There is no shift in the timing of the peak discharge.

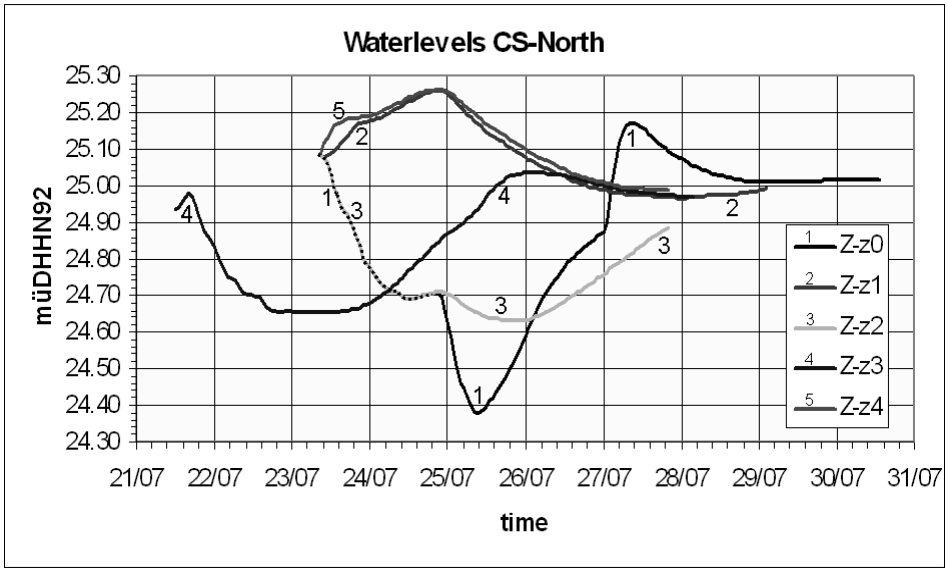

Figure 5.2. The downstream water levels of the four scenarios compared with the calibration scenario (Z0).

Table 5.2. Maximum simulated water levels in the Oder (in meters above the reference level - DHHN92). For the location of cross sections see Figure 5.3. Note that the Z4 scenario overtops the dike at two cross sections (indicated in bold print).

Cross Sections (CS)	**Dike height**	Z0	Z1	Z2	Z3	Z4
Oder at CS-South	**33.04**	32.44	32.46	32.44	32.44	33.01
Oder at CS-Ziltendorf	**31.87**	31.37	31.42	31.42	31.42	**31.89**
Oder at CS-Aurith	**30.10**	29.59	29.69	29.59	29.57	**30.10**
Oder at CS-Kunice	**29.02**	28.13	28.21	28.13	27.96	28.58
Oder at CS-Rybocice	**27.55**	26.48	26.56	26.48	26.28	26.76
Oder at CS-North	**26.40**	25.19	25.26	25.19	25.04	25.26

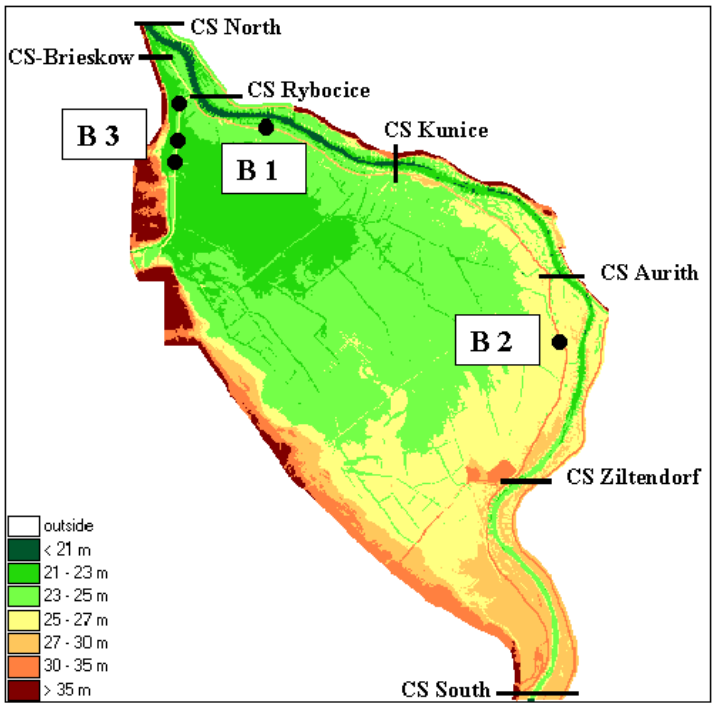

Figure 5.3. Elevations in the study area (in meters above sea-level DHHN92) with the location of the breaches (B1 to B3) and the location of the seven cross-sections.

Water levels and margin with the dike crest

The discharges of the different scenarios vary. This means that also the water levels of the scenarios will be different. Table 5.2 shows the maximum water level of the five scenarios at several cross-sections in the Oder (for the location of the cross-sections, see Figure 5.3). Figure 5.2 shows the variation of the water levels during the flood event. Figure 5.4 shows the margin between the maximum water level and the heights of the dikes on the German side of the Oder.

Z0

The consecutive dike breaches resulted in a reduction of the Oder water level at cross-section North (downstream boundary) to a level of 24.39 meters above sea-level (DHHN92). However, the back-bursts caused a surge of water into the Oder resulting in a maximum simulated water level of 25.17 meters.

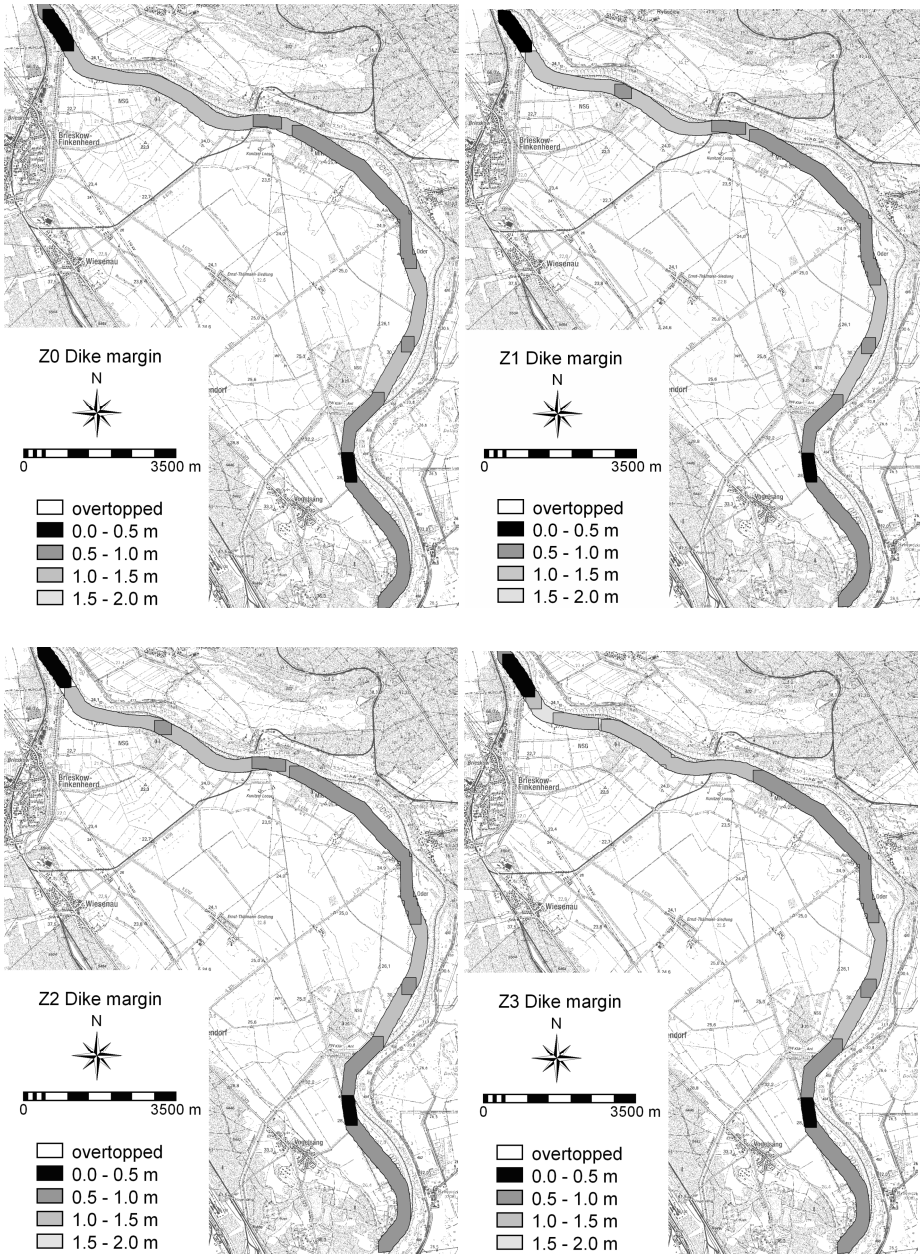

Figure 5.4. Margins between dike heights and maximum simulated water levels in the Oder River.

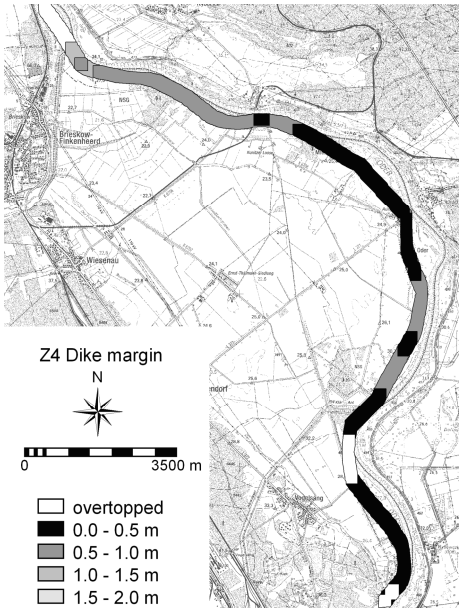

Figure 5.4 (continued). Margins between dike heights and maximum simulated water levels in the Oder River.

Z1 No dike breaches

With no dike breaches, the maximum water level in the Oder will rise approximately 5 to 10 centimetres higher that the maximum water level of scenario Z0. This will not result in an overtopping of the dikes.

Z2 Only the first dike breach

The scenario with only the first dike breach gives a maximum water level almost equal to the water level in scenario Z0. The minimum water level in the Oder is reduced to 24.63 meters above sea-level (DHHN92), approximately 25 centimetres higher than Z0. The maximum water level at downstream boundary was reached at the moment of the first breach: 25.19 meters – similar to the Z0-scenario.

Z3 Different timing of the first dike breach

The early opening of the dikes at the location of breach 1 results in a temporary reduction of the Oder water level of 30 centimetres to a level of 24.66 meters above sea-level (DHHN92). When the *Ziltendorfer Niederung* fills up, the water level downstream rises to a maximum level of 25.04 meters.

Z4 No dike breaches but increased roughness of the floodplain

Increasing the surface roughness results in a rise of the Oder water level of approximately half a meter, especially in the southern part of the Oder in the study area. In fact, near the cross-section "*Ziltendorf*" (Figure 5.3) the Oder overtops the dikes and water enters the *Ziltendorfer Niederung*.

Table 5.3. Summary of the inundation of the Ziltendorfer Niederung.

	Z0	Z1	Z2	Z3	Z4
Area (ha)	4879	0	4881	5008	184
Water-level (m.a.s.l.)	26.68		26.71	26.80	-
Total flood volume ($10^6 m^3$)	126.9	0	127.7	133.1	0.804
Time of max. depth (hours)	90	-	109	106	43 - 109
Average depth (m)	2.60	-	2.62	2.66	0.44
Max depth (m)	5.73	-	5.75	5.84	5.35
Max velocity (m/s)	3.07	-	2.99	2.83	1.72
Max impulse (m^2/s)	4.94	-	3.13	2.97	1.82
Max rising (m/h)	2.47	-	1.82	1.73	1.64

5.5 Effects on the inundation of the Ziltendorfer Niederung

In the scenario Z1 – no dike breaches – the dikes were not overtopped so no results for this scenario are shown in this section. In all other scenarios the *Ziltendorfer Niederung* was (partially) flooded. Table 5.3 shows that scenarios Z0, Z2 and Z3 are very similar with respect to total inundated area and in volume water stored. In the Z0 scenario the maximum water level is reached after 90 hours. In the scenarios with one breach the largest extent of the inundated area is reached after 109 and 106 hours, respectively. This means the *Ziltendorfer Niederung* fills faster when there are two dike breaches. This is also reflected in higher speed of rising, velocity and impulse. The five parameter maps for each scenario, except for scenario Z1, are shown and shortly described in the following sections.

Maximum water depth

The maps of maximum water-depth of scenarios Z0, Z2 and Z3 are very similar (see Figure 5.5). Apparently the location, number and timing of the dike breaches doesn't have a significant effect on the inundation depth. Only the Z4 scenario gives different results. Due to the increased roughness in the Oder-bed, the flow experiences more resistance, which results in higher water levels. Near cross-section "*Ziltendorf*" (Figure 5.3) a relatively small, but continuous amount of water from the Oder overtops the dikes and enters the *Ziltendorfer Niederung*. The dikes are also overtopped at the southern border of the study area, near Eissenhüttenstadt (see Figure 5.4) but this has no further consequences for the *Ziltendorfer Niederung* due to the presence of secondary dikes and embankments. In the Z4 scenario, the flood water propagates from South to North, contrary to the other scenarios It is at first blocked by the embanked road that connects a waste disposal site with higher ground near Vogelsang but in the evening of July 24th the flood propagation continues through the Pottack bridge. In the Z4 scenario the water depths do not reach higher than 1 meter in most parts of the inundated area. In the scenarios with a breach, the water depths are far greater, with the largest part of the area being submerged under more than 1.5 meters of water. The total stored volume of the Z4 scenario is less than 1 percent of the scenarios with a dike breach – see Table 5.3, and the area affected less than 4%.

Table 5.4. Surface area (ha) per depth class

Depth (m)	**Z0**	**Z1**	**Z2**	**Z3**	**Z4**
0.0 – 0.2	52	0	56	61	59
0.2 – 0.5	96	0	98	129	67
0.5 – 1.0	319	0	317	321	39
1.0 – 1.5	540	0	522	496	14
1.5 – 2.5	1288	0	1273	1245	8
2.5 – 3.5	1382	0	1383	1384	1
> 3.5	1199	0	1226	1324	0
Total	4876	0	4873	4960	188

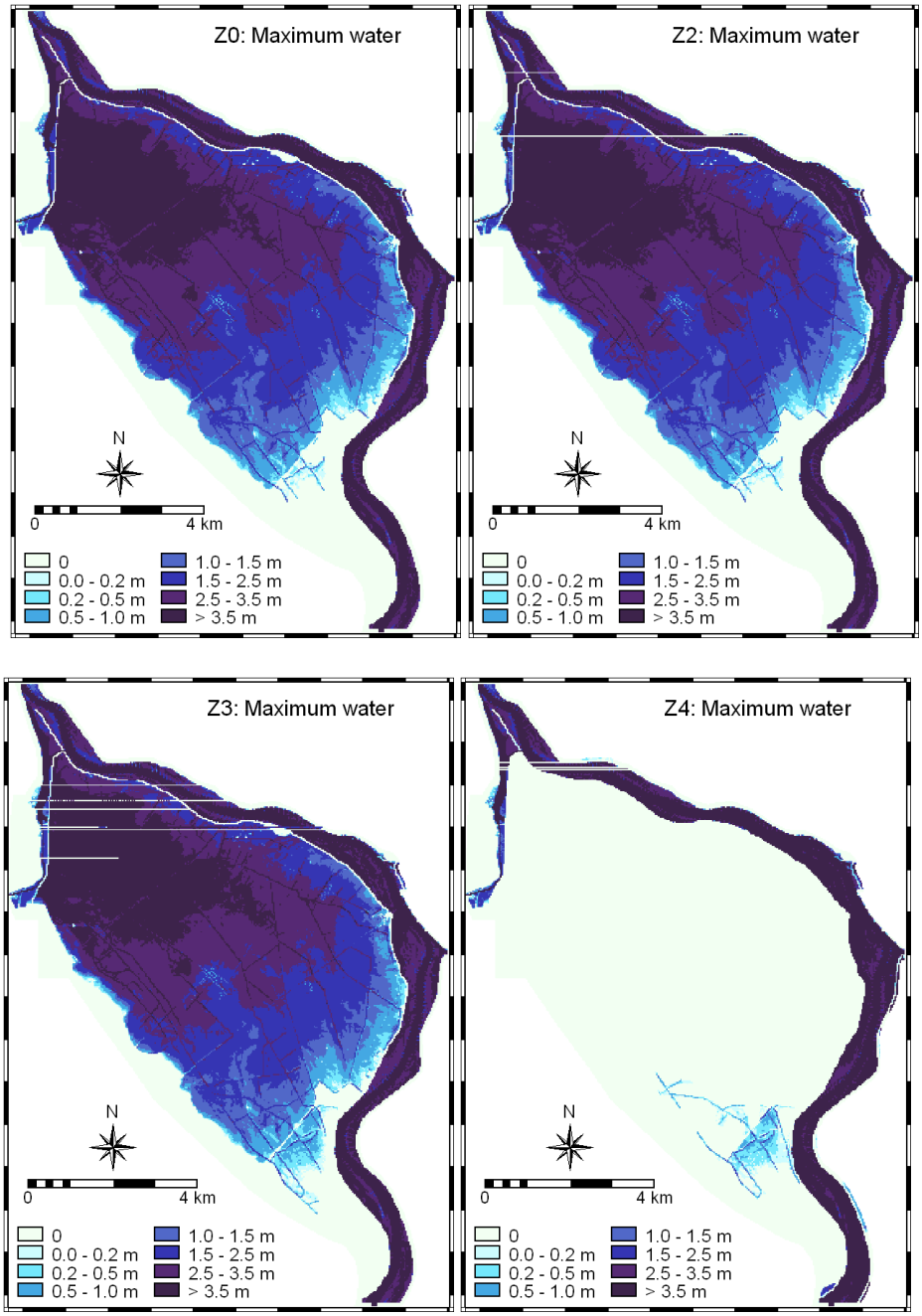

Figure 5.5. The spatial distribution of the maximum water depth of the four scenarios that resulted in the inundation of the Ziltendorfer Niederung: clockwise scenarios Z0 (top left), Z2, Z3 and Z4

Maximum flow velocity

Figure 5.6 shows the distribution of the flow velocity for scenarios Z0, Z2, Z3 and Z4. For most of the inundated area the flow velocities don't rise above 0.30 m/s. Higher velocities are found behind the breaches and near the location where the dikes are overtopped in scenario Z4. Table 5.5 and Figure 5.6 show that in scenario Z0, a larger area of the *Ziltendorfer Niederung* experiences higher flow velocities than the other scenarios. This can probably be attributed to the occurrence of the second dike breach which reactivated the flow of water through the area. In the Z0 scenario nearly 40% percent of the area experiences water velocities higher than 10 centimetres per second, whereas in the Z2 and Z3 scenarios, with only one breach, this percentage is less than 30. In scenario Z4 the flow velocities are much lower (<1 m/s).

Table 5.5. Maximum flow velocity – surface area (ha) per velocity class

Flow velocity (m/s)	**Z0**	**Z1**	**Z2**	**Z3**	**Z4**
< 0.01	256	0	381	344	7
0.01 – 0.1	2792	0	2872	2990	91
0.1 – 0.3	1472	0	1311	1318	80
0.3 – 0.5	235	0	241	243	9
0.5 – 1.0	101	0	55	54	1
1.0 – 2.0	18	0	11	10	0
> 2.0	2	0	1	1	0
Total	4876	0	4873	4960	188

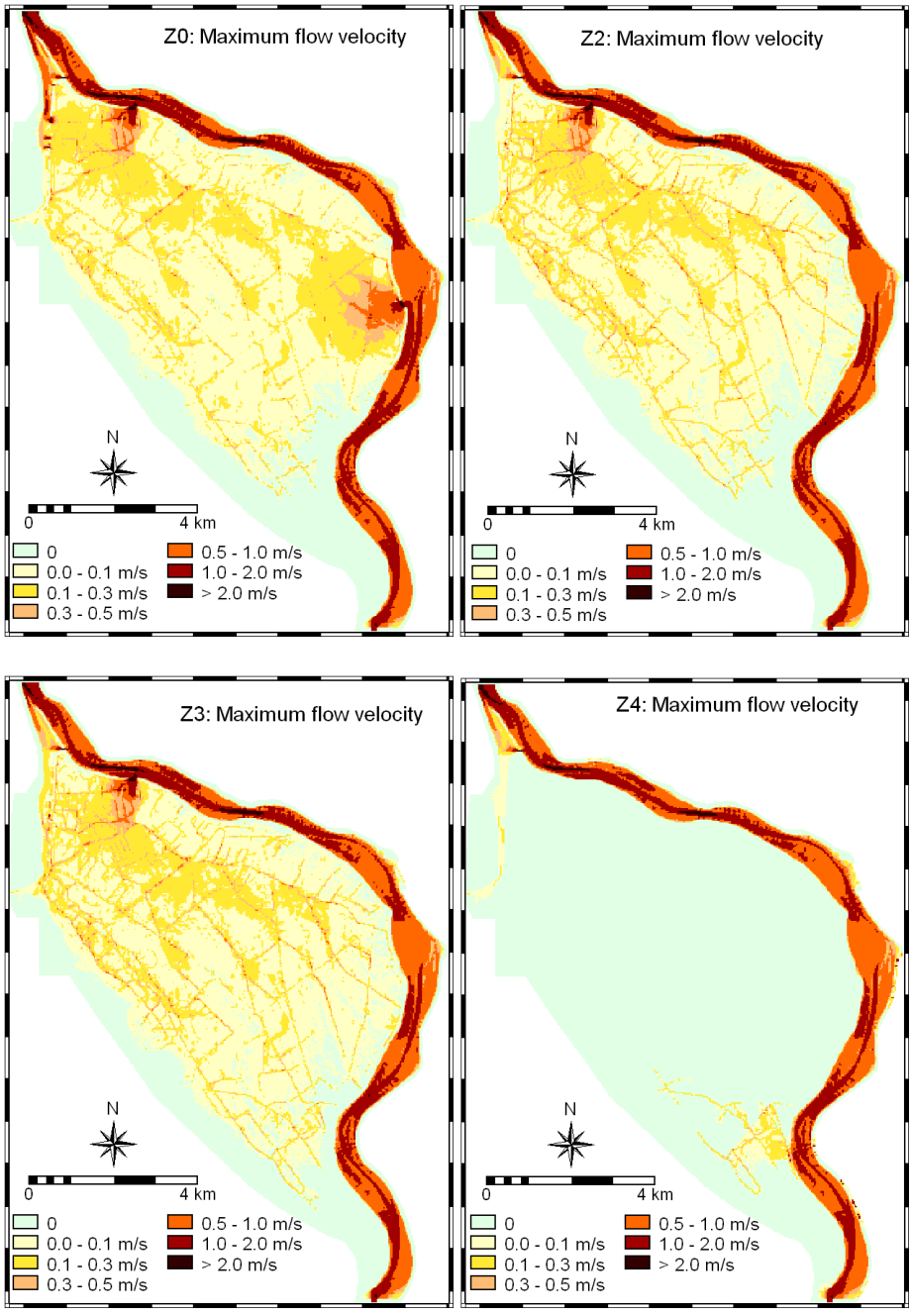

Figure 5.6. The spatial distribution of the maximum flow velocity of the four scenarios that resulted in the inundation of the Ziltendorfer Niederung.

Maximum impulse

Figure 5.7 shows the spatial distribution of the maximum impulse in the *Ziltendorfer Niederung*. The observations that were made for the flow velocity are also applicable to impulse, only even more pronounced. The area that suffered impulses over 0.10 m^2/s is 57% in the Z0 scenario, compared to 22%, 21% and 3% for the Z2, Z3 and Z4 scenarios respectively. The occurrence of the second breach triggered the displacement of a large volume of water, creating strong currents that may increase the risk of drowning and of structural damage to buildings. In the scenarios with one breach stronger currents are only found near the breach location. The absence of impulses over 0.1 m^2/s in scenario Z4 shows that the high flow velocities at the location where the dike was overtopped, were not accompanied by great water depths.

Table 5.6. Maximum impulse – surface area (ha) per impulse class

Impulse m . m/s	Z0	Z1	Z2	Z3	Z4
< 0.01	103	0	228	188	19
0.0 – 0.1	2053	0	3589	3728	158
0.1 – 0.2	1788	0	771	763	8
0.2 – 0.3	474	0	158	153	2
0.3 – 0.4	182	0	51	48	1
0.4 – 0.8	220	0	57	59	0
> 0.8	51	0	19	19	0
Total	4876	0	4873	4960	188

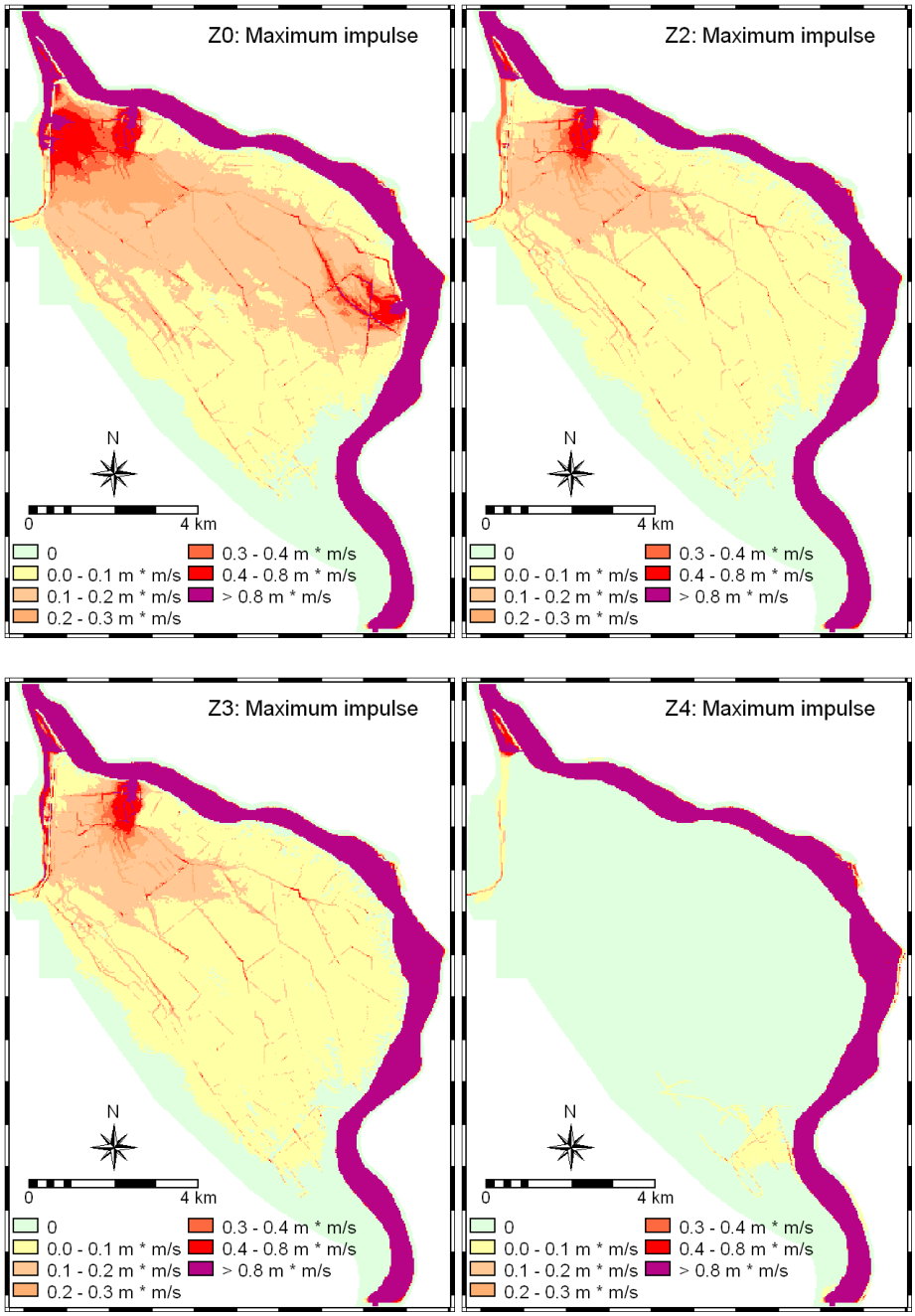

Figure 5.7. The spatial distribution of the quantity of movement (impulse) in the four scenarios that resulted in the inundation of the Ziltendorfer Niederung.

Maximum speed of rising of the water level

Figure 5.8 shows the spatial distribution of the maximum speed of water level rising. In Table 5.7 and Figure 5.8 can be seen that for all scenarios the water levels rises with a maximum speed of less than 30 cm per hour in approximately 90% of the inundated area. In scenario Z0 the area where the water level rises between 10 and 30 centimetres per hour is larger than in the other three inundation scenarios. This reflects the faster filling of the *Ziltendorfer Niederung* due to the two breaches compared to the one breach in scenarios 2 and 3 and overtopping in scenario Z4. In the lowest areas in the northern part of the *Ziltendorfer Niederung* the water level can rise as fast as 75 to 100 centimetres in 1 hour.

Table 5.7. Maximum rising of the water level – surface area (ha) per class speed of rising

Rising (m/h)	**Z0**	**Z1**	**Z2**	**Z3**	**Z4**
<0.01	5	0	0	0	6
0.01 – 0.1	2073	0	2300	2415	106
0.1 – 0.3	2139	0	1940	1934	51
0.3 – 0.5	371	0	369	350	13
0.5 – 0.75	184	0	177	185	6
0.75 – 1.0	74	0	71	72	4
> 1.0	28	0	23	24	2
Total	4876	0	4873	4960	188

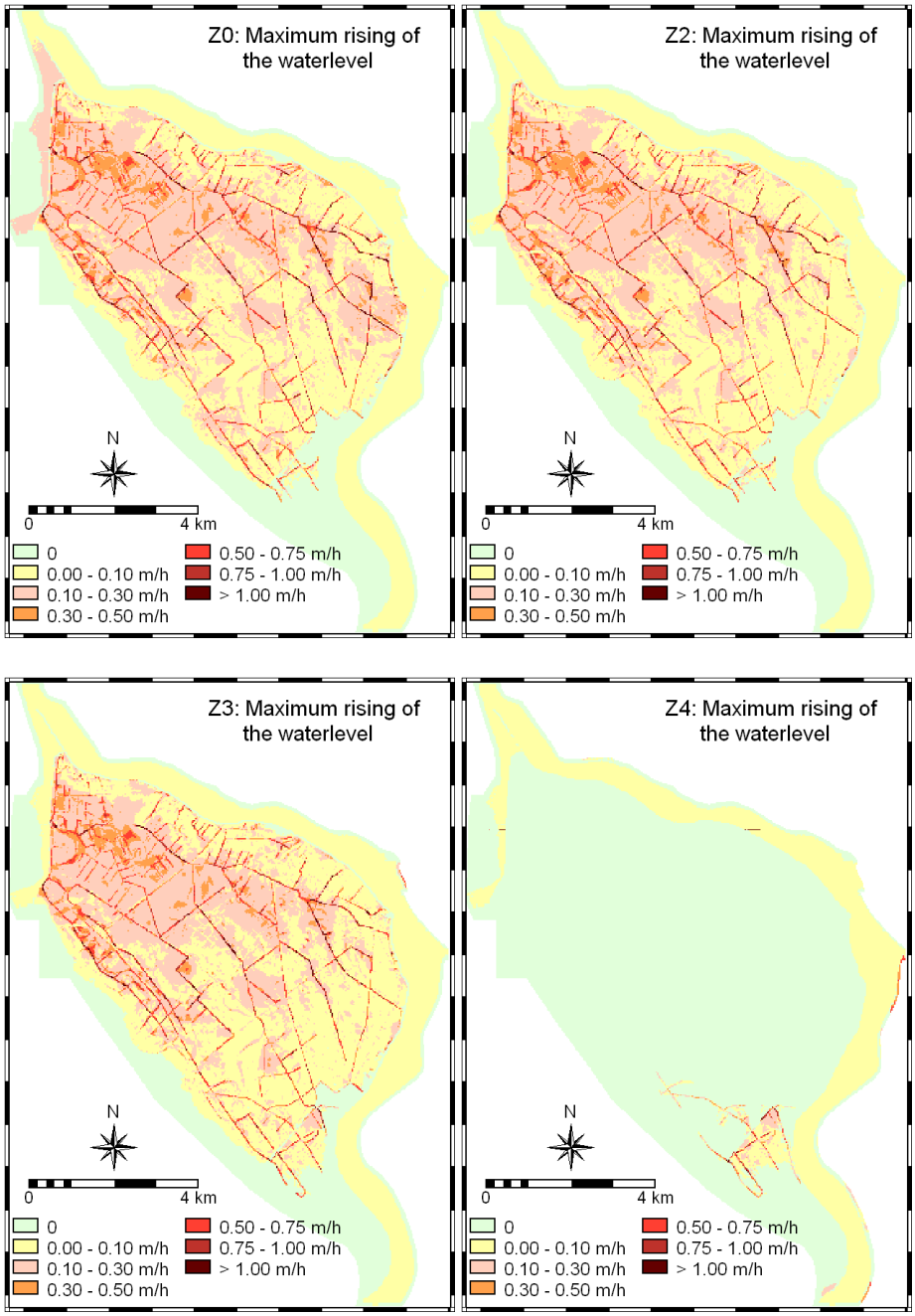

Figure 5.8. The spatial distribution of the maximum speed of rising of the water-level in the four scenarios that resulted in the inundation of the Ziltendorfer Niederung.

Warning time

Figure 5.9 shows how the water propagates through the *Ziltendorfer Niederung*. For scenarios Z0, Z2 and Z3 the time is given in hours after the first breach. For scenario Z4 t=0 corresponds with the moment that the dikes were overtopped. In scenario Z0 almost 90 % of the Niederung is flooded within 48 hours after the first breach. In scenarios Z2 and Z3 around 80 % is flooded at 48 hours. This reflects the faster filling of the *Ziltendorfer Niederung* due to the two breaches.

Table 5.8. Warning time – surface area (ha) per time class

Warning-time (h)	**Z0**	**Z1**	**Z2**	**Z3**	**Z4**
< 3	114	0	77	81	21
3 - 6	322	0	325	321	8
6 - 12	593	0	597	577	14
12 - 24	1354	0	1359	1344	27
24 - 48	2025	0	1703	1675	110
> 48	471	0	825	986	21
Total	4876	0	4873	4960	188

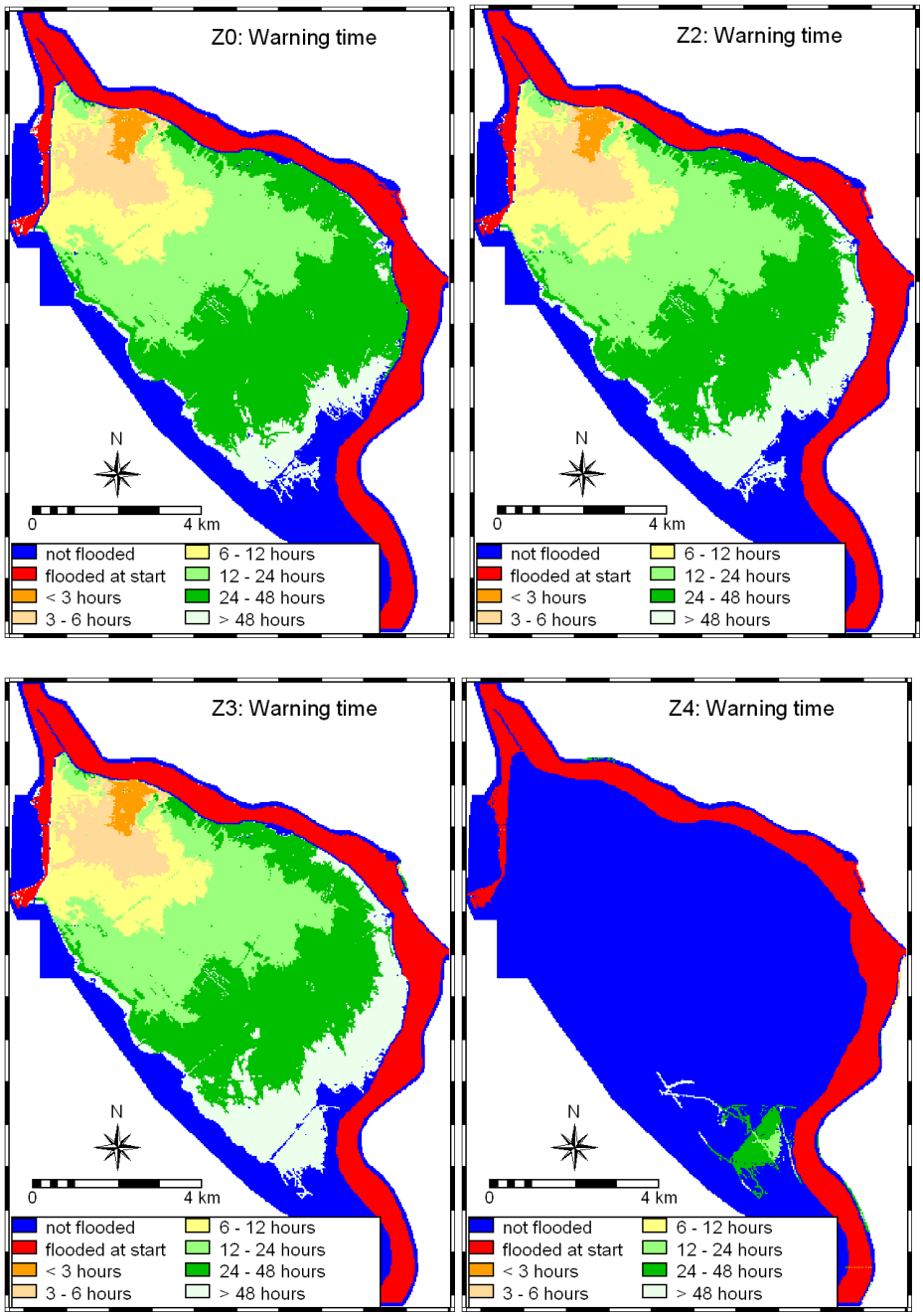

Figure 5.9. The spatial distribution of the arrival time of the first floodwater (warning time) – in hours after the first dike breach (or moment of overtopping).

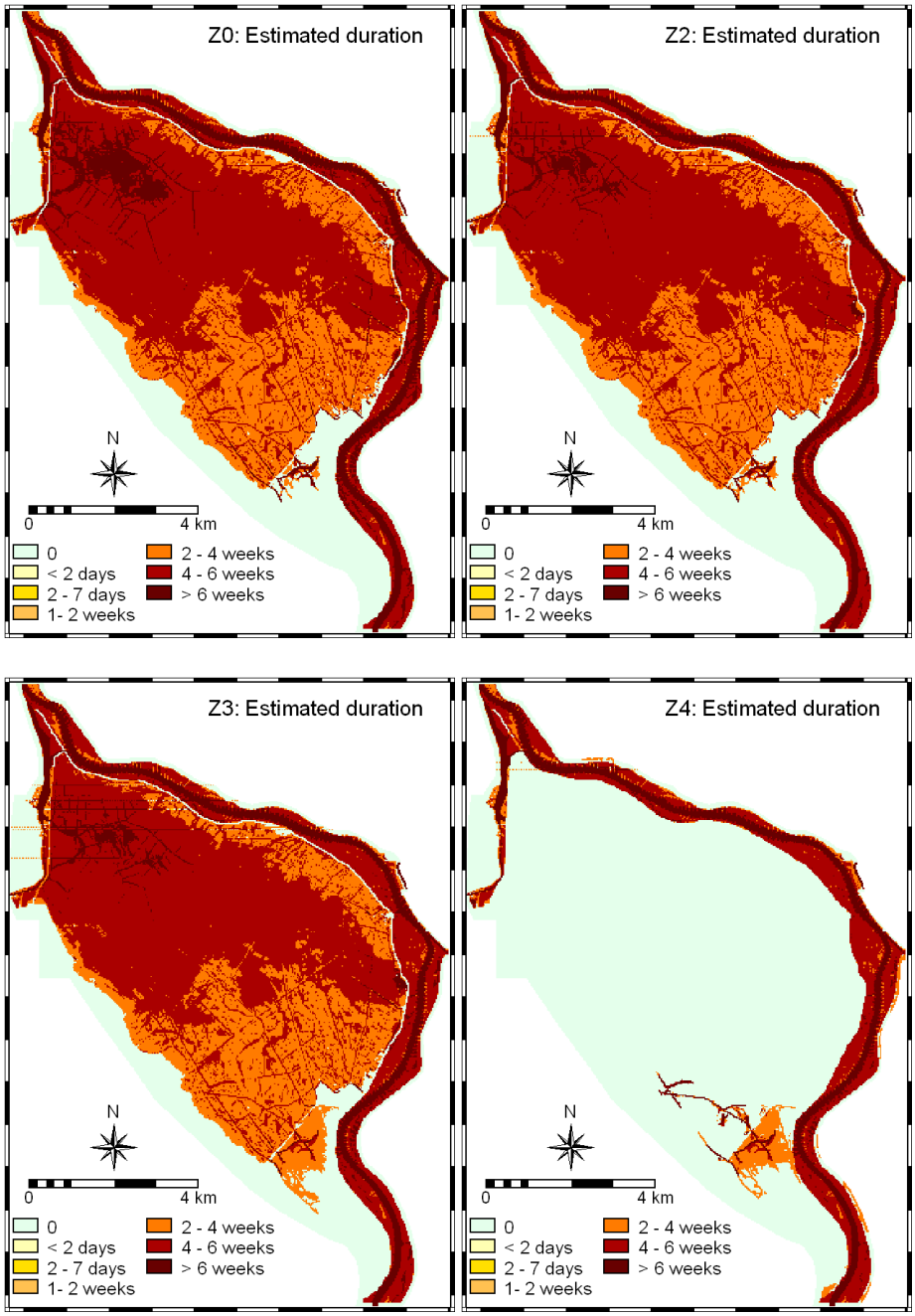

Figure 5.10. The spatial distribution of the estimated duration of the flood – in weeks after the start of the flood event – assuming the water will drain naturally to the river.

Duration

Figure 5.10 shows the estimated duration of the flood for the four scenarios. Again scenarios Z0, Z2 and Z3 give very similar results. Most parts of the *Ziltendorfer Niederung* will be submerged for a period of 2 to 6 weeks. In the lowest parts the duration could be even longer than 2 months because natural draining of these parts is very difficult due to their low elevation. Also the relatively small inundation of scenario Z4 still takes quite long to drain. This is due to the limited drainage capacity of the canals in the area.

5.6 Conclusion

This chapter has demonstrated the usefulness of applying a flood model in order to compare several flood scenarios, using multiple flood parameters. The scenarios were based on real questions by the regional authorities during the evaluation of the flooding event. Through the analysis of "what -if" scenarios it was possible to quantify the effects of the flood event under different circumstances. For example, if there would have been no dikes breach, the *Ziltendorfer Niederung* would not have been flooded because the water level in the Oder would not have overtopped the dike at any location along the Niederung. Another lesson that was learned from these scenario studies is that increasing the surface roughness coefficients in the Oder riverbed did not result in lower discharges at the downstream boundary. This means that this is not a viable solution to reduce the downstream hazard. The only effect of increasing the roughness was a rise of the water level in the Oder, which resulted in overtopping of the dikes at two locations. Another interesting finding was that the timing and the number of breaches don't seem to have a big effect on the total inundated area and the maximum water depth in the *Ziltendorfer Niederung*. For the downstream discharge in the Oder and the related water levels however, the timing and number of breaches are significant as can be seen from the graphs in Figures 5.1 and 5.2. Also the effects of the three back-bursts can be clearly seen. These resulted in a sudden increase of discharge and water levels in the river downstream. The lesson that can be learned from this is that in case of retention areas, one has to be extremely mindful of the potential danger of such a sudden, accidental release to the river, because it increases the problems downstream.

Chapter 6 Flood-risk assessment for EIA

This chapter is a modified version of a paper by Alkema, D. (2003): *Flood-risk assessment for EIA; an example of a new motorway near Trento, Italy. Acta Geologica, Studi Trentini di Scienze Naturali. Museo Tridentino di Scienze Natural – Trento. Vol. 78. pp 147-154*

In the previous chapters, simulated flood events were evaluated by comparing the flood parameter maps. In discussions with regional authorities and institutes that have to provide information to decision makers, however, it became apparent that this is not the kind of information that decision makers need. They need information on the socio-economic consequences of floods and not on water levels. And they need to know how their decisions effect these consequences, for instance if certain measures will significantly reduce flood-risk. Chapter 2 discussed the topic of risk in general terms; this chapter is dedicated to exploring different approaches to quantify the impact of floods to valuate the effects of certain actions. In this case the construction of a motorway.

Abstract

New developments and constructions on an alluvial plain can seriously affect the characteristics of a future flood. 2D flood propagation models can simulate flood scenarios and quantify these changes in flood parameter maps. However, planners and decision makers need information regarding the impact of floods and not regarding changes in water levels. In order to quantify the flood, the flood parameter maps need to be combined with information on the vulnerability and value of the exposed elements. This chapter gives an example how flood parameter maps can be transformed to a spatial flood-risk assessment. Two approaches will be discussed, one to assess economic damage, which can be quantified in monetary terms and one for social risk that expresses the impact in terms of level of disturbance to the people exposed and priority for evacuation. These damage and risk maps show the spatial distribution of the consequences of the flood and, in the case of a new development on the floodplain, can help to indicate where risk will increase (negative effects) and where it will decrease (positive effects). To compare different scenarios, the cumulative risk shows which scenario has the greatest total impact and which one has the least. Such an analysis, however, may result in loss of the spatial component which will hide the fact that in the "best" scenario not everybody will benefit equally.

6.1 Introduction

This chapter shows how the development of a new motorway on a river floodplain can alter the propagation characteristics of a flood. The Adige valley near Trento, Italy is used as an example to show how these kind of major changes in terrain topography may divert the flow of water, exposing previously safe areas to floods. On the other hand, there might also be positive effects if the construction forms a barrier and protects flood prone parts of the floodplain. For flood-risk assessment in the Adige valley near Trento, a three-step approach has been adopted: first, preliminary historic and geomorphologic studies have identified floods as the most serious hazard to those living in the area. Second, the flood hazard was characterised using a the parameter maps that were discussed in Chapter 3. This chapter focuses on the third step, to quantify the consequences of flood interference with human activities.

6.2 Input data and boundary conditions

Chapter 3 discusses the data requirements of 2D flood propagation modelling. The most important boundary conditions are: 1) an accurate digital surface model (that includes man-made objects as well as the river bathymetry), 2) the surface roughness coefficients and 3) the hydrographic data of the river (discharge, rating curve).

The Autonomous Province of Trento provided the detailed DTM of the floodplain, which was complemented by field observations (Figure 6.1). These observations showed that the vertical accuracy of the elevation data was approximately half a meter. In order to obtain reasonable computation times (10 to 15 hours), the original map with a resolution of 10 meters was resampled to a resolution of 50 meters. To ensure that important flow-influencing features (dikes, embankments) retain their proper elevation values, the procedure that is described in section 4.3 is applied.

Table 6.1. Surface roughness coefficients (Manning) for the various land use units (based on the classification by Geneletti, 2001) – Chow, 1959; Selby, 1988.

Land use	Manning's Coefficient	Land use	Manning's Coefficient
Bare	0.005	Scots pinewood	0.16
Pasture	0.04	Fir wood	0.16
Grassland	0.03	River vegetation	0.12
Shrub lands	0.05	Orchards	0.10
Orno-Ostryetum	0.06	Vineyards	0.07
Beech wood	0.10	Road	0.005
Larch wood	0.12	Urban	0.20
Oak wood	0.12	Water	0.04
P. Nigra pinewood	0.16	Canal	0.01

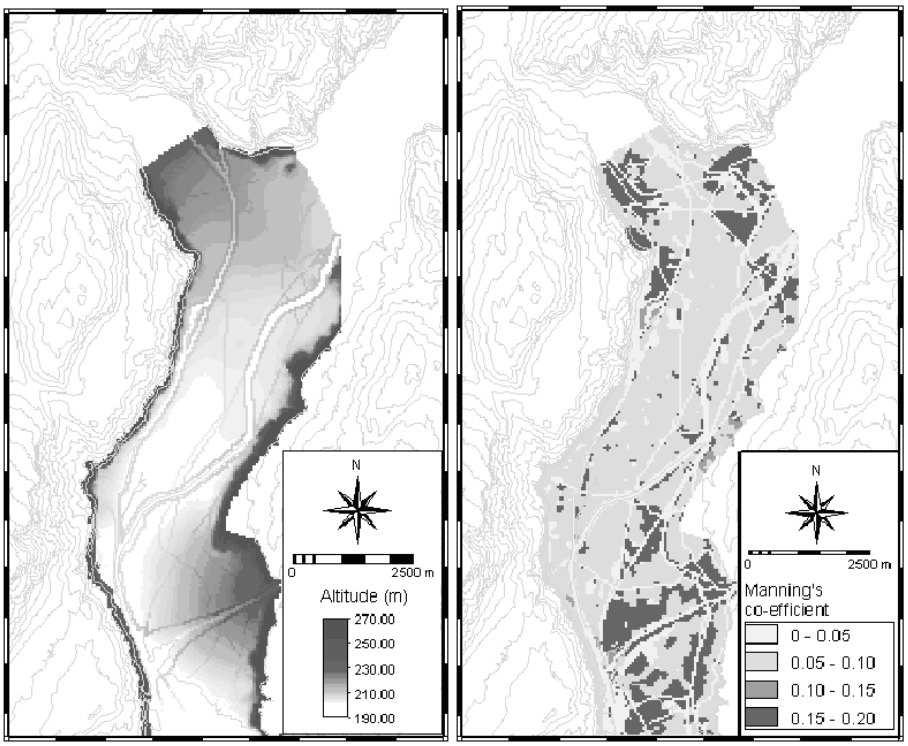

Figure 6.1. (left) The DTM including the Adige riverbed and main infrastructures.

Figure 6.2. (right) Map showing the surface roughness coefficients (Manning) for the study area.

The Adige Basin Authority (Trento office) provided the hydrographic data. For this study, special discharge curves for the upstream model boundary were derived from the historic discharge records of the "San Michele" river monitoring station – see next section. For the downstream boundary the rating curve (Figure 6.2) was derived from records of the "Trento" station (for locations, see Figure 6.4).

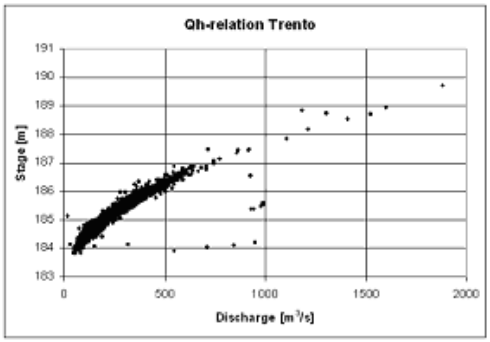

Figure 6.3. The water levels as function of the discharge of the Adige at the hydrographical station of Trento.

6.3 Scenario construction

A set of 48 floods scenarios was constructed, based on:

- Motorway alternative (3 alternatives);
- Rupture location (8 locations);
- Discharge Adige (2 return intervals).

Motorway alternatives

At the time of this study the layout of the new motorway was not yet clear. Geneletti and Alkema (2001) suggested for another study several options, of which two are used in this study. The third, so-called "zero-option" represents the current (2000) situation with no new motorway. This zero-option is used for reference. Figure 6.4 gives the location of the two motorway alternatives. Because no worked-out plans are available, the following assumptions were made for both the alternatives:

- The embankment rises 3 m above the present topography (this is similar to the railroad and highway embankments in the area);

- The embankments are impermeable and do not collapse during the flood event;
- Where the motorway crosses existing infrastructures and rivers, it is assumed that bridges will be constructed. For the model these will be "gaps" in the embankment.

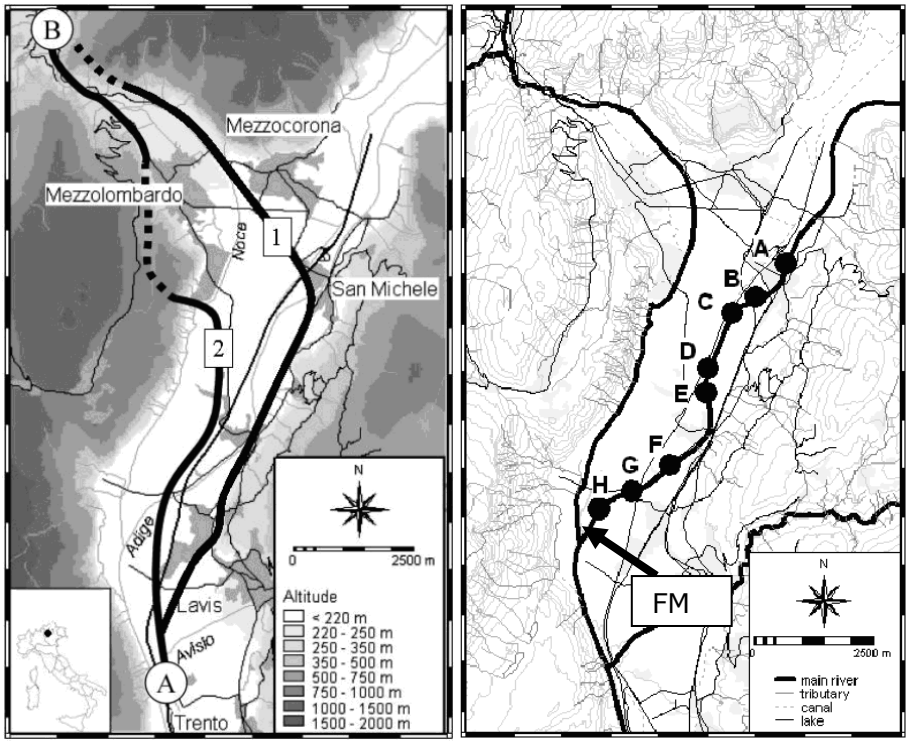

Figure 6.4. *(left) The bold black lines indicate potential routes for the new road connection between Trento North (A) and the valley of the Non (B). The dotted parts of the lines represent tunnel sections.*

Figure 6.5. *(right) Location of the 8 simulated dike breaches. "FM" indicates the sluice of the "Fossa Maestra".*

Dike breaches

In total, eight dike breach locations are – see Figure 6.5. The selection of locations is based on the following considerations:

- just after a curve where the talweg hits the outer bank;
- where the dike crosses a former riverbed;
- where tributaries and drainage canals join the Adige River;
- a more or less equal distribution along the river stretch that was analysed;
- all breaches were in the western dike, to ensure that the flood would interfere with the new motorway.

In addition to these considerations, the following assumptions were made regarding the breaches: the breach is 100 meters wide (2 pixels) and it reaches its maximum depth (5 meters) in 15 hours after the on-set of the rupture. There is no washout behind the failure locations. All the dike breaches have the same evolution and final profile.

River discharge

Two different discharge-regimes were considered: one with a peak discharge of 1000 m^3/s and another with a peak of 1800 m^3/s. A discharge of 1800 m^3/s corresponds more or less with bank-full discharge. The corresponding return periods are approximately 4 and 50 years (Adige Basin Authority, Bordato - oral communication). Figure 6.6 shows the synthesised hydrographs used for the upstream boundary. Synthesised curves were used rather than real discharge data to reduce the simulation period and hence the computation time.

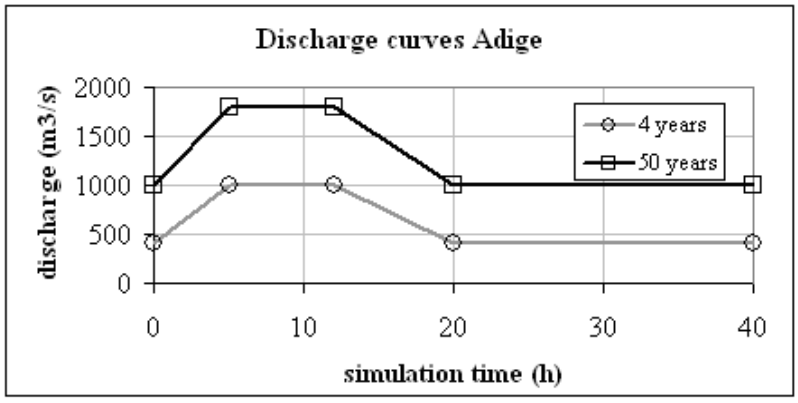

Figure 6.6. Discharge curves for the Adige that were used in the simulation.

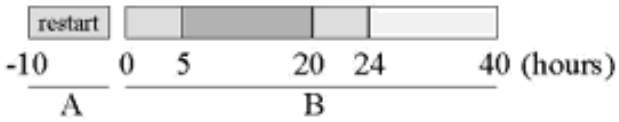

Figure 6.7. Time-frame used for the simulations

Simulation timeframe

Figure 6.7 schematises the time-frame of all computations. Phase A is a preparation simulation, that ensures that all simulations start with the same stable initial conditions. Phase B indicates the time-frame for the scenario simulations.

T = 0 Start of the scenario simulations.

T = 5 Peak discharge is reached. Breaching of the dike at a predefined location.

T = 12 End of peak discharge; water level in the Adige drops.

T = 20 Discharge Adige is reduced to initial discharge (see also Figure 6.6).

T = 24 Opening of a drainage canal "*Fossa Maestra*" at the most southern and low-lying part of the inundated area. Water is allowed to drain freely from the area.

T = 40 End of simulation.

The *Fossa Maestra* is the main irrigation/drainage canal in the area. A sluice near the confluence with the Noce River (see Figure 6.5) regulates the drainage into the Adige River. The version of Delft-FLS used in this study does not offer options to simulate a sluice, and thus the drainage was simulated by reducing the elevation value of the pixel at the sluice's location. This makes the modelled sluice 50 meters wide (the pixel size), which is major overestimation of the width of the actual *Fossa Maestra* (approximately 10 meters). The consequence is that the drainage and the descend of the water level is overestimated, resulting in an underestimation of the duration, see also section 3.5.

6.4 Flood hazard parameter maps

For each of the 48 scenarios, the hourly water depth and flow velocity maps of FLS are transformed into six parameter maps: maximum water depth, maximum flow velocity, maximum impulse, maximum speed of rising of the water level, duration and the propagation of the flood (see also section 3.5). The number of maps (48 sets of 6 parameter maps) is reduced by creating "worst case" scenarios for the 6 "main scenarios" based on the 2 return periods and the 3 road alternatives. The is schematised in Figure 6.8.

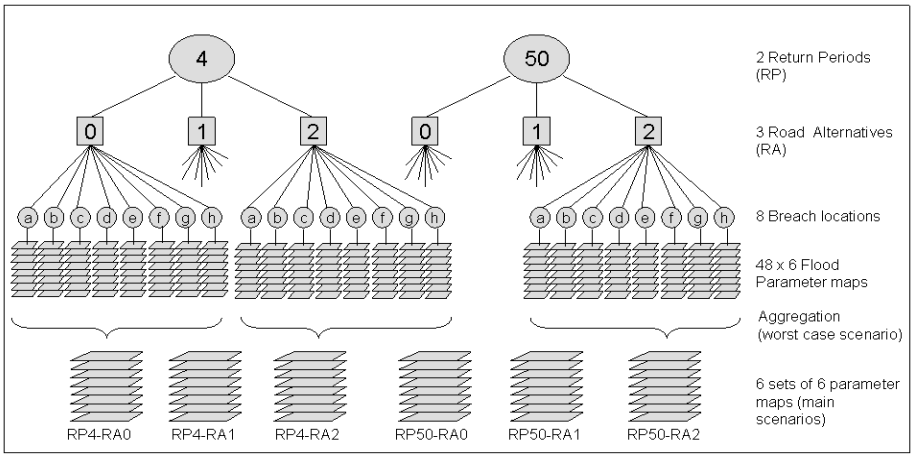

Figure 6.8. Aggregation of the 48 sets of 6 parameter maps into parameter maps for the six main scenarios based on return period (RP) and Road Alternative (RA)

The resulting maps for the 50 year flood are shown in Figure 6.9a-c. From these parameter maps can seen that road alternative 1 has less effects than alternative 2 Alternative 1 crosses the floodplain at its narrowest point due to the presence of the Noce alluvial fan, near San Michele. In addition to this, two bridges (gaps) were simulated in the new motorway where it crosses the Brenner highway and a major drainage canal. These allowed the flow of water through the embankment without much hindrance. It can be concluded that road alternative 1 is not a major obstacle to the floodwater. Road alternative 2 has larger effects. It affected the maximum water depth on both sides of the road: on the side behind the road it offered protection and resulted in lower depths or in no flood at all.

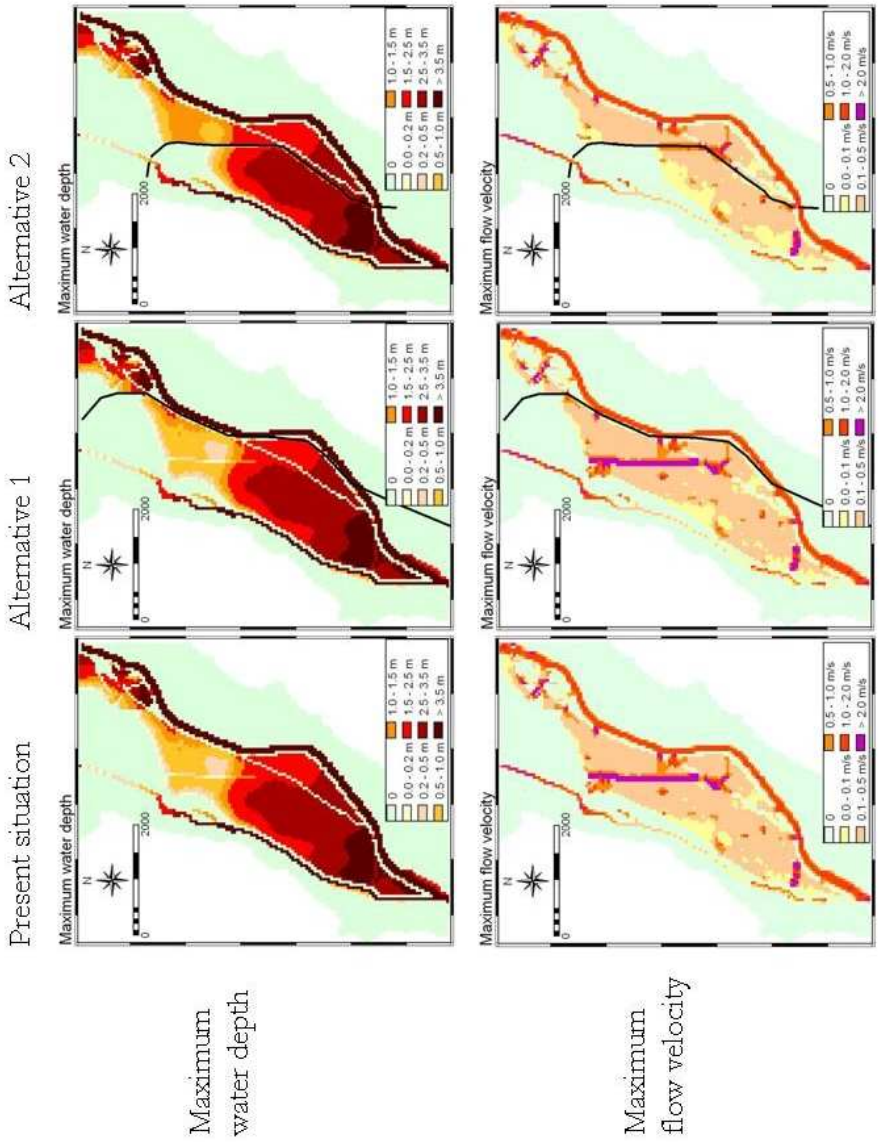

Figure 6.9a. Aggregated water depth and flow velocity maps of the 50-year flood for the three road alternatives.

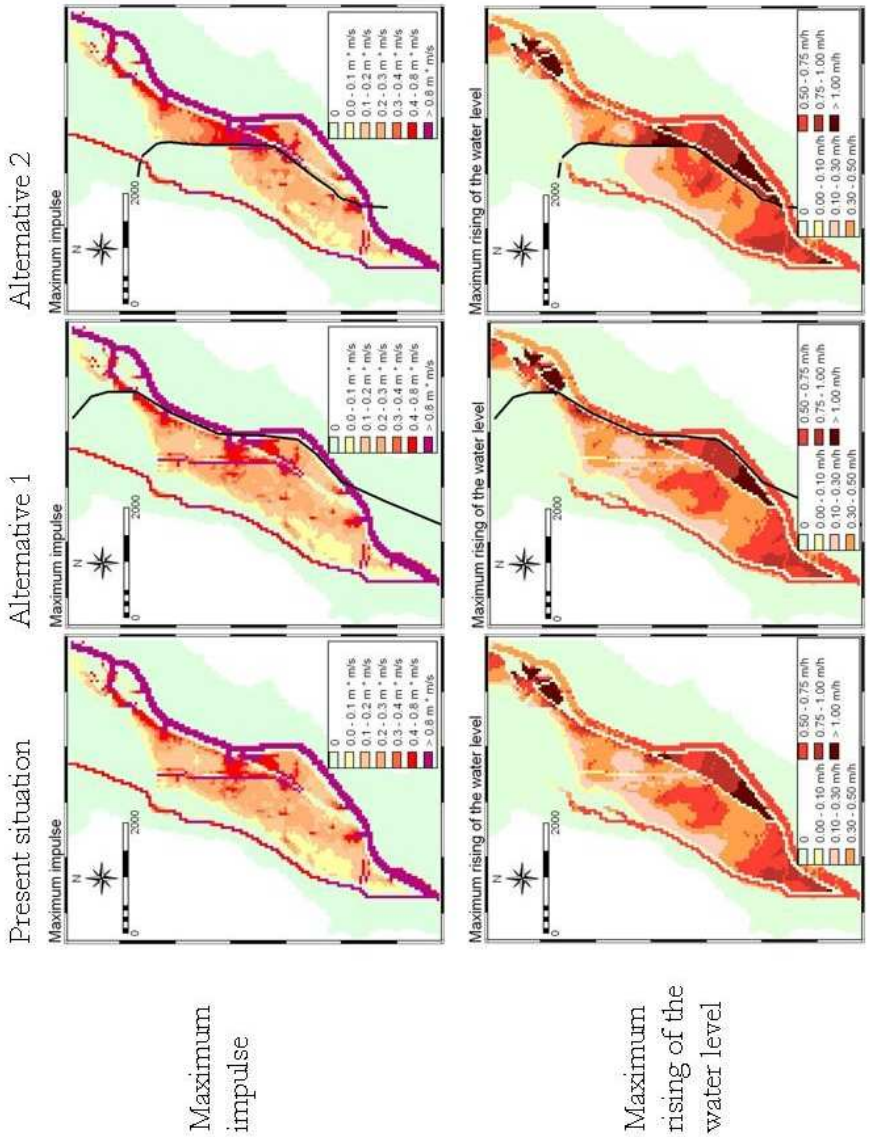

Figure 6.9b. Aggregated water impulse and rising of the water level maps of the 50-year flood for the three road alternatives.

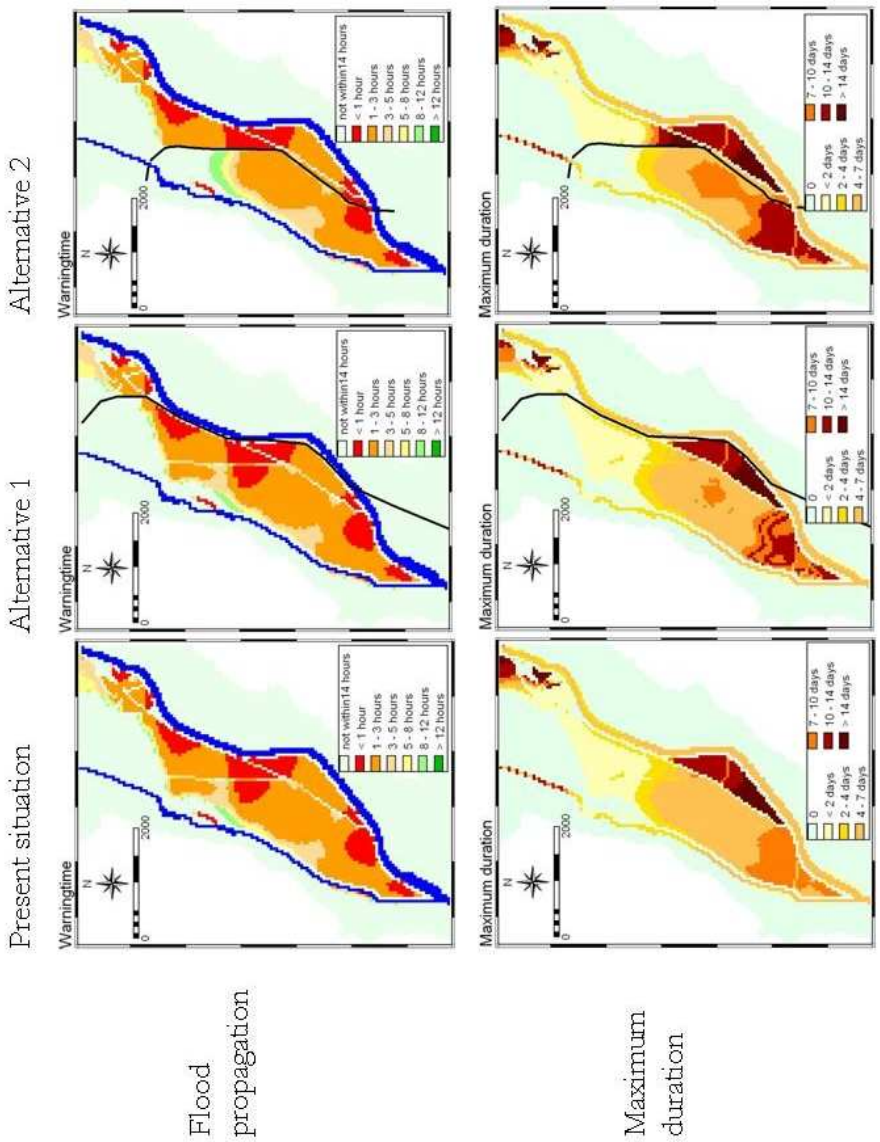

Figure 6.9c. Aggregated propagation and duration maps of the 50-year flood for the three road alternatives.

On the side between the river and the road, water levels are significantly higher (up to 1 meter). Also impulse and duration are higher in parts of the area, but the area behind the new road benefited in terms of the warning time that was reduced because the road acts as a barrier. It can thus be concluded that the introduction of an embanked structure has an affect the spatial characteristics, but the layout and design of the road is very important.

6.5 Risk assessment

To assess flood-risk, additional information is needed on the vulnerability of the various land-cover units in the inundated territory and their value. Data on the value of the three main land-cover units (orchards, vineyards and urban areas), like annual yield per hectare and average building price per square meter, were obtained from the annual statistical overview of the Province – see Table 6.2.

Damage

The economic damage estimate was based on two components: structural and non-structural damage. Structural damage to crops means that the harvest is destroyed. For multi-annual crops that (e.g. vineyards and orchards) this means that also the income of the following years is affected because new plants have to be planted which need time to grow before they start producing again. Structural damage to buildings means that (part of) the structure needs to be rebuilt. Non-structural damage in agricultural terms means that the harvest is not destroyed but that the yields have become less either in quality or quantity. Non-structural damage to buildings can be interpreted as damage due to the wetting and dirtying of carpets, wallpaper, furniture, machines, appliances, etc.

Structural damage estimation

The estimate of the structural damage is based on the parameter impulse: deep, fast-moving water will cause more damage than shallow water that practically stands still. Structural damage can happen to buildings (damage to walls, etc.) or to multi-annual crops like vineyards and orchards. Two critical thresholds were defined for each land-cover type:

- A minimum (critical) water level before damage starts (Table 6.2).

- A critical impulse where the element is considered as a total loss (Table 6.2).

The degree of damage is estimated as illustrated in Figure 6.10. At low impulses there is little damage, but as impulse nears the critical value, the damage percentage rises to 1 meaning that the crop or building is considered totally lost. When the crops or buildings are damaged beyond repair, additional costs are made for their replacement. For vineyards and orchards this means that the damage is not limited to the loss of one year's production, but several future harvests are lost as well until the newly planted crops start to produce again. For buildings "replacement costs" can be interpreted as the costs related to dismantling the destroyed house, temporary shelter, etc. At the critical impulse the curve becomes discontinuous and the degree of loss calculated as 1 + replacement factor.

Table 6.2. Critical values for the three main land-cover types; the estimates of the values for orchards and vineyards represent average annual yields per square metre.

Land-cover type	Critical water depth [m]	Critical impulse [m²/s]	Value: Euro / m²	Replacement factor (see Fig. 6.9)
Built-Up	0.1	3.0	40	1
Orchards	1.5	1.0	1	9
Vineyards	0.5	1.0	1,20	3

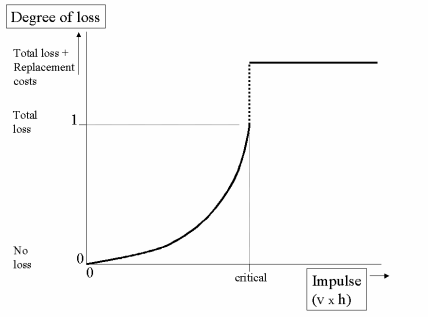

Figure 6.10. Damage as function of the impulse.

Non-structural damage estimate

The estimate of non-structural damage is based on maximum water depth and the duration of the inundation. With assistance of agro-economic experts at the local cooperative wine and apple societies, a matrix was constructed, containing an estimate of the degree of damage as a function of water level and duration, ranging from 0 (no damage) to 1 (complete loss). This was done for the main land-cover units in the area (orchards, vineyards and built-up). Table 6.3 shows an example of such a matrix for vineyards.

Table 6.3. Example of the non-structural damage matrix of vineyards, based on duration of the inundation and maximum water level.

Duration	Maximum inundation depth			
	0	0 – 0.2 m	0.2 – 0.5 m	> 0.5 m
0	0	0	0	0
< 2 days	0	0.3	0.6	1.0
2 – 7 days	0	0.6	0.6	1.0
> 7 days	0	1.0	1.0	1.0

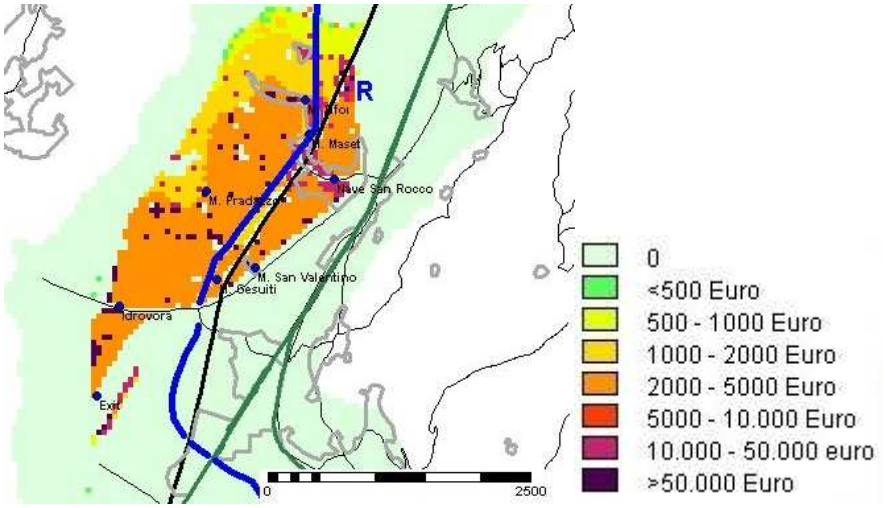

Figure 6.11. Total damage map (maximum of non-structural damage and structural damage) for a particular flood scenario: "R" indicates the breach location; the blue line represents the road alternative; the return period is 50 years. Costs are estimates per pixel (50 x 50 m).

Total damage estimate

The maps with degree of loss due to structural and non-structural damage were transformed into damage estimates, using the value and yield data obtained from the statistical overview of the Province of Trento – Table 6.2. For each scenario, the maximum values are shown in a total damage map, of which an example is given in Figure 6.11. The highest damage estimates are found in the built-up area and at isolated farms (> 10,000 euros per pixel covering 50 x 50 m).

Social flood-risk

Social flood-risk describes the degree of disturbance for the inhabitants of the flooded area. It is defined on the following three criteria:

- flooded within 6 hours after the dike breach;
- maximum water depth greater than 2 meters;
- maximum speed of rising of the water level greater than 20 cm per hour.

A special class was reserved for those areas where a water depth greater than two meters is reached within six hours after the dike breach. This is illustrated in Figure 6.12. The underlying assumption is that if people have sufficient warning time, they can be evacuated in time, safe their precious belongings etc. Even though damage cannot be avoided, this warning time will help them to cope better with the flood.

Social flood risk categories		Flood warning time < 6 hours	
		No	Yes
Maximum Waterlevel > 2 m	No	1 / 2	3 / 4
	Yes	5 / 6	7 / 8
Waterlevel > 2m in < 6 hours			9

a / b — a: maximum speed of rising < 0.2 m/h; b: maximum speed of rising > 0.2 m/h

Figure 6.12. Criteria for social risk Zonation

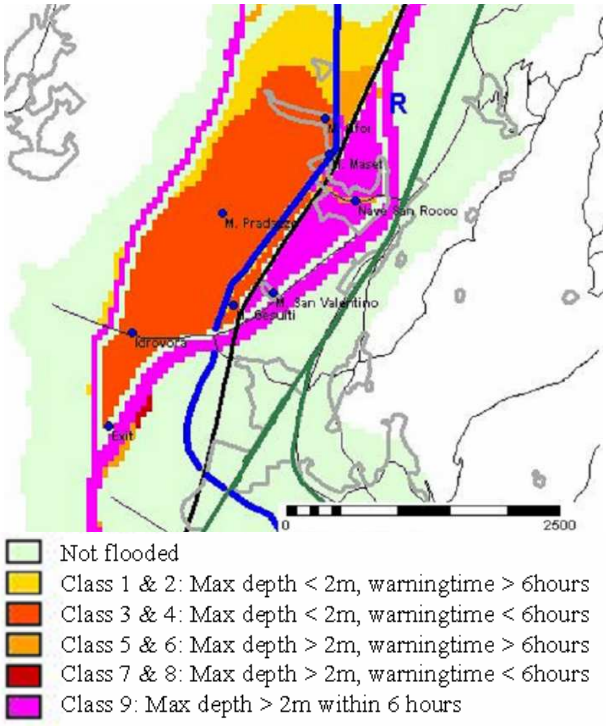

Figure 6.13. Social flood-risk map for a flood scenario: "R" indicates the breach location; the blue line is the road alternative; return period = 50 years.

A threshold of a water depth of 2 meters is chosen, because at this depth, risk of drowning is severe and because at greater depths the second floor of house may not stay dry anymore. A fast rise of the water level will hamper all kind of evacuation and relief efforts. The results of one scenario are shown in Figure 6.13.

6.6 Flood-risk comparison

The procedure described above results in a total damage map and a social risk map for the following six scenarios:

- Present topography + No new road 4 years flood;
- Present topography + No new road 50 years flood;
- Present topography + Alternative 1 4 years flood;
- Present topography + Alternative 1 50 years flood;
- Present topography + Alternative 2 4 years flood;
- Present topography + Alternative 2 50 years flood.

To see how total risk situation had changed and to see which areas had benefited and which areas had not, a comparison was made between the scenarios with a new road alternative were and those without. The map-total for economic damage and social risk are shown in Table 6.4. To facilitate the comparison, the damage and risk caused by the 4-year flood, with present topography is used as reference and is rescaled to 1.0. The difference between the values of the scenarios with the new road and the present situation can be attributed to the road alternative. The disadvantage of this method is that the spatial component is lost but the advantage is that the scenarios can easily be compared. In Table 6.4 can be seen that the total damage caused by the 50-year flood is 9,6 times higher than the total damage due to the 4-year flood. It can also be seen that road alternative 1 shows hardly any difference compared to the present situation, from which it can be concluded that its effect on the flood impact is negligible. This does not hold for road alternative 2. For smaller floods (4 years) it offers a benefit by reducing the economic damage by 31% and the social risk by 23%. However, for larger floods (50 years) it increases the total economic damage by a few percents, whereas for the social risk the benefit has shrunk by a few percents. The disadvantage of using the map-total values is that the spatial information is lost and that negative effects can be compensated by positive consequences elsewhere. This hides the fact that in the "best" scenario, some people might be worse off. To visualise which areas benefited and which areas suffered from the road project in terms of damage, the map-differences are calculated to obtain a map that shows where the damage is reduced (positive impact) and where the damage has increased - see Figure 6.14.

Table 6.4. Comparison of the total economic damage and social risk. The present topography / return interval 4 years is used as a reference (=1). The higher is the value, the higher is the damage or risk.

Economic damage	Present topography	Road Alternative 1	Road Alternative 2
4 years	1.0	1.0	0.69
50 years	9.6	9.7	9.8

Social risk	Present topography	Road Alternative 1	Road Alternative 2
4 years	1.0	1.0	0.77
50 years	6.7	6.8	6.5

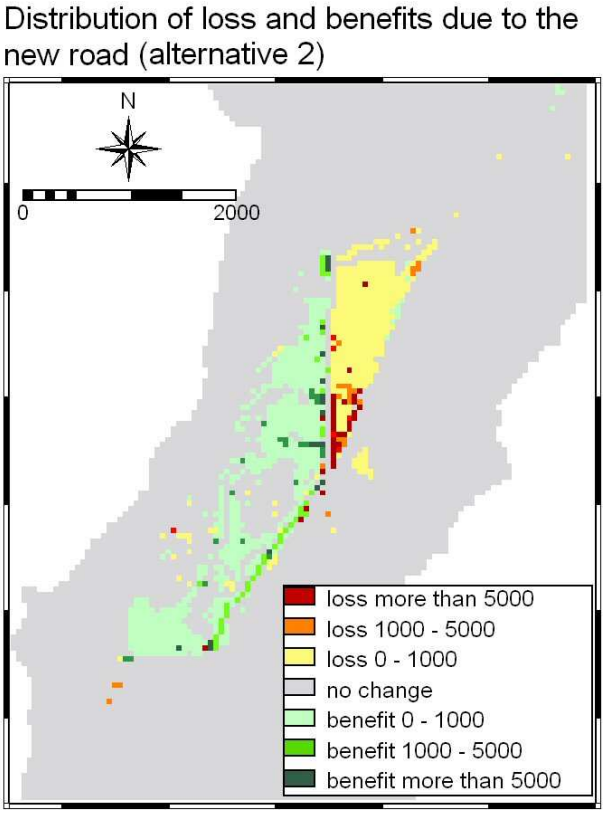

Figure 6.14. Example of the spatial distribution of difference in total damage (in Euros per pixel of 50 x 50 m) due to the new road (alternative 2); return period = 50 years.

6.7 Interactive demo on the Internet

All 48 scenarios can be accessed through at the GETS internet pages:. An interactive user interface allows the user to reconstruct each of the 48 possibilities and see the results. The URL is:
http://www.feweb.vu.nl/gis/research/gets/ResearchCenter/Demo%20Trento/frame_index1_trento_flood.htm
The demo can also be accessed through www.dinand.nl

6.8 Conclusion

This study demonstrates the applicability of a 2D flood propagation model to assess the flood consequences of new embanked motorway on a floodplain. It is concluded that the presence of such a structure can seriously alter the flood behaviour and thus affect the possible damage and risk distribution. In this study it was shown that road alternative 1 will not have a significant effect on the flood characteristics. This is for a large part due to its location on the side of the valley. It crosses the valley at a point where the Adige alluvial plain is at its narrowest, due to the presence of the alluvial fan of the Noce River – the *Piana Rotaliana*. Due to its lay-out characteristics (2 bridges), the new road does not seem the hinder the flood propagation. Road alternative 2, however, does have a significant effect on the flood behaviour and consequently on the economic damage and social risk. For smaller floods (4-year return interval) this is evident, but for larger flood events (the 50 years interval) the effect on the risk and damage is less clear. This study also shows that for some inhabitants the risk situation will improve, while for others the flood-risk has increased.

From this study is concluded that hydrodynamic modelling can help to foresee undesirable side effects of a development. During the planning stage the design of the new road can be adapted to the dynamics of the area (*direct hazards*) (see also Chapter 2) while considering construction costs, maintenance costs and safety of the users. For instance, on alluvial plains it is common engineering practice to design new infrastructure on embankments (to avoid flood-risk). But the construction of several of such structures will result in a landscape that is

compartmentalised by a maze of embanked railroads, highways, provincial roads and dikes. These elements form barriers that can change flooding characteristics and therefore result in *induced hazards:* small compartments will fill faster and to a higher level than they would have done without the embanked structures, which may cause unforeseen damage to the structure (*direct risk*). Tunnels, bridges and viaducts form connections between adjacent compartments through which water is funnelled, resulting in high flow velocities with a high potential to cause damage both to the structure itself (*direct risk*) and to the surrounding area *(indirect risk*).

6.9 Discussion

It is not hard to convince decision makers and planners of the fact that construction in flood-prone areas can have an affect on the behaviour of a future flood event and that his may have unwanted consequences for the people living and working in the area. With the use of 2D flood propagation models, like Delft-FLS, the changes in flood behaviour can be computed, as is demonstrated in the scenario-studies in this chapter as well as in Chapters 3 and 5. The flood model generates results in terms of changes in the behaviour of the flood: different water depths, flow velocities, warning times, etcetera. This, however, is not the information that decision makers need. They need to know how their decisions affect the people in the area in economic terms (change in potential damage) or in social terms (how many people are affected). In order to do this, the flood hazard assessment (the scenario modelling) has to be complemented with a risk assessment to quantify the socio-economic consequences. Such a combined hazard and risk assessment can provide decision makers with information to come to more balanced decisions. In this chapter the affects of two new road lay-outs on an alluvial plain have been assessed, both in terms of hazard (flood parameter maps) as well as in terms of the socio-economic consequences (damage and social risk). However, no procedure exists yet to transform the multi-parameter flood hazard assessment into risk maps. This chapter gives an example of possible ways to quantify structural and non-structural damage in a rural environment in monetary terms as a function of loss of harvest, loss of production means (plants and trees) and damage to buildings. The social risk is computed based on warning time, flood depth and rising of the water level. The transformation from hazard to risk is rather qualitative and based on estimates, generalizations and expert judgement,

which is inevitable due to the absence of real "data" in the form of damage maps and "risk inventories" after past flood events. Limited information about the exact damaging effects of floodwaters to the various land-use units makes it hard to evaluate the risk in absolute terms. The procedure described in this chapter is developed in collaboration with stakeholders in the area (Adige Basin Authority, the Provincial Geological Survey of Trento and Agricultural Institutes) serves as an example. The discussion on this topic continues in the next chapter and is the core of Chapter 8.

This approach to flood hazard and risk assessment can help to identify adverse consequences of new constructions and can thus help to avoid that a dramatic event like a flood turns into a disaster because of unwise planning. These kinds of studies should be integrated into environmental impact assessments that are usually mandatory for large projects like a new motorway, in order to balance flood-risk considerations against the other environmental, economic and social consequences of the project.

Chapter 7 Flood-risk and surface topography

This chapter is a modified version of the paper: Alkema, D and Middelkoop H. (2005): *The influence of floodplain compartmentalization on flood-risk within the Rhine-Meuse delta* in: Natural Hazards 36. pp 125-145.

The previous chapter discussed the application of flood propagation models for scenario studies and the transformation of the generated output into damage and risk maps. It was concluded that in flat, flood-prone areas dikes and embanked infrastructures will have a serious effect on the flow-behaviour of floods. This chapter will deal explicitly with the compartmentalization in a polder area to see if it can be used to reduce the consequences of a flood. To assess the damage, the Dutch standard flood damage estimate methodology is applied.

Abstract

The present compartmentalization layout within the river polders in the Dutch Rhine-Meuse delta is the result of abandonment and partial removal of secondary dikes and of the construction of modern infrastructure embankments. These structures will guide the flow of water in case the polder inundates. Through the application of a 2D flood propagation model in the polder "*Land van Maas en Waal*" this study explores whether restoration or removal of old dike remnants will contribute to a reduction of the damage during an inundation. A systematic set of 28 flood scenarios was simulated and for each scenario an additional damage assessment was carried out. It is concluded that a simple removal or total restoration will not reduce flood damage, but that this must be achieved by a strategic compartment plan. With such a plan old dike remnants and present embankments can be used to keep water away from vulnerable and valuable areas for as long as possible and to guide the floodwater to areas that are considered less vulnerable.

7.1 Introduction

This study explores the role of historic and modern compartmentalisations on the potential damage resulting from inundation of river polders in the Rhine-Meuse delta. These polders are protected against river floods by primary dikes that are designed to prevent inundation for discharge peaks lower than the 1250-year recurrence time flood (or annual probability of occurrence of 0.0008). For the Rhine River this corresponds to a discharge of 16000 m^3/s at the Dutch/German border and 3800 m^3/s for the Meuse River at the Dutch/Belgian border. However, because the magnitude of this design flood has to be determined by statistical extrapolation from a 100-year record of observations, there is a considerable uncertainty band around the estimated design discharge. Furthermore, it is anticipated that due to climate change, peak flows in the Rhine and Meuse might increase during the forthcoming century (Middelkoop et al. 2000; Silva et al. 2001). For this reason, water management in the Netherlands considers a 'worst-case' scenario with an increase of the design discharge of the Rhine to 18000 m^3/s and for the Meuse to 4600 m^3/s (Silva et al. 2001). This rise in discharge implies that - when no measures are taken - the probability of overtopping or breaching of the dikes will increase as well and the safety of the polder and its inhabitants will fall below the required safety standard. Furthermore, there is a growing awareness that it is impossible to guarantee a totally secure defence against floods: the inundation of river polders in the Netherlands therefore is no longer unimaginable. Recently, the option of using retention areas outside the present high-water bed of the rivers is considered as a flood reduction measure (Silva et al. 2001). The idea of appointing some river polders as temporary emergency retention basins has been put forward in order to alleviate flood-risk in the densely populated and low-lying downstream parts of the Netherlands in case a flood higher than the design discharge would occur. To allow controlled flooding of certain polders, parts of the dike will be designed as spill-over that can withstand overtopping by large amounts of floodwater without breaching. Before such decisions can be taken, the potential damage in different polders must be assessed, and measures to reduce damage in the eventual case of inundation must be thoroughly considered. This demands quantitative information on the hydraulic characteristics of the inundation process of a river polder, depending on the elevation, land use and the presence of embankments within the polder. These embankments subdivide a polder into different compartments, which greatly controls the rate and

propagation of the inundation. The present-day compartmentalization of the polders consists of the remains of compartment dikes that have been erected in historic times and embankments of modern infrastructures (highways, rail). Because of the effect of these embankments on the flood characteristics, impact reduction strategies should focus on the design of the compartmentalization layout.

The aim of this study is to determine the hydraulic characteristics (i.e. propagation rate, flow depth, inundation time) of the inundation of a river polder along the lower Rhine and Meuse rivers and the resulting damage, depending on the compartment layout of the polder. In addition to quantifying the effect of the present compartmentalization on the inundation propagation, we focused at assessing to what extent the inundation damage of river polders may be reduced by restoring the function of the old compartment dikes. For this purpose we simulated the inundation of a river polder using a two-dimensional flood propagation model for 28 inundation scenarios. The scenarios are based on a set of seven different dike-failures including catastrophic breaches and controlled overtopping of different sections of the primary river dikes along the Waal and Meuse Rivers, and four combinations of modern and (restored) historic topographic layouts of the polder. Each inundation scenario was evaluated by assessing the potential damage caused by the inundation. The study was carried out for the polder "*Land van Maas en Waal*", located between the Waal (the largest distributary of the lower Rhine River) and the Meuse River (Figure 7.1).

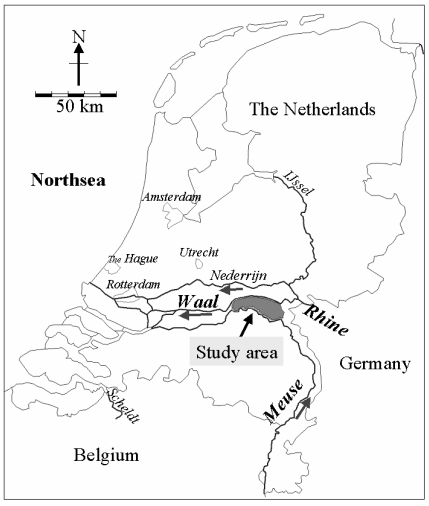

Figure 7.1. Location of the study area

7.2 Historic background

By nature, the Rhine-Meuse delta is characterized by alluvial ridges with natural river levees intersecting low-lying back-swamps. During periods of increased river discharge these swamps were flooded and remained inundated for a long period due to poor drainage. The natural levees along the rivers consist mainly of sandy material and formed the natural higher ground in the area. When the first inhabitants entered the area, the levees were their natural choice for settlement and the starting point for the further development of the back-swamps. For protection against river flooding artificial mounds and dikes were constructed. The first dikes were built perpendicular to the natural levees, upstream from the settlement to divert the floodwater around the settlement (Driessen, 1994). The enclosure of the river area by dikes was completed between the 13th and 14th century. To exploit the agricultural potential of the back-swamps, the drainage was improved by digging a network of canals. Also, compartment dikes were raised within the polders to control drainage, and in the event of a dike breach, to prevent areas from being flooded. Between the 16th and 19th century, a polder system was created surrounded by primary river dikes and with secondary dikes that formed closed compartments within the polder, each with its own drainage system of canals, sluices and pumps. The polder *Land van Maas en Waal* is a typical example of such a polder system (Figure 7.2).

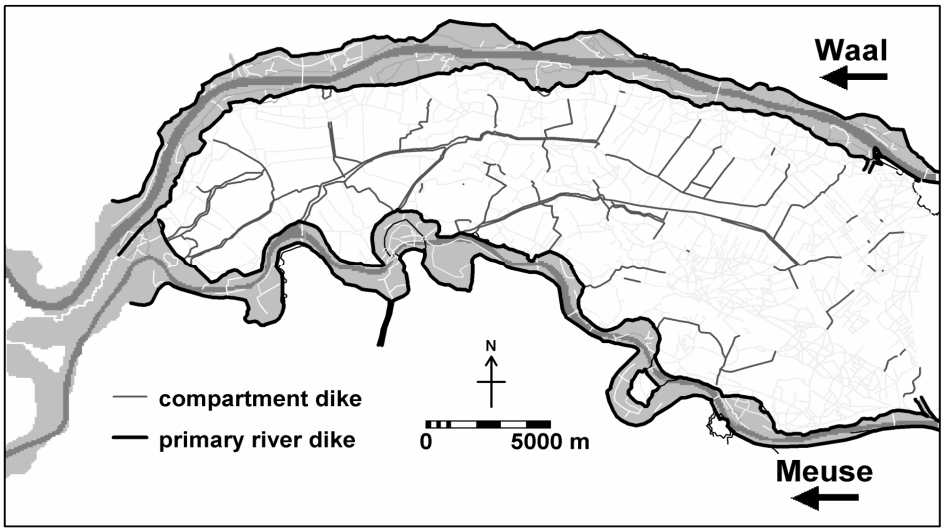

Figure 7.2. Historic map of the Land van Maas en Waal around 1850.

This defence system offered protection against smaller floods but it could not avoid that occasionally large floods overtopped or breached the primary river dikes (e.g. Driessen 1994). During the onset of the flood, the system of compartments diverted the flow of the floodwater and delayed the propagation by forcing the water to fill up the polder compartment by compartment (Hesselink et al. 2003). This increased the time for evacuation and distributed the impact of the flood more evenly over the polder.

During the 20th century the condition of the main river channels and quality of the primary river dikes had greatly improved, and inundation of a river polder in the Netherlands has not occurred since 1926. As a consequence, the appreciation and valuation of maintaining a secondary defence system within the polders declined and many compartmentalization dikes were subject of neglect or were completely removed. Large-scale development of the polder, with rapid expansion of urban and industrial areas and land reallocation contributed to their decline. Embanked infrastructures gradually developed as additional compartmentalizing elements within the polder. This started in the late 19th century with railway lines and progressively developed in the 20th century with the construction of highways and motorways. Although these embankments were not designed as flood barriers, they will play a significant role in directing the floodwaters in case of inundation. Bridges and tunnels will funnel water and create increased flow velocities. With the coinciding decline of the secondary dike system by the end of the 20th century, the old compartment system was replaced by a non-systematic compartmentalization of the polder consisting of old dike remnants and new embankments. The decline of secondary dike system was not appreciated by all, because it can be considered of a socio-historic value, and might play a role in flood mitigation in the Netherlands (see e.g. Nieuwenhuis, 1996). The evaluations of the inundations was carried out for different combinations of failure locations and mechanisms of the primary river dikes and topographic layouts of the polder. These are explained further in the following sections.

7.3 Inundation points

An inundation point is the location on the dike where the inundation of the polder starts. It can be either a catastrophic breach or a controlled overtopping of the dike

at a predetermined spill-over location. In this studies five different locations were defined: three along the Waal River and two along the Meuse River At the locations "Weurt" (Waal) and "Overasselt" (Meuse) a breach and a spill-over were simulated (Figure 7.3). The choice for the locations was based on three considerations: 1) they are distributed more or less evenly along the rivers, so that differences between the scenarios become sufficiently apparent; 2) they are not located too far downstream because that results in very small inundations; and 3) they are positioned in between urban areas, because it is unrealistic to construct a spill-over near a village. The location of Weurt for the breaching scenario was chosen because of the availability of historic data from the 1805 flood-reconstruction simulations carried out by Hesselink (2002).

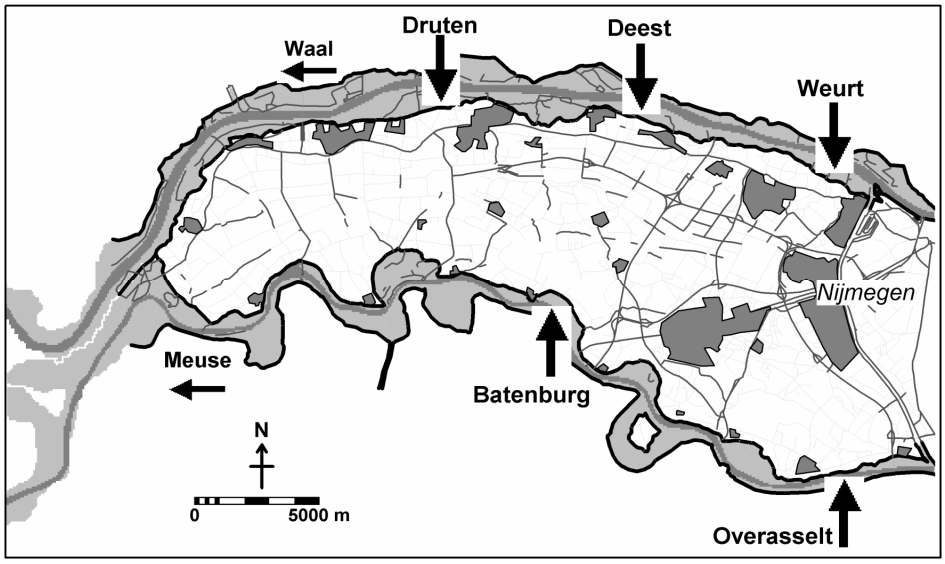

Figure 7.3. Location of the spill-overs and dike breaches

Spill-over

The aim of a spill-over into a retention area is to cut off the peak of a flood wave in order to alleviate the flood-risk in downstream areas. When compared to a dike breach, a spill-over allows controlled inundation over a predefined dike stretch, at an *a priori* known flood stage in the river. As no scour hole develops, the amount of water entering the polder depends on the river discharge and eventual technical means to reduce the crest level of the spill-over. To optimise the effect of the spill-

over on reducing the downstream river flood stages, the peak of the flood wave has to be cut off at exactly the right moment. In this study the spill-over would be activated as soon as the present-day design discharges of the Waal and Meuse Rivers are exceeded, which is 10,160 m^3/s and 3,800 m^3/s, respectively. At that moment the height of the dike is reduced by 20 cm over a width of 525 meters for the Waal River and 300 meters for the Meuse River in order to "open" the spill-over.

Breaches

The dimensions of the Weurt breach (i.e. its width and depth, Figure 7.4) are based on the historic dike breach that occurred at this location in 1805. This flood disaster is reconstructed in detail by Hesselink (2002). For the Meuse River the breach is located near Overasselt where a dike breach occurred in 1820 (Driessen, 1994). Unfortunately this event was not as well documented and analysed as the 1805 flood. So the dimensions of this breach and the scour hole are based on circumstantial evidence, like comparison with other Meuse dike breaches and shape of the reconstructed dike. The amount of water flowing into the polder is a function of the final dimensions of the dike breach (which can be measured or reconstructed) and the rate at which the breach develops (which has to be estimated). Based on the work of Hesselink (2002) it was assumed in this study that the final dimensions of the dike breach gap and scour hole at both locations are reached within 3 hours after the initial dike failure.

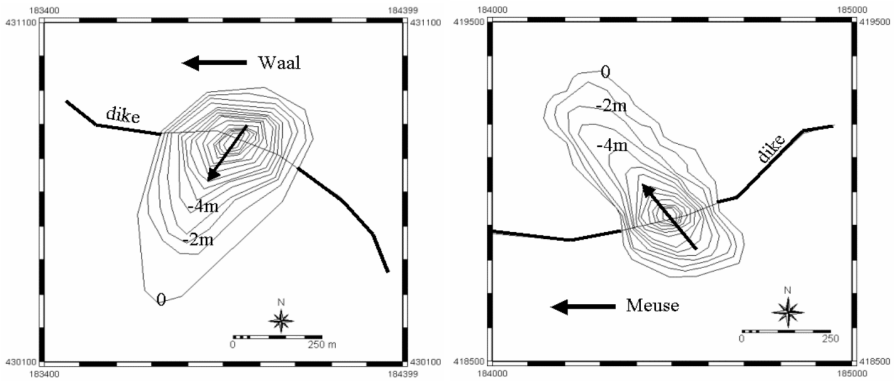

Figure 7.4. Dimensions of the dike breach near Weurt (left) and of the dike breach near Overasselt (right)

7.4 Topography

Four different lay-outs of the polder interior were constructed, based on: A) a current Digital Terrain Model provided by the Province of Gelderland (Van Mierlo et al. 2001) and B) on the DTM of the polder as it was in the first half of the 19th century, reconstructed by Hesselink (2002) with a complete compartmentalization (Figure 7.5a and 7.5b).
The historic DTM is based on 35,868 elevation points measured between 1950 and 1965 (before large land levelling and re-allocation schemes had taken place), complemented with data from a land survey carried out along five transects in the beginning of the 19th century and dike-height measurements carried out in 1801. The current DTM is derived from a laser-altimetric survey with a vertical accuracy of several centimetres. Comparing the present situation with topographic maps of 1850 showed which former secondary dikes had disappeared and which remnants had survived. Some of the major changes are seen on the two elevations models. For instance in the 1850 DEM, the secondary dikes in the lower part of the polder (left) can easily been seen, whereas these have disappeared nearly completely in the 2000 DEM. In the 2000 DEM some major infrastructures can be seen, such as highways (the A50 and A73) and a railroad. A field survey provided information of the height of these elements and of the embankments of modern infrastructure. It can also be seen that the rivers were changed significantly. Both the Waal and Meuse are much deeper due to dredging activities, and in the Meuse some meander curves were cut-off. In the East (right-hand side) the Meuse-Waal Canal is clearly visible. This canal was opened in 1927. For modelling purposes a grid size of 75 meters was chosen and a check with elevation points derived from the topographic map showed that vertical accuracy was within 10 cm for 90 % of the control points.

The four different layouts are (Figure 7.6):

- A: Present situation, including dike remnants and modern embankments (present);
- B: Present situation with all remnants removed (cleaned-up);
- C: Present situation with the 1850 compartmentalization complete restored (restored);
- D: Present situation with strategic adaptations to protect vulnerable (urban) areas (strategic).

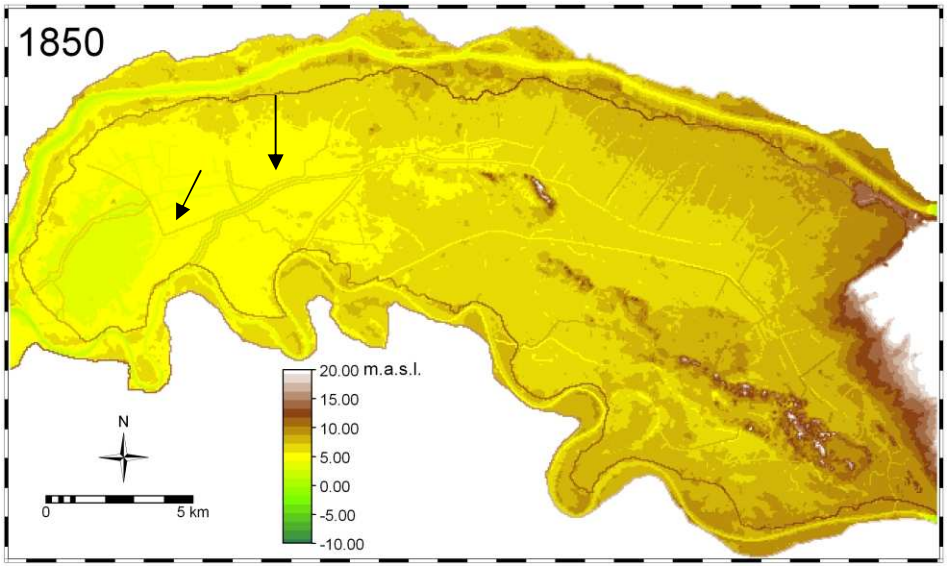

Figure 7.5a. Digital Elevation Model (DEM) of the study area around 1850 (in meters above sea level – NAP); Arrows indicate secondary dikes that have (partially) disappeared (see below).

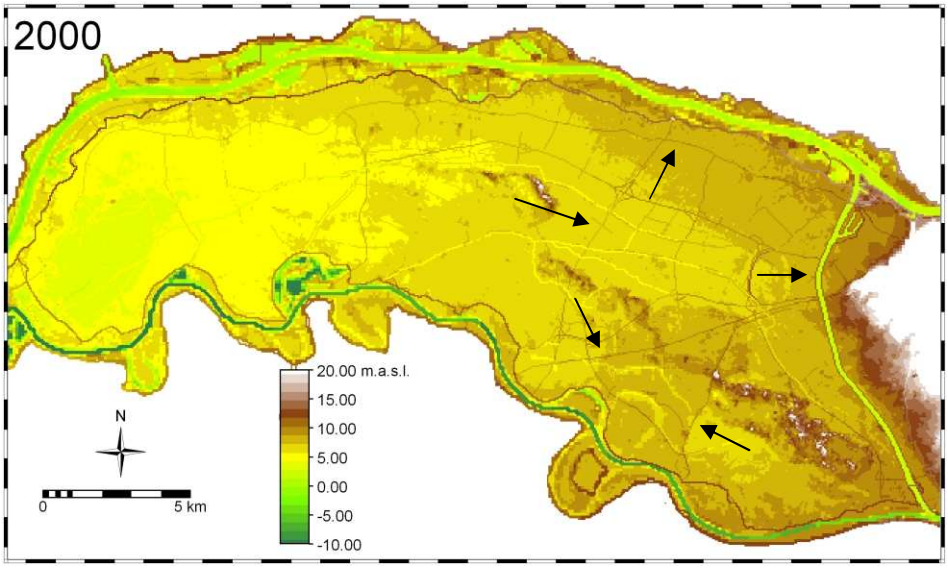

Figure 7.5b. Digital Elevation Model (DEM) of the study area around 2000 (in meters above sea level – NAP). Arrows indicate infrastructure (highway, railroad, canal) that were not yet present in 1850 (see above).

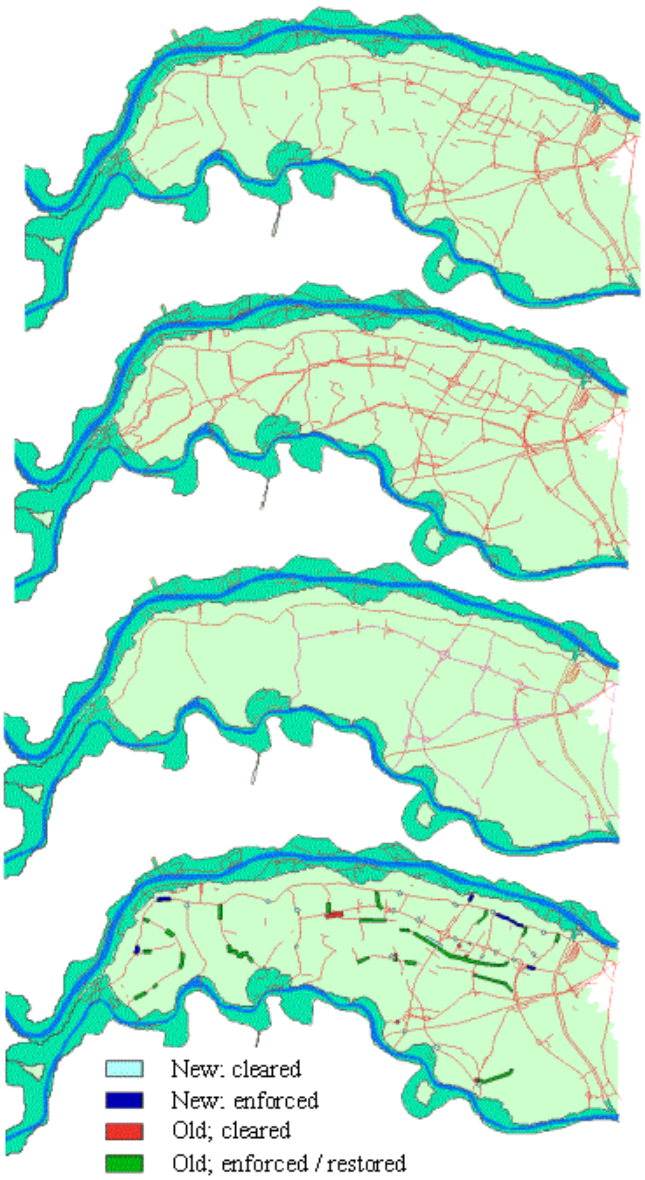

Figure 7.6. The 4 compartment layouts. From top to bottom: (A) present situation; (B) all old elements removed; (C) all old elements restored; (D) strategic adaptations – New; cleared = (partial) removal or lowering of new elements. New; enforced = (partial) strengthening or heightening of new elements. Old; cleared = (partial) removal of old, historic elements. Old; enforced / restored = (partial) restoration and/or enforcement of old, historic elements.

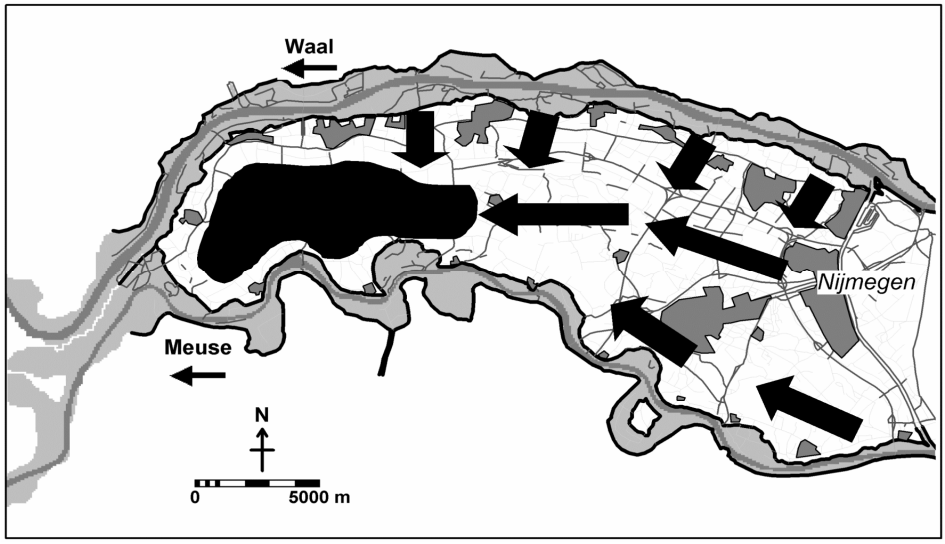

Figure 7.7. Strategic plan to use old and new barriers to keep the water away from vulnerable areas for as long as possible and to guide it towards less vulnerable parts of the polder.

The aim of layout D is to reduce the impact of the flood in terms of damage or risk by selective changes in the present compartment layout. This involves both repair of previously removed dikes as well as removal of dike sections. The adopted strategy aims at directing the water flow away from, or around the urban areas and to guide it towards the less vulnerable agricultural areas in the centre of the polder (Figure 7.7). Dike reconstruction or removal was done by changing the elevation value of the DTM at strategic locations. No attempt was made to optimise the impact reduction.

7.5 Boundary conditions and model calibration

Model sensitivity

Hesselink et al. (2003) carried out a sensitivity analysis of inundation patterns simulated with Delft-FLS for varying surface roughness and topographic detail in the same area of the present study. They concluded that hydraulic roughness affects the speed at which the polder fills, but that it does not influence the maximum inundation depth. Furthermore, the model results were highly sensitive

to the terrain topography and to the inclusion of secondary compartment dikes within the polder. In Chapter 5 of this volume the model was tested on the inundation of the Ziltendorfer polder during the 1997 Oder flood in Germany. This polder is comparable in size and land-use, although it is not as compartmentalized as the *Land van Maas en Waal*. The results of the Ziltendorf study also confirmed the model sensitivity and reliability, with the addition that for accurate water depth predictions a good rating curve is essential. In Chapter 5 it was demonstrated that Delft-FLS is well capable of accurately simulating inundation depth and propagation rate of an inundation. Validation of other parameters, such as flow velocity, was not possible.

River discharge

In accordance with the upper estimates of future design discharge (1250-yr recurrence time) due to the climate change considered by the Dutch water management (Silva et al. 2001) the model simulations were carried out for a design flood equal to 18,000 m^3/s for the Rhine River at the Dutch/German border and 4,600 m^3/s for the Meuse at the Dutch/Belgian border. Assuming that the Waal River then discharges 63,5 % of the Rhine discharge, the corresponding peak discharge in the Waal River equals 11,400 m^3/s. The discharge curves of the increased design flood wave for both rivers was obtained from the study to "design discharges for the Rhine and Meuse Rivers" or "*Randvoorwaardenboek*", 2001 by WL|Delft Hydraulics and the Institute for Water Management and Waste Water Treatment (RIZA). Both are shown in Figure 7.8. According to WL|Delft Hydraulics, the peak discharge of the Meuse River reduces as it travels downstream, while the length of the flood wave increases. Near the study area it is estimated that the peak discharge is reduced by approximately 1000 m^3/s, giving a peak discharge of around 3,650 m^3/s (WL|Delft Hydraulics, Asselman, oral communication).

Stage discharge relations Waal and Meuse

The water authorities of the Province of Gelderland (Mr. Overmars – oral communication) provided the Q-h relations of the Waal and Meuse Rivers at the downstream boundaries of the modelling area (near the villages of Opijnen and Empel). During the calibration the relation for the Waal River was slightly adapted to give better results (see next section). This correction compensates for errors in the representation of the riverbed in the DTM. For the Meuse this was not necessary. Figure 7.9 shows the Q-h relationships for both stations.

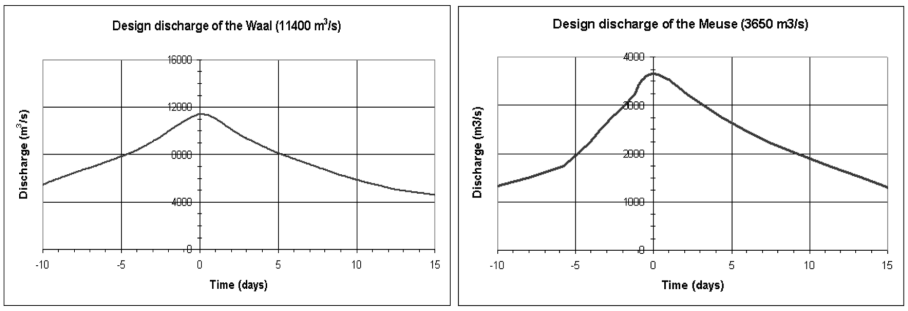

Figure 7.8. Discharge curve of the Waal used in this study (left) and that for the Meuse (right)

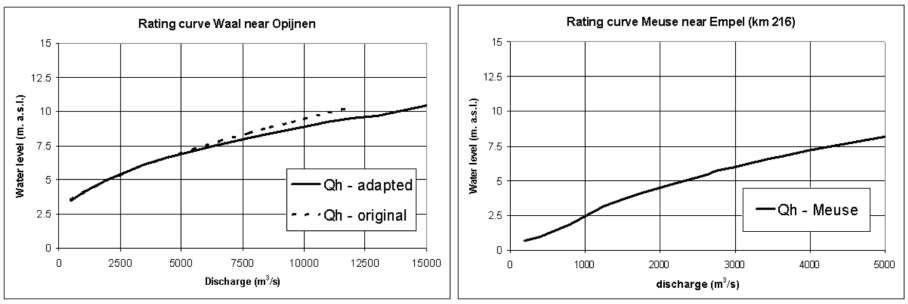

Figure 7.9. Stage-discharge curves for the Waal near Opijnen (left) and for the Meuse near Empel (right)

Surface roughness coefficients

The surface roughness depends largely on the type of land-cover and is often expressed as Manning's coefficient. Table 7.1 gives an overview of the land-cover classes and the corresponding values of Manning's coefficients as they are found in literature (e.g. Chow 1959, Albertson and Simons, 1964, Barnes, 1967) with the exception of the values for the riverbed and the floodplain. The latter were obtained by calibration the model results. They seem to be rather low compared to the values used in the other case studies presented in this volume. This is probably because this way they partially correct for inaccuracies in the representation of the riverbed. Figure 7.10 shows the resulting surface roughness map.

Table 7.1. Roughness values for different land-cover types used in the model simulations.

Land-cover type	Manning's coeff.	Land-cover type	Manning's coeff.
Riverbed	0.008	Heather	0.050
Floodplain	0.011	Main road	0.020
Urban area	0.100	Railway	0.020
Forest	0.150	Secondary road	0.015
Arable land	0.050	Water	0.012
Dike	0.030	Grassland	0.018

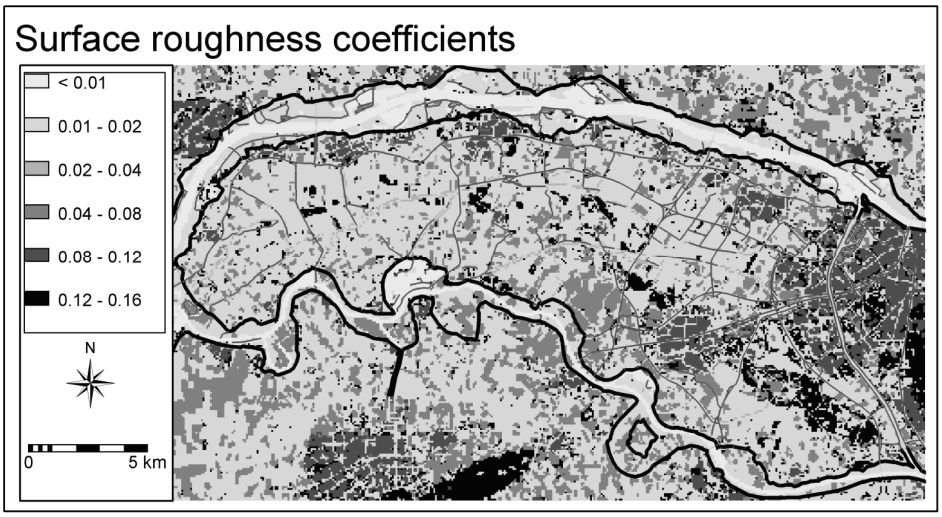

Figure 7.10. Manning's surface roughness coefficients.

7.6 Calibration

The discharges that are used as boundary condition in this study have never been recorded in the Waal and Meuse, so no measured water levels are available to calibrate the model. However, previous modelling studies by WL|Delft Hydraulics have provided estimates of flood water levels in the rivers occurring at these extreme discharges (Asselman, oral communication).

Table7.2. Comparison between water stage predictions of previous studies and the results of this study at various locations along the rivers.

WAAL	Nijmegen (km885)	Bridge A50 (km894)	Druten (km904)	Ben. Leeuwen (km911)	Dreumel (km920)
Previous studies	15.00m	13.60m	12.50m	11.80m	10.80m
This study	14.99m	13.64m	12.48m	12.07m	10.93m

MEUSE	Heumen (km(166)	Overasselt (km171)	Batenburg (km185)	Heerewaarden (km205)
Previous studies	12.70m	12.00m	10.10m	7.30m
This study	12.20m	11.90m	10.10m	7.54m

The outcomes of these studies were used to verify the water stages in the rivers calculated in this study (Table 7.2). As a result of this comparison, the Q-h relation for the Waal River was slightly adapted and were the Manning's coefficients estimated.

7.7 Model results

During a post-modelling analysis in a GIS, the model results, hourly maps of flow velocity and water depth, were transformed into seven parameter maps. In Chapter 3 is described how six of these parameter maps were calculated. The next section describes the estimation of the seventh parameter map "**erosion (scouring) /sedimentation**" in more detail.

Estimation of scouring and sedimentation

The estimation of the sedimentation and scouring is based on the Rouse number that gives the ratio of downward (falling) velocity of a particle to the shear velocity (turbulence acting to keep particles suspended). The method applied here was suggested by Kleinhans (2002).

$$Z = \frac{W_s}{\kappa . u^*} \quad -1 \qquad 7.1$$

Where:

Z	= Rouse number [-]
κ	= Kármàn constant (=0.4) [-]
u^*	= Shear velocity [m/s]
W_s	= Downwards velocity for a particle of certain grain size [m/s].

This criterion is calculated at the hourly time steps, for sediment particles with a diameter of 210 μm. When Z > 0, sedimentation is possible because the downward velocities are larger than the upward directed velocities. The particles present in the water will experience a net downward movement and may sediment on the surface. When Z < 0, then the upward directed velocities are higher than the downward velocities which means there is potential for uplifting of particles (scouring) and available particles will remain in suspension. The downward velocity W_s of a particle with a diameter between 100 and 1000 μm (fine sand) is given by:

$$W_s = 10 \frac{\nu}{d} \left(\sqrt{1 + \frac{(0.01(s_p - s_w)/s_w \, g \, d^3}{\nu^2}} \quad -1 \right) \qquad 7.2$$

Where:

ν	= viscosity of water = 1.2 * 10^{-6} [m^2/s]
s_p	= density of quartz = 1.65 * 10^3 [kg/m^3]
s_w	= density of water = 1 * 10^3 [kg/m^3]
d	= grain size diameter = (in this study) 210 * 10^{-6} [m]
g	= gravity acceleration = 9.81 [m/s^2]

Since all parameters in formula 7.2 are constant, W_s is approximately 0,01 m/s for a particle with a diameter 0f 210 μm. The shear velocity is given by:

$$u^* = \frac{\kappa \; U}{\ln \left(\frac{0.37 \, h}{3.97 \; 10^6 \, n^6} \right)} \qquad 7.3$$

Where:

U = flow velocity [m/s]
h = water depth [m]
n = Manning's roughness coefficient

The flow velocity and water depth are computed by the model, whereas the spatial distribution of Manning's coefficient is one of the known boundary conditions. All parameters are known at hourly time-steps. The final sedimentation / scouring gives the accumulated hourly values of the dimensionless parameter Z to identify areas where sedimentation or scouring are dominant. In this procedure, positive and negative values can cancel each other out: the higher the value, the more potential for sedimentation; the lower the value the more potential for scouring. Zero means no net sedimentation or scouring. To estimate the availability of sediment, three additional assumptions were made:

- the sediment-load of water flowing into the area decreases inversely with time (high at the start, then decreasing with time);
- the sediment is distributed uniformly in the floodwater and is never zero - the sediment fluxes are proportional to the water fluxes;
- sedimentation and scouring occurs only in the first 150 hours of the flood (the time period for which this parameter map was calculated).

This approach does not yield estimates for sedimentation and scouring in terms of deposition or scouring depth, but provides an indication where and to what degree sedimentation and scouring can be expected.

The results of the flood modelling of all 28 scenarios as well as the damage estimation can be found on the CD-ROM that accompanies this book. The interactive CD-ROM has a special interface to allow comparison at hourly time-steps between all possible scenarios.

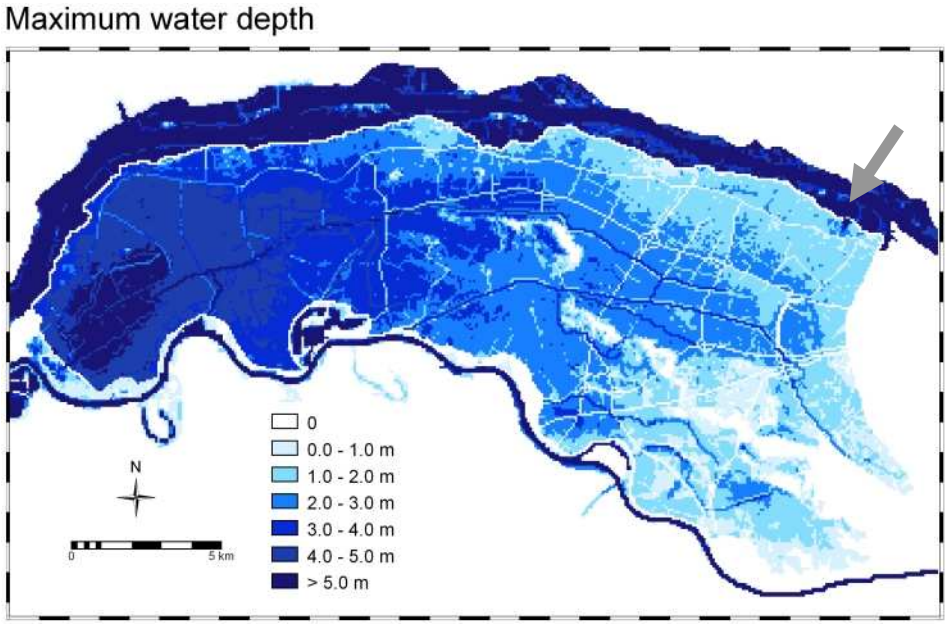

Figure 7.11a. Water depth map: dike breach near Weurt (indicated by the arrow), present topography.

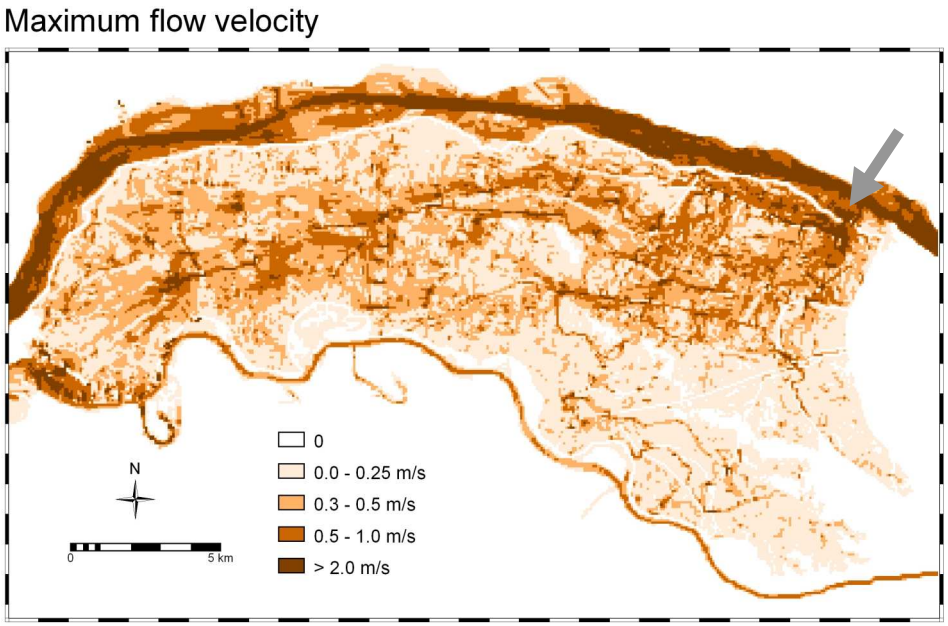

Figure 7.11b. Flow velocity map: dike breach near Weurt, present topography.

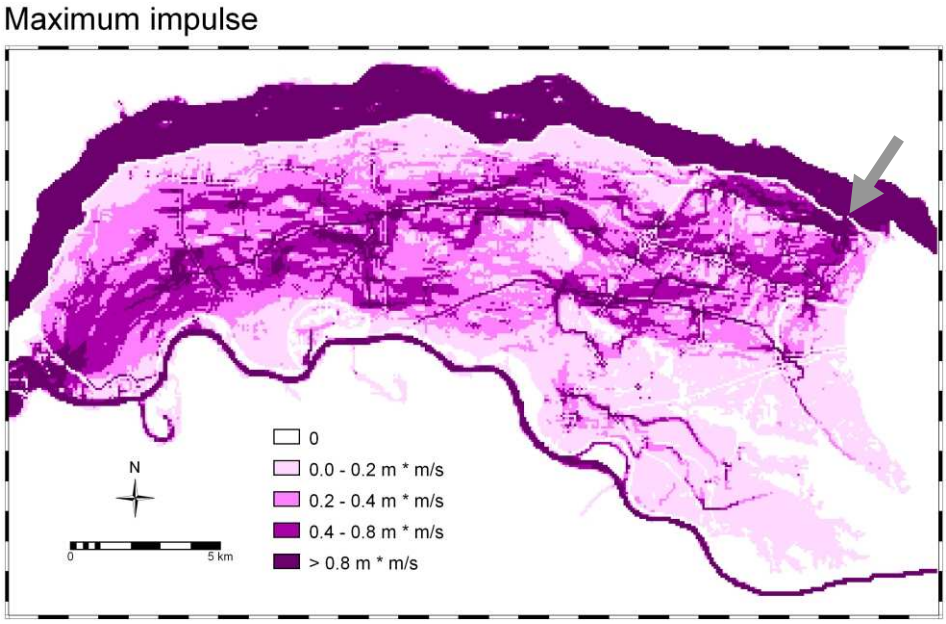

Figure 7.11c. Impulse map: dike breach near Weurt, present topography.

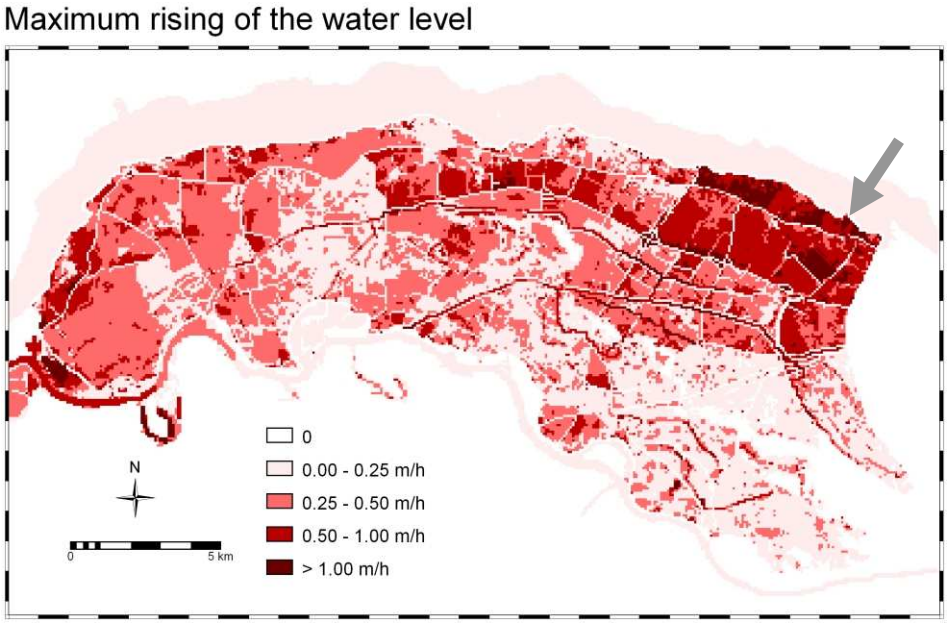

Figure 7.11d. Rising of the water level: dike breach near Weurt, present topography.

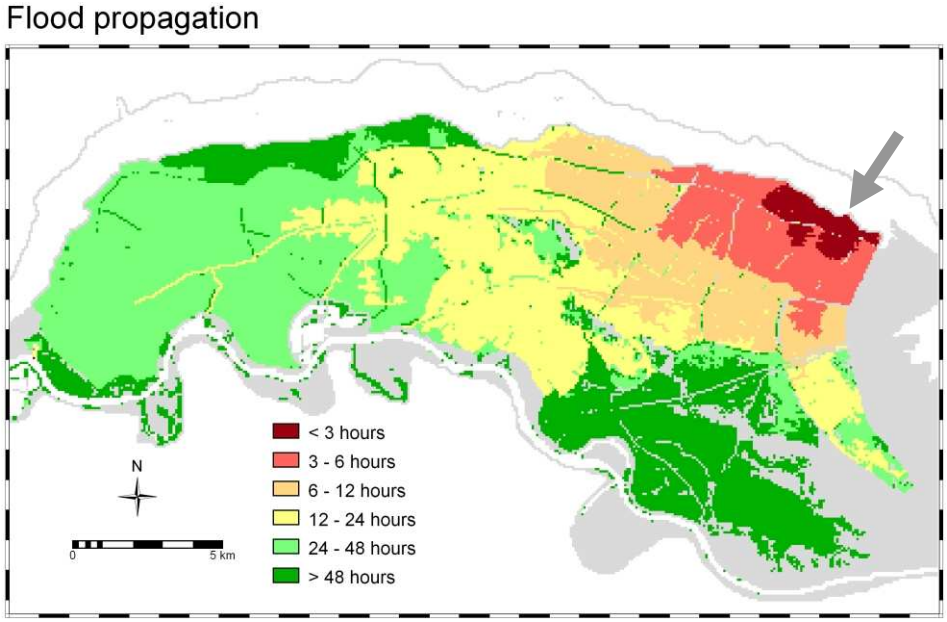

Figure 7.11e. Flood propagation map: dike breach near Weurt, present topography.

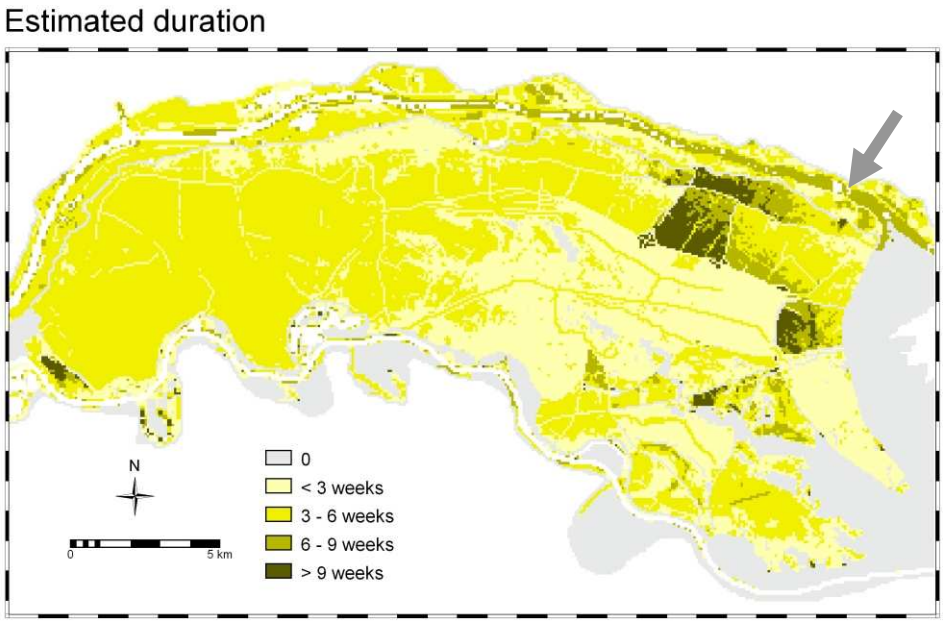

Figure 7.11f. Duration map: dike breach near Weurt, present topography.

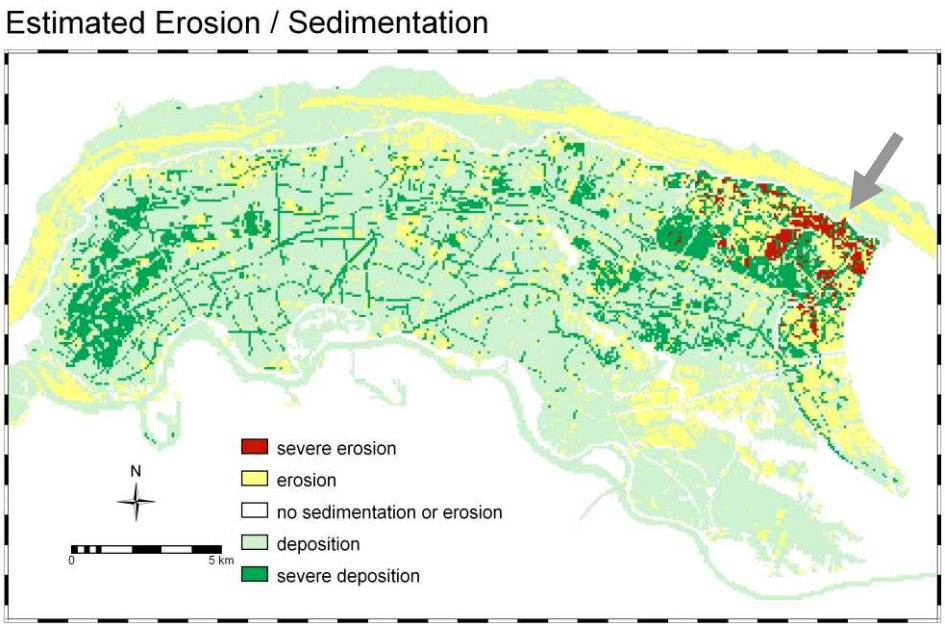

Figure 7.11g. Sedimentation/erosion (scour) map: dike breach near Weurt, present topography.

7.8 Flood damage estimation

In the Netherlands, a standardized method has been developed by the Directorate-General for Public Works and Water Management (*Rijkswaterstaat*) to estimate the possible monetary damage for flood scenarios (Kok et al. 2002). It uses a unit loss method to estimate the flood damage, the so-called stage-damage curve method. It is based on the assumption that for each land-cover type a relationship exists between the inundation depth and the degree of direct damage to units of that particular land-cover type. Van der Veen and Logtmeijer (2005) point out that this way only the direct costs are incorporated and that indirect effects are neglected. The degree of damage is expressed on a scale from 0 (no damage) to 1 (complete destruction). An example of such a relationship is given in Figure 7.12.

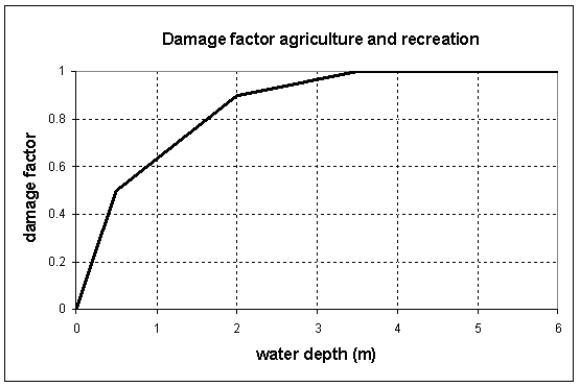

Figure 7.12. Stage-damage curve for agriculture and recreational areas (Kok et al. 2002)

The strength of this approach is that in some countries good records exist of the damage caused to all kind of land-cover types by the floodwater (e.g. by insurance companies) together with information on the maximum water levels at these locations. Especially in the U.S.A. a lot of work has been carried out in this field. see e.g. NRC (1999) and Pielke et al. (2002). In countries where this data is not collected systematically, the curve approach is also applied, but in these cases one has to realise that most curves are crude approximations, often based more on common sense than on hard evidence. Simply copying U.S. data to a European or African or Asian setting will not work because of differences in building materials, methods, crop types, mitigation measures, etc. Still they are widely applied and do give a good first idea on the direct consequences of floods, even though absolute damage estimates have to be taken cautiously. To apply this method, one needs the following pieces of information:

- Maximum water depth;
- Land-cover map;
- Stage-damage curves for all affected elements in the flooded area;
- Replacement costs of the affected elements.

If the value (replacement cost) of each land-cover elements is known (e.g. of a flooded house, or the yield of crops, the curves can be used to estimate the damage by multiplying the degree of damage with the value of these elements. The total damage is calculated by summing-up all the damages in the flooded area. Kok et al. (2002) have constructed stage-damage curves for all major land-cover units in the Netherlands. Their method was applied to the 28 flood scenarios in this study.

An example of the damage map for the scenario of a dike breach near Weurt and the present topography (the water depth map is shown in Figure 7.11a) is given in Figure 7.13. The accumulated totals for all scenarios are listed in Table 7.3.

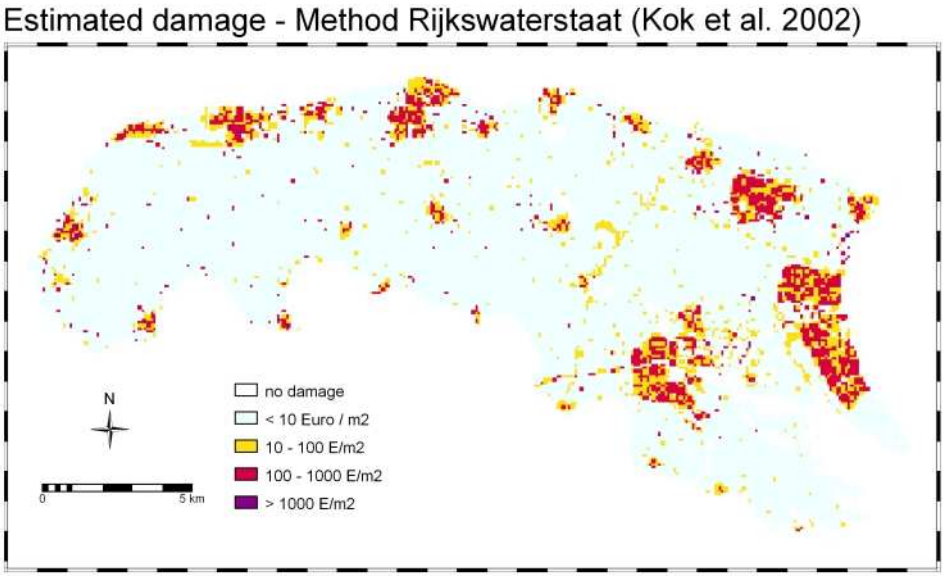

Figure 7.13. Flood damage map in Euros/m², based on the method of Rijkswaterstaat.

Table 7.3. Overview of flood damage for the 28 scenarios (in million Euros).

Location	Type	Present situation	Cleaned situation	Restored situation	Selective changes
Weurt (Waal)	Breach	5400	5300	5500	4300
	Spill-over	1900	1700	2000	905
Deest (Waal)	Spill-over	740	740	761	711
Druten (Waal)	Spill-over	627	629	645	588
Overasselt (Maas)	Breach	2600	2600	2700	2500
	Spill-over	1400	1400	1400	1300
Batenburg (Maas)	Spill-over	859	906	907	946

7.9 Strengths and limitations of the stage-damage curve method

Single parameter methods for flood-risk assessment simplify the complexity of a flood event because they reduce a dynamic spatial-temporal process to a single static map. Often the map showing the maximum water depths is used. It is this simplification that makes them relatively easy to apply and to link them with post-event damage surveys. During a damage inventory after a flood event, it is relatively easy to record the maximum water depth as well, either by interviews with the local people or by measuring the wetting marks on buildings and other structures. Also remote sensing techniques can be used to obtain the maximum flood extent. It is then possible to find relationships for different classes of structures and buildings between the degree of damage and the water depth. Their strength is that there (often) exists an underlying database that forms the foundation for these stage-damage relationships (see previous chapter), although they often fail to disclose the uncertainty around the curves. It is possible to quickly estimate the possible damage of a flood event if the following pieces information are available:

- Map of maximum water depths;
- Land-cover map;
- Stage-damage curves;
- Monetary replacement value of the buildings and structures affected.

The simplification of the single parameter method is also its limitation. It is clear that not only the depth of the flood defines the degree of damage, but also the flow velocity (kinetic energy or impulse), duration (indirect costs for shelters and production loss), sedimentation (clean-up costs) and warning time (evacuation and preparedness). These parameters are hardly ever included in post-event surveys and it is therefore nearly impossible to relate them to degree of damage to specific objects.

Another limitation is that stage-damage relationships are area specific. In different areas different methods and techniques are used for construction. Some areas are more inclined to construct with wood, other with bricks and again other with reinforced concrete. It is therefore not possible to use relationships from one area to any other without proper justification of the applicability of the relationships.

A final limitation is that this method tends to express the impact of the flood in economic, monetary terms. It neglects – or fails to quantify – other consequences of the flood that are often less tangible or more indirect.

7.10 Results and conclusions

From the damage estimates of the 28 flood scenarios it can be seen that the location of the breach or spill-over has great effects on the total damage. The further downstream the location, the lower the total damage. This is because a smaller part of the polder is inundated. Failure at the most upstream located point of the polder will result in the highest damage. Furthermore, the damage associated with a catastrophic dike breach is significantly higher than in case of a spill-over inundation. The breaching of the dike creates an enormous gradient between the water level in the river and the low-lying polder surface. This results in a much higher flux of floodwater into the polder than during a controlled overtopping at a spill-over location. So from a safety and damage reduction point of view it can be concluded that it makes sense to prefer controlled overtopping over catastrophic breaching.

Comparison of the damage estimates of the scenarios showed that neither the complete restoration of the old secondary dike systems nor its complete removal would result in a significant reduction of the damage. This can be explained as follows. Most secondary dikes are too low to block the water flow completely and therefore have no significant affect on the maximum water depth in the polder. Since the method of *Rijkswaterstaat* uses only the maximum water depth to estimate the total damage, the damage results will consequently also be similar. In the D-scenarios a strategic plan was developed with the aim of guiding the water away from the vulnerable urban areas where a lot of valuable property is concentrated. The water was guided to the more rural parts of the polder. This strategic approach does reduce the damage in the inundated area. It can therefore be concluded that complete restoration or removal of the secondary dike systems will not improve the safety situation in the polder, unless a strategy is followed to protect the more vulnerable parts. A well-designed compartment layout, comprising both modern and (repaired) historic embankments can reduce the

damage caused by an inundation. Whether this reduction is economically feasible is not addressed in this thesis.

It should also be noted that embankments and internal dikes not only control the inflowing floodwater, but also create storage locations that drain badly and could extend the inundation time up to 2 months. This is not reflected in the damage estimates, but will cause additional problems for the recovery after the flood event has passed. Furthermore it should be noted that this kind of inundations may also result in back-bursts, that is dike failures at the downstream end of the polder when water levels in the river have already dropped. These may cause a sudden release of water from the polder back into the river resulting in a fast rise in discharge and water levels in the rivers causing additional problems downstream. See also the *Ziltendorfer Niederung* case study described in Chapter 4 where this actually happened.

Chapter 8 Multi-parameter flood-risk assessment

The previous chapters in this thesis deal primarily with flood simulation. Delft-FLS is used for flood scenario studies and the results of these simulations can be expressed in parameter maps to describe the main characteristics of a flood event. The main difficulties regarding the applicability of flood modelling as a provider of information to decision makers, lie with the transformation of the hazard assessment to risk or damage. In this chapter Spatial Multi Criteria Evaluation is introduced as a tool to support this transformation process and to define multi-parameter flood-risk maps.

Abstract

This chapter describes the application of Spatial Multi Criteria Evaluation (SMCE) for multi-parameter flood-risk assessment. SMCE is already widely applied to integrate spatial data to support decision-making and for environmental impact assessment. The strength of SMCE is that it structures complex spatial problems and that it offers a procedure to reach a balanced decision while taking many different parameters in consideration. In this chapter, SMCE is used for the multi-parameter risk assessment in the *Land van Maas en Waal* case study (see previous chapter). The first requirement of SMCE is to clearly state the goal of the evaluation. For flood-risk assessment this is important because it forces the evaluators to clearly define the objectives of the risk assessment: what is it going to be used for? Who will be the users? Do they have a specific purpose in mind, for instance to prioritise evacuation or should the map be generic – or multi-purpose. Once the goals are set, the procedure guides the (group of) evaluators along several steps that eventually results in a final output, a decision. If all agree on all steps along the way, they also have to agree on the decision. In this chapter two different specific purpose maps are shown as a result of two different goals: 1) assessment of evacuation priority, and 2) assessment of potential damage for a specific dike breach scenario. It is concluded that SMCE is a useful tool to guide stakeholders in flood-risk assessment through the process of combining flood hazard maps with (implicit) vulnerability data.

8.1 Introduction

In the previous chapters it was shown that to quantify the magnitude of a flood, it does not suffice to provide only water depth or flood extent. Flood events are complex spatial-dynamic processes and to quantify their impact on exposed elements in the flooded area, a multi-parameter approach is required. In the case studies discussed in this volume is shown that by using a 2D flood propagation model, a series of parameter maps can be generated that describe the dynamic behaviour of the inundation process and that give valuable information for assessing the socio-economic consequences of a flood event. The idea of using multiple parameters to evaluate the flood impact is not new, as can be seen by numerous publications on this topic. Most use two or at maximum three parameters, for instance Gendreau (1998) combines inundation depth, duration and maximum acceptable return period, Témez (1992) and Penning-Rowsell and Tunstall (1996) who combine flow velocity and inundation depth, and Borrows (1999) who combines flow velocity, inundation depth and warning time. Also the risk maps in Chapter 6 can be viewed in this light. A limited set of flood parameter maps has been used to obtain a map with *structural damage* – based on impulse (water depth x flow velocity), and *non-structural damage* – based on water depth and duration. The *social* risk map is based on water depth, warning time and maximum speed of rising of the water level.

No procedure exists yet that includes all seven flood parameter maps that were presented in this book (water depth, flow velocity, impulse, warning time, duration, rising of the water level and sedimentation/scouring). The difficulty is, of course, that it is hard or perhaps impossible to develop such a procedure because information on the spatial distribution of the flood impact is often unavailable (or is classified) which inhibits establishing relationships between flood parameters and flood consequences. However, implicitly each parameter does hold information on its consequences: deeper water depths create higher flood-risk, and so does longer duration and shorter warning times. This implicit information can be used to assess flood-risk. This approach differs from previous multi-parameter flood-risk procedures because it does not rely on vulnerability relationships between magnitude of the hazard and the impact on the elements exposed, like stage-damage curves or graphs that predict under what circumstances pedestrians and cars are washed away, see e.g. Smith (2002). It is based on expert knowledge from hydrologists, engineers, disaster managers, economists, relief workers, local and

regional authorities, farmers, etc. but it can also be based on experiences of those exposed to floods and their perception of its impact. In short, this approach is based on the knowledge of the stakeholders and experts involved in a flood disaster. This chapter will show that spatial multi-criteria evaluation (SMCE) offers opportunities to formalise the procedure for multi-parameter risk assessment using this expert knowledge. The vulnerability is implicitly included in the transformation process from multiple flood parameter maps to a potential flood-risk map.

8.2 Spatial Multi Criteria Evaluation (SMCE)

Spatial multi criteria evaluation can be thought of as a process that combines and transforms geographical data (input) into a resultant decision (output) – see Figure 8.1 (Malczewski, 1999). This process includes, apart from geographical data, also the decision maker's preferences and the manipulation of the data and preferences according to specified decision rules. The result is an aggregation of multi-dimensional information into a single parameter output: the decision.

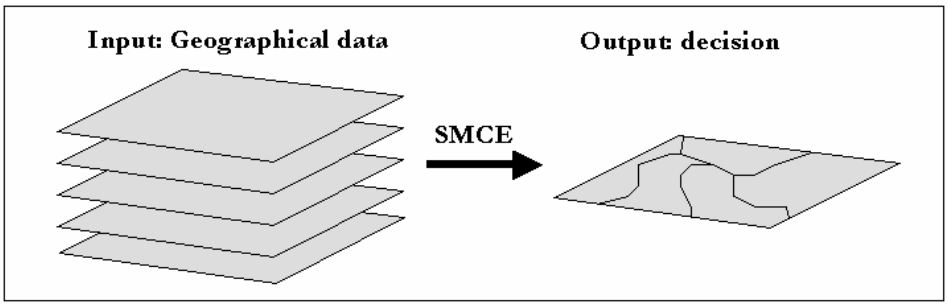

Figure 8.1. Spatial multi criteria evaluation (after Malczewski, 1999)

The strength of these support systems is that they force the users (decision makers) to structure their problem (Scott Morton, 1971; Densham, 1991) and thus clearly outline their information requirements. Initially decision support systems were developed for complex business decisions, but in the last 20 years they have become applied to spatial problems as well, see e.g. Carver (1991), Chen et al. (2001), Sharifi et al. (2002), Pfeffer (2003) and Zucca (2005).

Before starting with an SMCE it is important to clearly define the goal, or set of goals of the decision maker or group of decision makers. Goals are the desired end states of the decision-making activities, for instance in the case of flood-risk the

goals is to decrease flood-risk in a given area or to avoid that flood-risk increases as a consequence of certain activities. In defining the goals for a multi-parameter flood-risk assessment two dichotomies can be distinguished: 1) specific purpose flood-risk maps versus general purpose flood-risk maps, and 2) evaluation of the present situation versus evaluation of a future situation (after a change has occurred).

Table 8.1. Goals for multi-parameter flood-risk assessment.

	Specific purpose	**General purpose**
Present situation	Specific flood-risk definition	General flood-risk definition
Future situation	Specific flood-risk impact assessment	General flood-risk impact assessment

These two dichotomies are shown in Table 8.1. The dichotomy specific versus general purpose can be related to a distinction between a team assessment and a coalition assessment (Rothenberg, 1975): a team is defined as a group of people with a mutually consistent set of preferences. Even though a team may consist of many people, they seem to act as a single entity because they have a common vision on the goal and the criteria evaluation to reach that goal. A coalition on the other hand can be defined as a group of people who compromise their partly similar, partly divergent outlooks (Rothenberg, 1975). Coalition partners can agree on the structure of the problem and on the general goal (a single model), but may disagree on the relative importance of the evaluation criteria. The consequence of these different opinions is that it necessitates multiple analyses to accommodate the various preferences of the coalition participants, whereas a single analysis is possible for team members (Malczewski, 1999). For example, relief workers can generate a specific purpose flood-risk map, based on a set of criteria, like warning time, rising of the water level and maximum water depth. The result is a map that will help them in designing evacuation plans. An insurance company can generate a specific purpose map based on maximum water depth, duration, impulse, etc. to estimate damage. Within the group of relief workers or insurance experts there may be discussion on how to evaluate these criteria, but in the end they should be able to synthesise their combined expertise into a single model and analysis to

produce a final product that serves their needs. A general-purpose flood-risk map should accommodate the preferences of all stakeholders, that is relief workers, insurance experts and a multitude of others involved in flood-risk assessment. It is therefore a compromise of divergent objectives and may thus not serve the specific needs of specific (groups of) stakeholders, but it may serve the needs of a higher-level decision maker like a local, regional or national authority.
The distinction of present versus future situation is linked to the requirements of the multi-parameter flood-risk assessment. Does it serve to inform the stakeholders on the present situation, or is it required to study the consequences of a proposed action that could alter the flood-risk situation? In any case agreement is required within the team (specific purpose) or within the coalition (general purpose) on the goals, the problem structure and the importance of the evaluation criteria. A study focussed on the present situation serves to inform the stakeholders, decision makers and authorities about possible critical locations. In case a future situation needs to be evaluated – for instance as part of an Environmental Impact Assessment (EIA), the study of the present flood-risk situation serves as a reference or baseline study to identify areas where the flood-risk will increase or decrease.

8.3 SMCE for decision-making

Rational decision-making requires a careful analysis of the problem. A frequently applied approach is to decompose the problem into smaller, understandable parts that express relevant concerns. These smaller parts are the evaluation criteria (Malczewski, 1999; Pfeffer, 2003), standards by which a proper decision can be made. Saaty (1980) discusses this process, also called analytical hierarchy process (AHP), in further detail. The evaluation criteria can be further decomposed into objectives and attributes (Saaty, 1980; Malczewski, 1999; Pfeffer, 2003). An objective conveys a desired state that an individual or group would like to achieve, while an attribute is used to characterise an objective. Attributes can be quantified by parameters (some authors use the term indicator, e.g. Lorentz, 1999) – see also Figure 8.2.

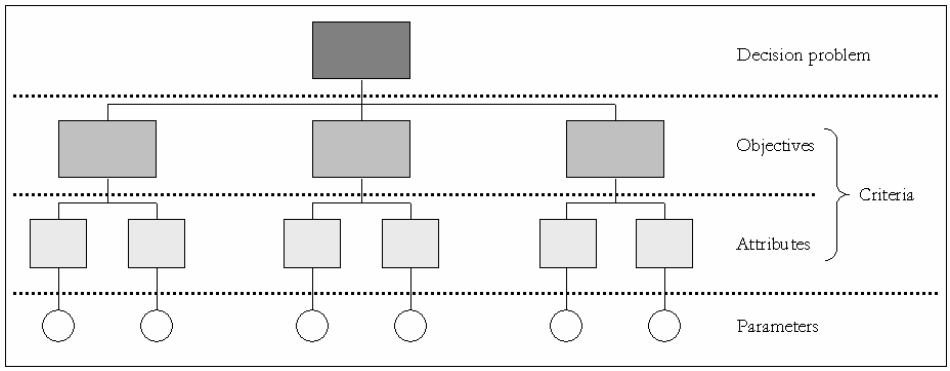

Figure 8.2. Decomposition of a decision problem into objectives, attributes and parameters. In principal there is no restriction to the number of hierarchical levels of objectives and attributes.

In this respect it is important to make another distinction and that is between discrete and continuous methods. Discrete methods tackle choice problems in which alternatives are selected from a discrete (and limited) set of alternatives, whereas continuous methods are more suitable for design problems (Beinat, 1997). Some authors define the latter type of evaluation as multi-objective decision-making (e.g. Hwang and Masud, 1979; Malczewski, 1999). In this chapter the decision problem is related to the definition of flood-risk, which does not evaluate a set of alternatives but rather seeks to find a good definition of flood-risk that provides the best possible information required for the decision-making – either for a specific purpose or for a general purpose. To select from an (in potential) infinite set of solutions, the stakeholders can use the procedure of SMCE to reach agreement on the objectives of the risk map, the set of criteria and the processing of this information. If agreement exists at all stages of the SMCE-procedure, they must also agree on the outcome: the flood-risk map. In this way SMCE adds to the decision-making process in the sense that it identifies agreements and disagreements between the stakeholders, that it brings understanding, supports learning-by-doing and that it reveals areas where thinking is necessary (Beinat, 1997). Furthermore, SMCE supports the solution of a decision problem by analysing its robustness with respect to uncertainty (Geneletti, 2002).

In the transformation process of the parameter maps into an output map four consecutive steps have to be taken: 1) identification of the parameter maps as costs or benefits; 2) standardisation of the parameter maps; 3) establishment of the

importance of each individual criterion with respect to the decision problem; and 4) establishment of the aggregation procedure. An additional sensitivity analysis can be included to test the robustness of the outcome.

1 Cost and benefit parameters

The distinction between costs and benefit criteria is critical because with benefit criteria a high parameter value will have a positive effect on the achievement of the objective, where as with cost criteria a high value is disadvantageous. In the case of flood-risk, high maximum water depth values are advantageous for flood-risk – the higher the better; thus water depth is a benefit criterion. Warning time is the opposite: longer warning times result in less flood-risk, which makes it a cost criterion. Whether or not positive effects can balance disadvantageous effects depends on the choice for compensatory or non-compensatory techniques. In compensatory techniques poor performances on one criterion can be compensated by good performances on another, of course within specific limits (Beinat, 1997) – for instance the high-risk effects of high maximum water depths may be compensated by long warning times. In non-compensatory techniques this counterbalancing is not possible. This can be the case if certain thresholds or limits are surpassed that are considered as absolute, for instance all locations flooded within 3 hours fall within the highest risk category, regardless of the performance of the other criteria. Identification and definition of such limits must be included in the SMCE procedure, either by agreement of all stakeholders, or because of outside forces, like legislation and directives.

2 Standardisation

Each criterion has its own scale of measurement. Water depth is often expressed as a length, for instance in meters, flow velocity is measured as meters per second, or kilometre per hour; duration in hours, days or weeks, etc. It is clear that it makes no sense to simply add-up or multiply the values from the parameter maps. Apart from the fact that this would result in physically meaningless numbers, it would also make the result a function of the scale of measurement (depth in millimetre or in meter, duration in hours or weeks – the result would be very different). To overcome this problem a standardisation is required. This step – the value assessment (Geneletti, 2002) - transforms the parameter values of each parameter map into scores on an equal, dimensionless scale – often between 0 and 1. This operation is performed by generating a value function, i.e. a mathematical relationship that represents human judgements, knowledge and goals. The value

function explicitly links the factual information in the parameter maps to the corresponding parameter scores. The value function can be linear, meaning that equal increments of the parameter value result in equal increments in the parameter scores, but can also be non-linear or discontinuous. Figure 8.4 gives an example. During the establishment of the appropriate form of the function model, the value assessment, the assessors face a dilemma (Beinat, 1997): on the one hand, the assessment aims at a numerical specification of the value function model, implying high precision and good knowledge of the transformation process; in practice, on the other hand, the assessors often find it difficult to provide reliable numerical judgements and prefer qualitative and tentative responses. Beinat (1997) deals in depth with the value assessment and shows that this duality is at the basis of the many attempts that have been made to provide adequate solutions. Defining the value functions is one of the major discussion topics in the multi-criteria evaluation procedure. The assessor is most likely to be a group of people (experts, stakeholders). They either form a team or a coalition, but together they have to reach agreement on the value functions for each parameter included in the assessment. This should avoid possible bias from individual members, but raises new problems like composition of the expert group (number and backgrounds of the experts) and the interaction within the group (see e.g. Ferell, 1985; Van Steen, 1991 – in Beinat, 1997).

3 Prioritisation

During the prioritisation, the preferences of the stakeholders with respect to the evaluation of the criteria are incorporated in the decision model. This is typically done by assigning weights to the criteria. The weights reflect the importance of each criterion relatively to the other criteria under consideration (Malczewski, 1999). The assignment of the weights is the second crucial step that, like the value assessment, is likely to be a group process in which the group members will have to reach agreement. To facilitate this discussion several techniques have been developed to assist the process of normalised weight assignment. Normalised in this context means that the sum of the weights equals 1. Among these are the following (Malczewski, 1999):

- Ranking methods in which the assessor ranks the criteria in order of preference. The numerical weights are then assigned as function of the rank;
- Rating methods in which the assessor assigns weights on a predetermined scale to each criterion using a predefined procedure. The numerical

weights are then assigned by normalisation (dividing each weight by the sum of all weights);

- Pair-wise comparison method in which the assessor compares each possible pair of criteria and rates one relative to the other on a scale from "equal importance" to "extremely more important". Comparison of all possible pairs results in a so-called ratio-matrix. The numerical weights are determined by normalizing the eigenvector associated with the maximum eigenvalue of the ratio matrix (Saaty, 1980).

4 Aggregation

The outcome – or decision – depends on both the value functions (standardisation) and the weight-factors for each criterion (prioritisation) but also on how these are combined in a decision model. This is called the aggregation step (Geneletti, 2002). The most widely used aggregation method is the weighted linear combination, also called simple additive weighting or scoring method. This method is based on the concept of weighted average (Malczewski, 1999). In its simplest form a decision could be defined as:

$$F(x) = \Sigma_n(W_k\,(f_k(x))) \qquad 8.1$$

Where:

$F(x)$ = the outcome (the decision) as a result of n criteria.
W_k = the normalised non-negative weight of the k^{th} criterion.
$f_k(x)$ = the value function of the k^{th} criterion.

Because the results of the value functions are on a scale from 0 to 1 and because the sum of the normalised weights equals 1, the resulting map F(x) is a dimensionless scalar map with scores between 0 to 1. Scores close to 0 identify areas where the criteria are absolutely disadvantageous and scores close to 1 indicate areas that meet the criteria perfectly. This method assumes that the criteria provide independent evidence and that there is no uncertainty in the decision situation. The first assumption means that there is no correlation between any two criteria. The second assumptions means that all relevant information about the decision situation is known and that there is a known deterministic connection between every decision and the corresponding outcome (Malczewski, 1999). In practice these two assumptions are hard or impossible to test. To deal with uncertainty in a deterministic decision situation, sensitivity analysis can be performed to study the effects of uncertainty. Malczewski (1999) describes in-

depth alternative methods that are based on probability and on fuzzy-set theory as well as other decision models like several programming methods.

5 Sensitivity analysis

Until now we have implicitly assumed that all information required for decision-making is available to the decision makers: no errors in the criterion maps, no uncertainty in the assignment of weights and value functions and choice of decision model. Although methods exist to include uncertainty directly into the decision-making process, the most often applied approach is to incorporate them into the decision-making process indirectly, using a so-called sensitivity analysis. Sensitivity analysis is concerned with the way in which errors in a set of input data affect the error in the final outcome. In other words, it serves to test the robustness of the decision with respect to uncertainties in the parameter maps, weights, value functions and decision rules. Errors in the parameter maps can be classified into positional and attribute errors (e.g. Burrough and McDonnell, 1998). The first type of errors deals with uncertainty regarding the location, i.e. errors in the X-, Y- and Z-coordinate. The second type of errors deals with uncertainty regarding the measurement value or with misclassification of objects. Since most maps in flood-risk assessment are based on modelling results, the latter type of errors also includes uncertainty generated during the modelling phase (due to inaccuracy in model input, boundary conditions, initial conditions and by approximations in the modelling procedure). There are ways to assess the map errors, for instance using root-mean-square error, or with a confusion matrix (Burrough and McDonnel, 1998).

Errors introduced in SMCE during the standardisation, prioritisation and aggregation are also called preference uncertainty (Malczewski, 1999). Decision makers are not able to provide precise judgements due to limited or imprecise information and knowledge. These types of errors do not always result from mistakes, although mistakes create errors of course, but are rather the result of a margin between the best judgement and alternative estimates. Within a group process, the range of possible weights and value functions can be estimated (with some level of confidence). During the sensitivity analysis this range-estimate can be used to test the robustness of the outcome. For instance the minimum and maximum limits of the range can be used instead of the best estimate, leaving all other factors constant. Another possibility is to specify a distribution model for each uncertainty range (normal, triangular, block, …) and to run a so-called Monte-Carlo simulation. In a Monte Carlo simulation a high number of runs are executed,

where during each run parameter values are taken from the distribution models. The result is not a single outcome, but an outcome with an error distribution.

8.4 SMCE for multi-parameter flood-risk maps – an example

Chapter 7 shows the results of scenario simulations using a 2D flood propagation model. The recurrence probability (annual probability of occurrence) of these scenarios is estimated to be once in 1250 years. This estimate is based on the on the return period of the flood wave in the river (*Randvoorwaardenboek*, 2001). For each scenario, a stack of seven flood parameter maps is computed: 1) maximum water depth, 2) maximum flow velocity, 3) maximum impulse, 4) maximum rate of water level rise, 5) flood propagation time, 6) flood duration, and 7) sedimentation and scouring. In this example this stack of flood parameters indicates the flood hazard (the probability of occurrence of an event of a certain magnitude in a given area within a specific period of time) – see Figure 8.3. The vulnerability is implicitly included through the decision rules in the SMCE procedure. If the elements exposed to the hazard are known, e.g. buildings, people, etc. the specific risk for this flood event can be calculated.

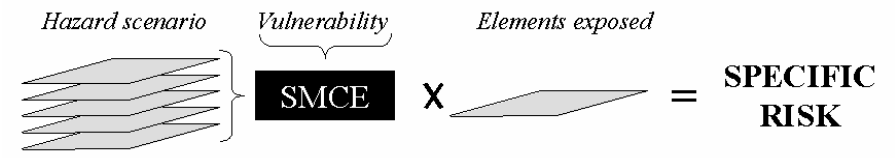

Figure 8.3 Procedure to calculate specific risk, using SMCE.

The aim of this example is to develop 2 different specific purpose flood-risk maps for the present situation in the "*Land van Maas en Waal*". The specific purposes are: 1) a flood-risk map for evacuation plans and 2) a flood-risk map for property. The analysis was carried out with ILWIS SMCE. The input for the application is a number of raster maps of a certain area (so-called 'criteria' or 'effects'), and a criteria tree that contains the way criteria are grouped, standardized and weighed. The output is one or more maps of the same area (the so-called 'composite index' maps) that indicate the extent to which criteria are met or not in different areas.

For more information see for instance Sharifi and Retsios (2003) and the ILWIS website: http://www.itc.nl/ilwis/. Filling the criteria-tree takes the decision maker through steps 1 to 4 (see below). It defines the decision problem in terms of "groups" (objectives), which can in turn be subdivided in "factors", and "constraints" (attributes). Factors allow for compensation whereas constraints are binding criteria that allow no compensation. In the criteria tree parameter maps can be linked to the factors and constraints.

Step 1: identification of cost and benefit parameters

The aim is to assess flood-risk which means that parameters maps where high values correspond to high risk are considered to be benefits: they contribute positively to the risk situation. These parameters include: water depth, flow velocity, impulse, rate of water level rising and flood duration. Cost parameters are the inverse of benefit: high values correspond with lower level of risk. This holds for the parameter map warning time – longer warning times is less risk. It is unlikely that any stakeholder involved in the flood-risk assessment would disagree with these classifications. However the situation for the map sedimentation and scouring is bit more complex. Positive values on the map represent sedimentation and negative values scouring (erosion). The further away from zero the values are, the more sedimentation or scouring is expected. To simplify the example, only the sedimentation part is included in the analysis – i.e. only positive values. Determination of whether the parameter is a cost or benefit depends on the situation and the assessor's objectives: when the sediment is unpolluted and fertile, farmers might be positive about it (less risk), however if it is polluted or unfertile, they might disapprove. Other inhabitants will most likely consider sediment as a nuisance that requires cleaning-up. In their opinion, more sediment adds to flood-risk: a benefit! In this example sedimentation will be considered as a benefit.

Step 2: standardisation

For each parameter map a value function is required to transform the parameter values into parameter scores on a scale from 0 to 1. The value functions depend on the objectives of the stakeholders (in this example a team of relief workers and a team of insurance experts).

In ILWIS-SMCE one can choose from several different types of possible value functions, but in this example only the type known as "goal" standardisation method will be used. It allows the inclusion of expert knowledge where the assessor defines a minimum and a maximum threshold for each parameter. All

values below the minimum threshold will be assigned a score of 0; all values above the maximum threshold receive a score of 1. In the range between minimum and maximum thresholds a linear interpolation transforms the value range into a score range between 0 and 1 (Figure 8.4). The resultant value functions are given in Table 8.2 and 8.3.

Step 3: prioritisation

The assignment of normalised weights to the objectives and attributes was done using the so-called rating method (see section 8.3). The rationale behind the choices made in Tables 8.2 and 8.3 is that for evacuation purposes the evacuation objective is the most important, whereas for insurance purposes the direct physical damage is considered as the most important.

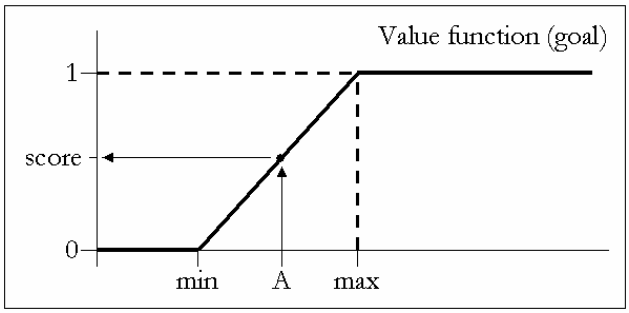

Figure 8.4. Example of a value function (type "goal"): on the horizontal axis are all possible values of a certain parameter map. Values below the lower threshold (min) get a corresponding score of 0, values above the higher threshold (max) get a corresponding score of 1; value A gets a corresponding score based on linear interpolation.

Step 4: aggregation

The aggregation method applied was the weighted linear combination. The result is a relative potential specific risk map that indicates where priority should be given with respect to evacuation or where high damages can be expected for this given flood scenario (see Figures 8.5 and 8.6). To get the actual specific risk map, the potential specific risk map needs to be overlaid with the map containing the location of the exposed elements. In the case of a risk map for evacuation purposes, spatial information is required on the number of people living and working in he area. In case of potential damage, additional information about the value of buildings and crops is needed.

Table 8.2. *(left) Value functions for a flood-risk assessment to prioritise evacuation (B/C stands for benefit or cost). Reference (1): Smith, 2004.*

Table 8.3. *(right) Value functions for a flood-risk assessment to assess potential loss.*

Objective	Attribute	B/C	Unit	Min	Max	Rationale	Weight	
Deposition of material	Deposition	B	-	0	0.08	Based on histogram of the deposition map: the 5% of the area with most deposition gets score=1	0.06	
Duration of disruption	Duration	B	hours	12	48	Duration less than half a day: no need for action. Duration more than 2 days action is required (food and water safety, relocation, ..)	0.21	
Physical destruction	Water depth	B	meter	0.2	3.0	Depth < 20 cm is a nuisance; water depth > 3 meter means 2nd floor is not safe for hiding and storage	0.75	0.21
	Impulse	B	m^2/s	0.1	0.5	< 0,1: no dangerous combination of water depth and flow velocity; > 0,5: danger for pedestrians and cars (1).	0.25	
Evacuation time	Rising of water level	B	m/h	0.2	1.0	< 0.2 m/h is gradualrise; > 1 m/h reduces time to adapt seriously.	0.25	0.52
	Warning time	C	hours	0	48	Everyone with more than 2 days of warning time has sufficient time to prepare and evacuate.	0.75	

Objective	Attribute	B/C	Unit	Min	Max	Rationale	Weight	
Deposition of material	Deposition	B	-	0	0.08	Based on histogram of the deposition map: the 5% of the area with most deposition gets score=1	0.21	
Duration of disruption	Duration	B	hours	6	36	Duration less than 6 hours is no serious disruption. Duration more than 1,5 days brings relocation costs (hotels) and damage to multi-annual crops begins.	0.21	
Physical destruction	Water depth	B	meter	0	6	Damage to contents and crops starts immediately; At depths > 6 meters complete houses are submerged	0.50	0.52
	Impulse	B	m^2/s	0	1	Damage to crops and buildings (also due to debris) starts immediately; > 1 serious damage can be expected to brick buildings (1).	0.50	
Evacuation time	Rising of water level	B	m/h	0.2	1	< 0.2 m/h is gradualrise; > 1 m/h reduces time to adapt seriously.	0.25	0.06
	Warning time	C	hours	0	48	Everyone with more than 2 days of warning time has sufficient time to prepare to reduce damage and evacuate.	0.75	

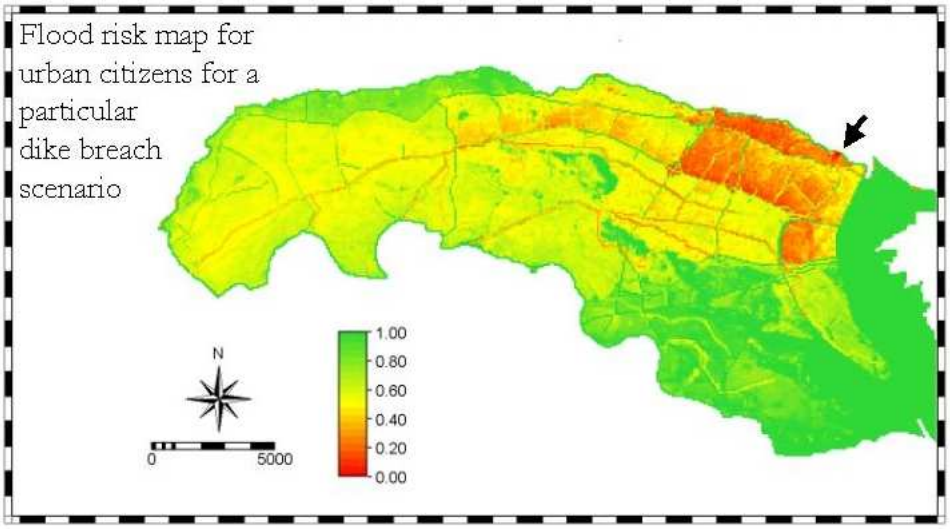

Figure 8.5. Relative potential specific risk map for evacuation purposes (evacuation priority) in case the dike breaches at the location indicated by the arrow with a 1:1250 years discharge in the river.

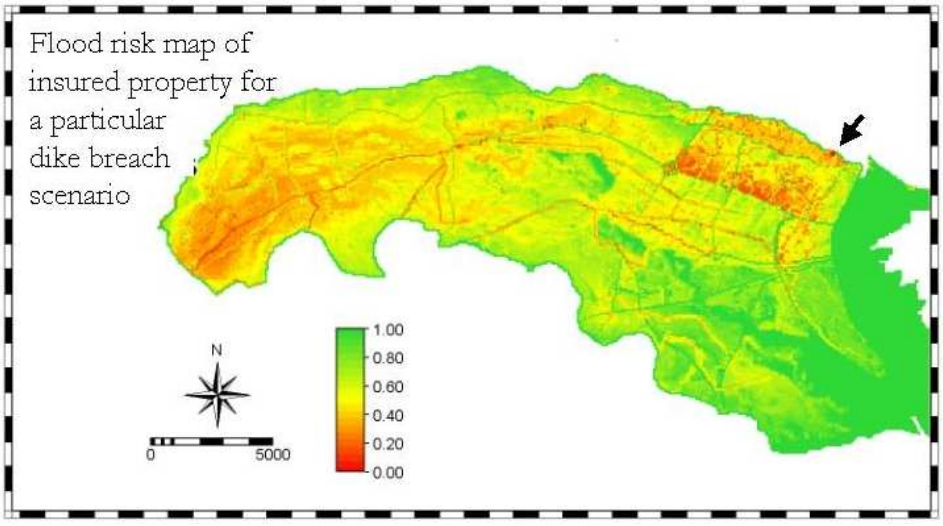

Figure 8.6. Relative potential specific risk map for to estimate potential damage (for e.g. insurance purposes) in case the dike breaches at the location indicated by the arrow with a 1:1250 years discharge in the river.

8.5 The multi-parameter specific flood-risk maps

The results of the SMCE, shown in Figures 8.5 and 8.6, are quite different, which illustrates well that the objective(s) of the assessors have to be well-stated at the start. For the map in Figure 8.5 emphasis was put on evacuation prioritisation. This resulted in high weights for warning time (the amount of time between the moment of dike breaching and the arrival of the first flood water) and the speed with which the water level rose – see Table 8.3. However these two parameters alone were not considered sufficient to prioritise evacuation, because low maximum water depths decrease the need for evacuation. And the same reasoning goes for the duration: if the water remains somewhere only for a short period of time, evacuation might not be necessary either. In Figure 8.5 it can be seen that the priority area for evacuation lies directly behind the breach, which is a result of the short warning times (< 6 hours), but also a result of the compartments created by the provincial road, the motorway A73 and the railroad. These resulted in high inundation depths (> 2m), quick rising of the water level (> 0,5 m/h) and long duration of the inundation (> 6 weeks) - see Figures 7.11 a, d, e and f.
The second specific risk map puts emphasis on the potential for damage. High weights were given to the damaging components of the inundation: the amount of moving water (impulse) which can cause structural damage and the maximum water depth which is an indicator of how much property is getting wet. Duration of the flood and deposition of material may also contribute significantly to the damage. Duration is a factor because certain materials will decay if exposed to water for too long and (tree-)crops will perish if they are submerged for too long. Duration is also an indicator of how long businesses are discontinued (economic damage) and how long people will have to be evacuated (relocation costs). Sedimentation adds to the damage component because it requires clean-up operations, that especially in urban areas can be quite costly. These considerations resulted in priority areas of expected damage in the lower parts of the polder because of the high water depths (> 4m) and severe deposition of material, and directly behind the breach due to the high impulse (>0.4 m^2/s) and long duration (>6 weeks) – see Figures 7.11 a, c, f and g.

8.6 Conclusion

Floods cannot be described in general by one single parameter. A set of parameters is required to characterise the multiple aspects a flood event. Furthermore, different end users of flood-risk maps have different needs and requirements (objectives). These need to be taken into account before a useful and understandable flood-risk zonation can be made. Even though different groups of end users are discussing the same flood, some relate high risk to short warning time; others to high flow velocities and again others might define flood-risk simply by water depth. Thus, each user will assign different priority to different flood parameters and will use a different standardisation procedure. The result is that different actors will construct different flood-risk zonations for one and the same flood. The difference lies in the definition of the vulnerability. This chapter demonstrates that vulnerability can be introduced implicitly into the procedure using SMCE by defining the standardisation, prioritisation and aggregation rules. The results can be interpreted as priority areas for a predefined goal or objectives. If the goal is to define priority areas for evacuation (which people have to be evacuated first) the map presented in Figure 8.5 can be used. If the objective is to identify areas where the largest damage will occur, the map in Figure 8.6 can be used.

Chapter 9 Synthesis

9.1 Summary

This thesis deals with the application of a 2D hydraulic flood propagation model (Delft-FLS) for flood hazard and risk assessment. It focuses on two components: 1) what is the performance of the model or, how well does it predict the characteristics of the simulated floods and 2) how can the model results be transformed into a flood hazard and flood-risk assessment.
Before these questions are answered, this thesis first gives an overview of the interaction of geo-hazards with the socio-economic environment. **Chapter 2** introduces the widely accepted risk concept of Varnes who defines risk as the product of hazard and vulnerability. Furthermore it is shown that it is insufficient to assess the direct consequences of an event, but that also indirect effects need to be addressed, especially when large scale terrain modifications are planned. In the case of floods this almost automatically directs the assessor towards deterministic modelling tools because these are capable of translating changes in input parameters (like modified terrain) into change in flood characteristics. **Chapter 3** explains that the traditional definition of hazard applied to low-land areas is not very useful and that in these areas additional information is needed to differentiate the hazard in the hazardous area, like how long does it take before an area (polder) is flooded, what are the maximum water depths, flow velocities etc.? 2D flood models are identified as the appropriate tools for simulating the flow of water over (nearly) flat terrain and complex topography and the theory behind numerical flood modelling is shortly described. A flood simulation in Trento – Northern Italy – is used to introduce the flood model Delft-FLS and it is explained how a series of flood parameter maps are derived from the model results. **Chapter 4** demonstrates a thorough testing of the model by reconstructing a flood event in Germany in 1997. With an independent validation data set it is shown that Delft-FLS is capable of giving a realistic reconstruction of this flood event. Water levels were predicted up to 30 cm accurate and it is argued that a large part of this error can be attributed to errors in the boundary conditions. One of the findings presented in this chapter is that the reduction of the downstream river discharge due to a dike breach is controlled by the development of the breach growth and the surface roughness coefficient in the inundated area. In Chapters 5, 6 and 7

scenario studies show the use of Delft-FLS for different purposes. In **Chapter 5** "what-if" scenarios were simulated to gain more understanding of the 1997 flood event and to see what effect certain mitigation measures might have on the inundation of the polder and on the downstream river discharge. **Chapter 6** deals with the applicability of Delft-FLS to assess the impact of a new motorway on an alluvial plain, as part of an Environmental Impact Assessment. In this chapter the concept of risk is reintroduced and it is observed that decision makers are usually willing to include flood considerations in their decision-making process, but that information about changes in water levels are of no use to them. Therefore the changes in flood characteristics are quantified in terms of economic damage and social risk so that these can be incorporated in the EIA instead of the flood parameter maps. **Chapter 7** focuses on the effect of sub-compartments in a polder and it is concluded that (low) compartmentalizing dikes have a significant effect on the propagation of the flood through the area. On one hand they can be used to delay water flow towards vulnerable areas. On the other hand, the water level will rise much faster in the smaller sub-compartments which will increase the impact on the inhabitants living there. The compartment dikes may also hinder the draining of the area, prolonging the duration of the flood in certain areas. Eventually, during large floods, the compartment dikes themselves are overtopped and the whole polder is flooded without any significant reduction of the maximum water depth. The Dutch standard method - based on stage-damage relationships - is applied to estimate the damage of the flood scenarios. This method uses the maximum inundation depth as input, and because these do not show much variation between the different scenarios, the total damage estimates for the scenarios depend more on the breach location (the more downstream, the less the damage) than on the compartment lay-out. **Chapter 8** deals with a new tool to define flood-risk as a function of seven flood parameter maps: 1) maximum water depth, 2) maximum flow velocity, 3) maximum impulse, 4) maximum speed of rising of the water level, 5) estimated duration of the flood, 6) the propagation speed of the flood water (or warning time) and 7) an estimate of the sedimentation and scouring. With clearly defined objectives, Spatial Multi-Criteria Evaluation (SMCE) can be used to integrate these seven maps are into a flood-risk map. Two examples of specific purpose flood-risk maps are given: 1) to prioritise evacuation for a given flood event and 2) to estimate potential structural damage. This method does not create a risk map as defined by Varnes, because vulnerability is introduced implicitly into the procedure. However, it is concluded that SMCE is useful for creating specific and general purpose multi-parameter flood-risk maps. It

guides the (group of) assessors through a well structured procedure and if everyone agrees on each step along the way, they also have to agree on the outcome: the risk map.

9.2 Conclusions

Societal consequences of floods

From a geomorphologic point of view floods are natural processes that are part of the dynamics of fluvial systems. A geomorphologist considers the alluvial plain as the domain of the river that is flooded every once in a while. Some parts are flooded more frequently than other parts, but all parts were inundated at some point in history as witnessed by the fluvial sediments. And there is a chance that they'll be flooded again in the future. To reduce the impact of floods, mitigation measures can be introduced that serve to keep the river water separated from the socio-economic activities that developed on the alluvial plain. These protection measures can fail either because they were not well designed, constructed or maintained or because an event occurred that was not anticipated (beyond the design criteria). Whatever the reason, as soon as the flood water enters areas where people live and work, it will cause enormous damage and will result in suffering. And this happens all over the world. People get killed or injured, buildings and infrastructures are destroyed or damaged and socio-economic activities come to a halt or are severely hindered. And these are only the direct effects of floods. Indirect effects may include the spread of diseases, loss of jobs and social unrest. In this study is further demonstrated that human activities and constructions on the alluvial plains can have a significant effect on the flood characteristics, resulting in inundation of previously unaffected areas, shorter warning times and greater flood depths. These unforeseen induced hazards should also be included in flood hazard studies.

The increase in flood disasters that is observed nowadays, might partly be attributed to changes in flow regimes of the rivers due to land use change, climate change and river engineering (increase of hazard). But other important factors are the growing accumulation of property in flood-prone areas and the increasing susceptibility to disruption of our increasingly complex society (increase of vulnerability). A relatively small event may then quickly turn into a disaster. There is growing awareness among the public and decision-makers that flood

considerations need to be included in the decision-making process and to be better prepared for the next flood.

Objectives of this study

This study deals with the application of flood propagation models for hazard and risk assessment. It does not just deal with the application of existing techniques to simulate the behaviour of floods (hazard assessment), but it explores their application to assess the consequences of flood interference with our socio-economic environment (risk assessment). This last step is crucial because flood considerations will only be included in the decision-making process when the consequences of floods can be expressed in terms like damage or humans affected. The research question that is addressed in this thesis is "*how to apply flood propagation models for hazard and risk assessment?*" One part of the question deals with the flood propagation model itself - what are its data requirements, what are the results (output) it generates and how well do those simulations compare with real flood events? The second part of the question deals with the transformation of these model results into meaningful flood-risk maps that can be integrated in the decision-making process.

The quality of the flood model

This thesis presents three case studies using Delft-FLS to simulate the propagation of the floods. It was demonstrated how the model results, hourly maps of flow velocity and water depth can be converted to a set of parameter maps that describe the complex, dynamic behaviour of a flood event. The three case studies demonstrated that flood modelling studies are capable of evaluating the effects of changes in flood controls (surface topography, land-cover, flow regime) in terms of flood characteristics: spatial distribution of water depth, flow velocity, rising of the water level, flood propagation. It is concluded that major alterations of surface topography can significantly alter the behaviour of flood events.

Reconstruction of a flood event in Germany has shown that the results of Delft-FLS are close to the measured values (< 0.3 meters), not only for the water depth, but also for the timing of the first arrival of the floodwater and the speed of rising and falling of the water levels. Differences could be largely attributed to inconsistencies in the input data, especially in the hydraulic boundary conditions like the upstream discharge boundary and the downstream stage-discharge relationship. Another important factor in accurate flood modelling is a correct representation of the surface topography. High resolution, high accuracy terrain

models are available, but computation time limits the number of grid-cells and thus presently prohibits the use of terrain models with too many grid-cells (>100,000). This poses a dilemma for the modeller who has to find a balance between acceptable computation times and accurate representation of the surface topography. When high resolution terrain models are resampled to a coarser resolution, critical elevation values for flow influencing structures like dikes and embankments have to be maintained. These elements compartmentalize the alluvial plain and can alter the flow behaviour. Tunnels and bridges must also be included in the surface model because these elements play an important role in the connectivity of the compartments. Especially for the flood propagation characteristics and speed or rising of the water level, a correct representation of the compartmentalization of the area is crucial. The use of satellite imagery and land-cover maps to get a spatial distribution of surface roughness coefficients, obtained from literature, seems to yield satisfying results.

Flood modelling as support for decision-making

With the use of flood models, we are now capable of studying floods without getting our feet wet. Flood propagation models give us better insights in flood characteristics like water depth, flow velocity, warning time, duration, etc. The simulation of possible future floods can also assist in assessing the consequences of human activities and – if necessary – adapt the activities to minimize the negative effects. For instance in the Trento case study (Chapter 6) and in the case study "*Land van Maas en Waal*" (Chapter 7) it is clear that large modifications in the surface topography have a pronounced effect on the characteristics of a flood event. These changes may have negative consequences for the people living and working in that area. It is therefore concluded that hydraulic modelling should therefore be an integrated part in any study to large scale alterations of topography and land-cover in vulnerable and flood-prone areas. Flood modelling should be integrated in the Environmental Impact Assessment that is usually mandatory for these kinds of activities in most countries.

Flood disasters have an enormous impact on a local, regional and sometimes national level. The floodwater destroys and disrupts lives, property and economic activity. Understanding of this process is pivotal for quantifying the impact of floods. Without justified quantification of the flood impact, it is not possible to compare two flood scenarios and to evaluate which scenario is best. Furthermore it is concluded that flood considerations can only be included in the decision-making process if societal consequences are quantified in a meaningful way. Only this way

can they be balanced against other factors that decision makers have to consider. The process of transforming flood parameters into a risk assessment is a difficult, multi-disciplinary endeavour. Often only direct effects are considered (like direct damage to buildings), while wider range effects are neglected. In this thesis it is shown that different approaches can be followed, for instance quantifying the risk in monetary terms (damage) or in "social" terms (amount of suffering, number of people affected, etc.). It is concluded that mono-parameter approaches to quantify the effects (Varnes' definition of risk, stage-damage curves) are insufficient to comprise the complex interaction of floods and society. The difficulty of multi-parameter approaches is they are more subjective and often focus on specific components of flood impact. It is shown in this thesis that Spatial Multi Criteria Evaluation can assist in multi-parameter risk assessment. SMCE guides the (group of) assessors through a well structured procedure and if everyone agrees on each step along the way, they also have to agree on the outcome. It is concluded that SMCE is useful tool for creating specific and general purpose multi-parameter flood-risk maps.

9.3 Flood simulation for disaster preparedness

In the last few decades a lot of progress has been made in understanding potentially hazardous geologic and geomorphologic processes. The flood model that was deployed in this study is a good example of this development. We can learn from floods and use that knowledge to better deal with them through hydraulic simulations. The model tells us – given specified boundary conditions – where the water will go to, what water depths can be expected, how fast the water flows, how long it will take to reach a certain point, how long it will stay there, etc. This study has shown that these flood parameters can be fairly well estimated. Sufficiently in any case, to use them as basis for policy making, decision support and planning.

It is impossible to predict when the next floods will happen. Also other factors like breach location and breach development cannot be predicted. However these problems can be overcome by simulating flood scenarios, analysing them and seeing what we can deduce from the simulations.

The major challenge of today – in my opinion – in reducing the impact of flood disasters, is to put these models to use. What lessons can be learned from flood

simulations and how can these lessons be implemented? Many examples of flood disasters – also recent ones, like in New Orleans, USA – have shown that a major part of the real tragedy lies not so much in the flood event itself, but in the handling of the consequences in the aftermath. Authorities and relief workers seem to be overwhelmed by the scale of the flood and response is often seen as too slow, too little. Of course immediate resources are scarce, but that makes it even more critical that they are used efficiently and without delay.
Simulation of floods can help here. The state-of-the-art hydraulic models represent the accumulated knowledge of hydraulic engineers and many other scientists that have contributed to their development. It is now a challenge to incorporate this knowledge of the spatial and dynamic nature of floods in the training of those working in disaster management, relief coordination, etc. and to include these models in the decision process to enable better decision-making. This requires efforts from both sides. The scientific community has to reach out and attempt to understand the information requirements from decision makers; this study should be seen as an attempt to do so. On the other hand those working in disaster management have to have an open mind to information coming from computer simulations and use that knowledge to optimise their decisions. Perhaps then the next big flood will not become the next big disaster.

9.4 Recommendations

The main conclusions of this thesis are that flood propagation models are suitable tools to simulate floods. But their accuracy is only as good as the input data that is provided. Recently accurate terrain representation has become available in the form of LIDAR DTMs and high resolution satellite imagery. In this study was found that regarding the hydraulic boundary conditions – discharge, rating curves – often less accurate data was available, or was non-existent. It is therefore recommended that more attention must be paid to the monitoring of rivers, specially in urbanized, flood-prone areas.
The quantification of the impact of floods still requires a lot of research. After flood events, inventories should be made to get insight in the spatial distribution of the damage and other forms of impact. This must be done systematically so that consequences of different flood events can be compared and analysed. A useful technique for this is the participatory approach to assess the perception of flood-

risk and coping strategies of people living in flood-prone areas. This kind of multi-disciplinary research should be stimulated.

References

Abbott, M. B. and Price, W.A. (1994): Coastal, estuarial and harbour engineer's reference book. E and FN Spon, London. UK.

Abbott, P.L. (1996): Natural Disasters. Wm. C. Brown Publishers, Dubuque, U.S.A.

Abt, R.S. Wittler, R.J. and Taylor, M. (1989): Predicting human instability in flood flows. Hydraulic engineering; Proc. Of the ASCE Hydraulic Division Conference.

Albertson, M.L. and Simons, D.B. (1964): Fluid mechanics, flow in open channels. In: Chow, V.T. (Ed) Handbook of applied hydrology. McGraw-Hill book company, New York, USA.

Alcrudo, F. and Garcia Navarro, P. (1994): Computing two dimensional flood propagation with a high resolution extension of McCormack's method. In (eds) Molinaro, P. and Natale, L.: Modelling of flood propagation over initially dry areas. American Society of Civil Engineers, New York. pp. 373.

Alkema, D. (2003): Flood-risk assessment for EIA; an example of a new motorway near Trento, Italy. Acta Geologica, Studi Trentini di Scienze Naturali. Museo Tridentino di Scienze Natural – Trento. Vol. 78. pp 147-154

Alkema, D. and Cavallin, A. (2003): Geomorphologic risk assessment for EIA. Acta Geologica, Studi Trentini di Scienze Naturali. Museo Tridentino di Scienze Natural – Trento. Vol. 78. pp 139-146.

Alkema, D and Middelkoop H. (2005): The influence of floodplain compartmentalization on flood-risk within the Rhine-Meuse delta in: Natural Hazards 36. pp 125-145.

ANUFLOOD: Natural Hazards Research Centre Division of Environmental & Life Sciences. Macquarie University North Ryde, NSW 2109, Australia.

Arcement, G.J. and Schneider, V.R. (1990): Guide for Selecting Manning's Roughness Coefficients for Natural Channels and Flood Plains; USGS Water-supply Paper 2339. pp 67.

Barnes, H.H. (1967): Roughness characteristics of natural channels. USGS Water-supply paper 1849.
http://www.engr.utk.edu/hydraulics/openchannels/Index.html

Bates, P.D. and De Roo, A.P.J. (2000): A simple raster based model for flood inundation simulation. Journal of Hydrology 236 (p 54-77). Elsevier, the Netherlands.

Beinat, E. (1997): Value functions for environmental management. Kluwer Academic Publishers, the Netherlands. Pp. 241.

Beinat, E. and Nijkamp, P. (1998): Multi-criteria evaluation for land use management. Kluwer Academic Publisher, Dordrecht, the Netherlands.

Beinat E. Bressan, M. Jones, M. and Fabbri, K. (1999): Geographical Information Systems and Environmental Impact Assessment. UNIGIS introduction module, Faculty of Economics, Vrije Universiteit Amsterdam, the Netherlands.

Benkhaldoun, F. and Monthe, L. (1994): An adaptive nine-point finite volume Roe scheme for two-dimensional Saint-Venant equations. In (eds) Molinaro, P. and Natale, L.: Modelling of flood propagation over initially dry areas. American Society of Civil Engineers, New York. Pp. 373.

Beven, K. Calver, A. and Morris, E.M. (1987): The Institute of Hydrology distributed model. Institute of Hydrology report 98, Wallingford UK.

Blyth K. Baltas, E. Benedini, M and Givone, P. (2001): Risk of Inundation – Planning And Response Interactive User System (RIPARIUS) final report. Centre for Ecology and Hydrology (CEH), Wallingford, UK. Internet document: http://www.nwl.ac.uk/ih/riparius/

Borrows, P. (1999): Issues for flood warning in extreme events. Report of RIPARIUS Expert Meeting 1. Centre for Ecology and Hydrology (CEH), Wallingford, UK.

Brunner, G.W. (2002): HEC-RAS River Analysis System; Hydraulic Reference Manual. US Army Corps of Engineers, Davis, USA.

Burrough, P.A. and McDonnell, R.A. (1998): Principles of Geographical Information Systems. Oxford University Press, UK.

Carver S. J. (1991) Integrating multi-criteria evaluation with geographical information systems, International Journal of Geographical Information Systems, 5(3); 321-339.

Cavallin, A. Marchetti, M. Panizza, M. and Soldati, M. (1994): The role of geomorphology in environmental impact assessment. Geomorphology 9. Elsevier, the Netherlands.

Cavallin, A and Marchetti, M. (1995): Geomorphology and environmental impact assessment: a practical approach. Proc. of 1st and 2nd workshops on

human capital and mobility project. Quaderni di Geodinamica Alpina e Quaternaria, 3. pp 99-107.

Chen, K. Blong, R. and Jacobson, C. (2001): MCE-RISK: integrating multicriteria evaluation and GIS for risk decision-making in natural hazards. Environmental modelling and software 16. pp 387-397.

Chagas, P. and Souza, R. (2005): Solution of Saint Venant's equation to study flood in rivers, through numerical methods. Hydrology Days, pp 205-210.

Chow, V.T. (1959): Open channel hydraulics, McGraw – Hill, Inc. New York, USA.

Chung, C.F. and Fabbri, A.G. (1999): Probabilistic prediction models for landslide hazard mapping, Photogrammetric Engineering & Remote Sensing, Vol.65, No.12, Pages 1389-1399.

Conway, J. (2000): Flood in Europe, a peril not to be ignored. GenRe research publication. November 2000.

Densham, P.J. (1991): Spatial decision support systems, In: D. J. Maguire, M. S. Goodchild and D. W. Rhind (eds) Geographical information systems: principles and applications, London: Longman, pp. 403 - 412.

De Roo, A.P.J. Wesseling, C.G. and Van Deursen, W.P.A. (2000): Physically based river basin modelling within a GIS: the LISFLOOD model. Hydrological Processes 14, 1981-1992.

Dhondia, J.F. and Stelling, G.S. (2002): Application of one dimensional – two-dimensional integrated hydraulic model for flood simulation and damage assessment. Hydroinformatics 2002.

De Saint Venant, B.M. (1871) : Théorie du movement non permanent des eaux, avec application aux crues des rivières et à l'introduction des marées dans leur lit. Académie des sciences (France). Comptes rendus hebdomadaires des séances de l'Académie des sciences. (T. 73). Pages 1544 p. (pp 147-154 and pp 237-240).

Di Giammarco, P. and Todini, E. (1994): A control volume finite element method for the solution of 2D overland flow problems. In (eds) Molinaro, P. and Natale, L.: Modelling of flood propagation over initially dry areas. American Society of Civil Engineers, New York. Pp. 373.

Dresback, K.M. Kolar, R.L. and Dietrich, J.C. (2005): On the form of the momentum equation for shallow water models based on the generalized wave continuity equation. Advances in Water Resources 28, 345-358.

Driessen, A.M.A.J. (1994): Watersnood tussen Maas en Waal. Overstromingsrampen in het rivierengebied tussen 1780 en 1810. Walburg Pers Zutphen, the Netherlands.

Ferell, W.R. (1985): Combining individual judgements. In G. Wright (ed) Behavioral decision-making. Plenum, USA.

Fread, D.L. (1992): Flow Routing. In: Maidment, D.R. (Ed) Handbook of Hydrology. pp 10.1 – 10.36 McGraw – Hill, Inc. New York, USA.

Gendreau, N. (1998): Protection objectives in flood-risk prevention. Proceedings of the British Hydrological Society International Conference, Exeter, UK 6-10 July 1998, p. 145-154.

Geneletti, D. (2001): Metodologia per la realizzazione di una carta di copertura del suolo nell'area compresa tra Trento Nord e la bassa Val di Non; Acta Geologica, Studi Trentini di Scienze Naturali, vol 78; Museo Tridentino di Scienze Naturali – Trento, Italy, p. 103-107.

Geneletti, D. and Alkema D. (2001): A case study in Environmental Impact Assessment: the decision problem, the project and the area affected; Acta Geologica, Studi Trentini di Scienze Naturali, vol 78; Museo Tridentino di Scienze Naturali – Trento, Italy, p. 97-102.

Geneletti, D. (2002): Ecological evaluation for environmental impact assessment. PhD thesis. Netherlands Geographical Studies 301.

Grayson, R.B. Moore, I.D. and McHahon, T.A. (1992): Physically based hydrological modelling 1. A terrain based model for investigative purposes. Water Resources Research 28(10), pp 2639-2658.

Grünewald, U. (1998): The causes, progression and consequences of the Oder floods in summer 1997. Including remarks on the existence of risk potential; an interdisciplinary study – abridged version. Translation from German by M. Seymour. German IDNDR-committee for Natural Disaster Reduction. Bonn, Germany.

Harris, G. (2002): Integrated assessment and modelling: an essential way of doing science. Environmental modelling and software 17, 201-207.

Hervouet J.M. and Janin, J.M. (1994): Finite element algorithms for flood propagation. In (eds) Molinaro, P. and Natale, L.: Modelling of flood propagation over initially dry areas. American Society of Civil Engineers, New York. Pp. 373.

Hervouet, J.M. and Van Haren, L. (1996): Recent advances in numerical methods for fluid flows. In: Anderson, M.G. Walling, D.E. and Bates, P.D. (Eds) Floodplain Processes. Pp 183 – 214. John Wiley & Sons Ltd. England.

Hesselink, A.W. (2002): History makes a river. Morphological changes and human interference in the river Rhine, The Netherlands. PhD-thesis Faculty of Geographical Sciences, University of Utrecht, Netherlands Geographical Studies 292.

Hesselink, A.W. Stelling, G.S. Kwadijk, J.C.J. and Middelkoop, H. (2003): Inundation of a Dutch river polder, sensitivity analysis of a physically based inundation model using historic data. Water Resources Research, 39(9), art. no. 1234.

Horritt, M.S. and Bates, P.D. (2002): Evaluation of 1D and 2D numerical methods for predicting river flood inundation. Journal of Hydrology 268, 87-99.

Hwang, C.L. and Masud, A.S.M. (1979): Multi-objective decision-making – methods and applications: a state of the art survey. Springer, Berlin.

Kamrath, P. Disse, M. Hammer, M. and Köngeter, J. (2006): Assessment of discharge through a dike breach and simulation of flood wave propagation. Natural Hazards 38, 63-78.

Keeney, R.L. (1996): Value-focused thinking: Identifying decision opportunities and creating alternatives. Eur. J. of Operational Research 92; Elsevier Science B.V. Amsterdam, the Netherlands. p 537-549.

Keskin, M.E. and Agiralioglu, N.A. (1997): Simplified synamic model for flood routing in rectangular channels. Journal of Hydrology 202, pp 302-314.

Kleinhans, M. (2002): Derivation of the Froude number. Utrecht University, Faculty of Geosciences. Personal Communication.

Kok, M. Huizinga, H.J. Meijerink, T.C. Vrouwenvelder, A.C.W.M. Vrisou van Eck, N. (2002): Standaardmethode 2002 Schade en Slachtoffers als gevolg van overstromingen. Eindrapport. Dienst Weg en Waterbouwkunde, Rijkswaterstaat. Delft, Nederland.

Lorenz, C.M. (1999): Indicators for sustainable river management. PhD-thesis, Vrije Universiteit Amsterdam, the Netherlands.

Malczewski, J. (1999): GIS and multi-criteria decision analysis. Wiley and sons, Inc. USA. Pp 392.

Mandleburger, G. (2001): Digital Elevation Model of the Grenzoder. Institute of Photogrammetry and Remote Sensing, Vienna University of Technology.

Moser, D.A. (1994): Assessment of the economic effects of flooding. In: Rossi et al (Eds) Coping with Floods. Kluwer Academic Publishers, the Netherlands

Munich Re (2004): Annual review: Natural catastrophes 2003. Münchener Rückversicherungs-Gesellschaft. München, Germany.

Nieuwenhuis, J.D. (1996): Flood mitigation in the Netherlands; plans for the flood plain of the Meuse. River Flood Disasters. Report of the ICSU SC / IDNDR workshop, Koblenz, Germany, 1996 (IHP-OHP-Berichte : Sonderheft ; 10).

NOAA/NWS (2000) Flood Losses - Compilation of Flood Loss Statistics; web document: http://www.nws.noaa.gov/oh/hic/flood_stats/Flood_loss_time_series.htm

NRC - National Research Council (1999). The Impacts of Natural Disasters: A Framework for Loss Estimation. National Academy Press, Washington, DC.

Penning-Rowsell, E.C. & Tunstall, S.M. (1996): Risks and resources: Defining and managing the floodplain. In: Andersen, M.G. Walling, D.E. and Bates, P.D. (Eds) Floodplain resources. John Wiley and Sons, Ltd. London, UK.

Pfeffer, K. (2003): Integrating spatio-temporal environmental models for planning ski runs. PhD thesis. Netherlands Geographical Studies 311.

Pielke, R.A. Jr. Downton, M.W. and Miller, J.Z.B. (2002): Flood damage in the United States, 1926 – 2000; A reanalysis of National Weather Service estimates. National Center for Atmospheric Research, Boulder Colorado,. US.

Randvoorwaardenboek (2001): Design discharges for Rhine and Meuse. WL|Delft Hydraulics.

Refsgaard, J.C. and Storm, B. (1995): MIKE-SHE In: V.J. Singh (Ed) Computer models in watershed hydrology. Water Resources Publications.

RIPARIUS: see e.g.Borrows, P. (1999): Issues for flood warning in extreme events. Report of RIPARIUS Expert Meeting 1. Centre for Ecology and Hydrology (CEH), Wallingford, UK.

Rivas, V. Rix, K. Francés, E. Cendrero, A and Brunsden, D. (1994): The use of indicators for the assessment of environmental impacts on geomorphologic features. In: Marchetti, M. Panizza, M. Soldati, M. and Barani, D. (Eds) Geomorphology and Environmental Impact Assessment (Quaderni di Geodinamica Alpina e Quaternario. CNR. Milano, Italy, p.157-180.

RIZA: Institute for Inland Water Management and Waste Water Treatment; Research and advisory body for the Directorate-General for Public Works and Water Management (Rijkswaterstaat) of the ministry of

Transport, Public Works and Water management. Lelystad, the Netherlands. http://www.riza.nl/index_uk.html

Rothenberg, J. (1975): Cost-Benefit analysis: A methodological exposition. In (eds) Guttentag, M. and Strüning E.L. Handbook of evaluation research. Sage Publications, USA.

Rotmans, J. (1998): Methods for IA: The challenges and opportunities ahead. Environmental Modelling and assessment 3 155-179.

Saaty, T.L. (1980): The analytical hierarchy process: Planning, priority setting and resource allocation. McGraw-Hill, USA.

Scott Morton, M. S. (1971): Management Decision Systems; Computer-based support for decision-making. Boston, Division of Research, Graduate School of Business Administration, Harvard University.

Selby, M.J. (1989): Earth's changing surface. Clarendon Press. Oxford, United Kingdom.

Sharifi, M.A. Van den Toorn, Rico, A. and Emmanuel, M. (2002): Application of GIS and Multicriteria Evaluation in locating sustainable boundary between the Tunari National Park and Cochabamba city (Bolivia). Journal of Multi-Criteria Decision Analysis 11, pp. 151-164.

Sharifi, M.A. and Retsios, V. (2003): Site selection for waste disposal through spatial multiple criteria decision analysis. In: Proceedings of the 3rd International conference on decision support for telecommunications and information society DSTIS, 4-6 September 2003, Warsaw, Poland. 15 p.

Silva, W. Klijn, F. and Dijkman, J. (2001): Room for the Rhine branches in the Netherlands: What research has taught us. Report of the Ministry of Transport, Public Works and Water Management, Directorate-General for Public Works and Water Management, the Hague, the Netherlands.

Stelling, G.S. Kernkamp, H.W.J. and Laguzzi, M.M. (1998): Delft Flooding System, a powerful tool for inundation assessment based upon a positive flow simulation. In Babovic and Larsen (Eds) Hydro-informatics 1998; Balkema; Rotterdam the Netherlands. pp 449-456.

Stelling, G.S. (2000): Delft-FLS user manual, WL | Delft-Hydraulics, version 2.47, May 2000.

Stelling, G.S. and Duinmeijer, S.P.A. (2003): A staggered conservative scheme for every Froude number in rapidly varied shallow water flows. Int. Journal for Numerical Methods in Fluids, 43. pp 1329-1354.

Stelling, G.S. and Verwey, A. (2005): Numerical flood simulation. Encyclopedia of Hydrological Sciences. John Wiley and Sons Ltd. UK. Vol 1, pp 257-270.

Smith, D.I. (1994): Flood damage assessment - a review of urban stage damage curves and loss-functions. Water South Africa, vol. 20, no 3, July pp 231-238.

Smith, K. (2002): Environmental Hazards, assessing risk and reducing disaster. Routledge, London. pp306.

Témez, J.R. (1991): Planificación hidrológica-ordenación de zones inundables, CEDEX, Madrid, Spain.

US ACE - U.S. Army Corps of Engineers (1996): Risk-based analysis for evaluation hydrologic/hydraulics, geotechnical stability, and economics in flood damage reduction studies. Engineering regulation 1105-2-1-1 dated March 1,1996.

US ACE - U.S. Army Corps of Engineers (1997): HEC: Hydraulic Engineering Software, Davis, CA. USA.

US EPA – U.S. Environmental Protection Agency (1998): Guidelines for ecological assessment. EPA/630/R-95/002F. Washington, DC, USA.

Van Asch T.W.J. and Van Dijck, S.J.E. (1994): The role of geomorphology in Environmental Impact Assessment in the Netherlands. In: Marchetti, M. Panizza, M. Soldati, M. and Barani, D. (Eds) Geomorphology and Environmental Impact Assessment. Quaderni di Geodinamica Alpina e Quaternario. CNR. Milano, Italy, p. 63-70.

Van Beek, R. (2002): Assessment of the influence of changes in land use and climate on landslide activity in a Mediterranean environment. Netherlands Geographical Studies 294.

Van der Veen, A. and Logtmeijer, C. (2005): Visualizing vulnerability to flooding. Natural Hazards 36: 65-80. Springer Publishers.

Van Herwijnen, M. (1999): Spatial decision support for environmental management. PhD-thesis Faculty of Economic Sciences and Econometry, Free University, Amsterdam, the Netherlands.

Van Leussen, W. (2002): Leven met water; vermaatschappelijking van het waterbeheer – consequenties voor de civiel ingenieur en waterbeheersorganisaties. Inauguration speech to the chair of River Basin Management, Technical University of Twente, the Netherlands.

Van Mierlo, M.C.L.M. Overmars, J.M.S. and Gudden, J.J. (2001): Delft-FLS inundatie simulaties van de Ooij-Düffelt polder en de Land van Maas en Waal polder. http://www.compuplan.nl/pe-resultaten-delftfls.htm

Van Steen, J.F.J. (1991): A perspective on structured expert judgement. Report 91-245, Netherlands Organisation for Applied Scientific Research (TNO), the Netherlands.

Van Westen, C.J. ,1993. Application of Geographic Information Systems to Landslide Hazard Zonation. Ph-D Dissertation Technical University Delft. ITC Publication Number 15, ITC, Enschede, The Netherlands, 245 Pages

Van Westen, C.J. (2004): Geo - information tools for landslide risk assessment : an overview of recent developments. In: Proceedings of the 9th International symposium on landslides, June 28 - July 2, 2004 Rio de Janeiro. London: Balkema, 2004. pp. 39-56

Varnes, D.J. (1984): Landslides hazard zonation: a review of principles and practice. UNESCO, Paris, Natural Hazards, v3, 63 p.

Wathern, P. (1988): Environmental Impact Assessment: theory and practice. Unwin Hyman. London, UK.

White, I.D. Mottershead, D.N. and Harrison, S.J. (1992): Environmental systems, an introductory text; 2nd edition. Chapman & Hall, London, England.

Wood, C. (1995): Environmental Impact assessment. A comparative review. Pearson Education Limited, Harlow, Essex, UK.

WL|Delft Hydraulics: http://www.wldelft.nl/gen/intro/english/index.html

Zucca, A. (2005): Sviluppo sostenibile del territorio: Agenda 21 locale e valutazione ambientale strategica. Proposta di metodologie per la gestione dell'informazione spaziale nei processi decisionali. Unpublished PhD thesis, Università degli studi di Milano-Bicocca.

Curriculum Vitae

Dinand Alkema was born on June 20th, 1969 in Groningen (the Netherlands). He finished his secondary school, the Praedinius Gymnasium in Groningen in 1988. Thereafter, he studied astronomy at Groningen University for one year before he decided to change to Physical Geography at Utrecht University. In 1995 he graduated from this study with a specialization in land degradation with the MSc-thesis "Slope stability zonation in Colombia".

After his graduation he worked for two consulting engineers. First at "Witteveen en Bos" in Deventer until 1996, then at "Ingenieursbureau Milieu Gemeentewerken Rotterdam" (Municipal Engineers). He worked as specialist in geostatistics for large scale soil remediation works in the Rotterdam Harbour. He also developed the "Bodem Zonerings Kaart" for the city of Rotterdam, a data base that gives information on background levels of heavy metals and poly-cyclic aromatic hydro-carbons in the city.

In 1998 he started to work for the GETS project in Milan, Italy. For three years he worked on the Trento case study (presented in this thesis) at the University of Milano-Bicocca. After that he continued his flood research at the EU Joint Research Centre in Ispra, Italy, working on the Oder River dataset. In 2002 He returned to the Netherlands and worked on a "Belvedere" project at Utrecht University (the "*Land van Maas en Waal*" case study). These three case-studies form the core of his work.

Since May 2003 he is employed at the International Institute for Geo-Information Science and Earth Observation (ITC) in Enschede, the Netherlands as lecturer/researcher. His tasks are teaching (flood modelling, flood hazard and risk assessment), research (flood related studies in the Philippines, Sri Lanka, Thailand, and Nepal) and consulting (training courses in Guatemala, Philippines, Thailand and development of training material in Vietnam and Sri Lanka).

He is married and has one son.

Bibliography

Hack, R. Alkema, D. Kruse, G. Leenders, N. and Luzi, L. (2007): Influence of earthquakes on the stability of slopes. Engineering Geology, Elsevier, the Netherlands.

Bin Usamah, M and Alkema, D. (2006): Simulating scenario floods for hazard assessment on the Lower Bicol Floodplain, the Philippines. In Advances in Geosciences, vol. 4 Hydrologiocal Science ed. by Park, N. World Scientific Publishing, Singapore. Pp 69-74.

Alkema, D. and Middelkoop H. (2005): The influence of floodplain compartmentalization on flood-risk within the Rhine-Meuse delta. In: Begum, S. (Ed.) Flooding in Europe: Risk and challenges. Natural Hazards, special issue. Kluwer Academic Publishers, the Netherlands.

Alkema, D. Tennakoon, T. Otieno, J. and Kingma, N. (2004): Strengthening local authorities in flood-risk management: a case study from Naga, the Philippines. In: Brebbia (Ed.) Risk analysis IV; Wessex Institute of Technology.

Alkema, D. (2004): Remote Sensing and Geographical Information Systems in flood forecasting. Proceedings of the National Workshop on Flood Disaster Management – Space inputs. National Remote Sensing Agency, Hyderabad India.

Alkema, D. Cavallin, A. De Amicis, M. and Zanchi A.:(2003): Valutzione degli effetti di un alluvione: il caso di Trento; Studi Trentini di Scienze Naturali – Acta Geologica v. 78 (2001) pp 55-62.

Geneletti, D. and Alkema, D.(2003): A case study in Environmental Impact Assessment: The decision problem, the project and the area affected. Studi Trentini di Scienze Naturali – Acta Geologica v. 78 (2001) pp 97-102.

Alkema, D. and Cavallin, A. (2003):Geomorphologic risk assessment for EIA. Studi Trentini di Scienze Naturali – Acta Geologica v. 78 (2001) pp 139-146.

Alkema, D. (2003): Flood-risk assessment for EIA. Studi Trentini di Scienze Naturali – Acta Geologica v. 78 (2001) pp 147-154.

Alkema, D. Zanchi, A. and De Amicis, M. (2003): Geomorphologic map of the Adige valley north of Trento, Italy. Studi Trentini di Scienze Naturali – Acta Geologica v. 78 (2001) pp 165-172.

Alkema, D. (2001): How landuse changes influence flood effects. The 11th Stockholm Water Symposium: Building bridges through dialogue. Pp 258 - 261

Alkema, D. Cavallin, A and De Amicis, M. (2001): Strategic application of flood modelling for infrastructure planning and impact assessment. Integrated Water Resources Management, proceedings of a symposium held at Davis, California, April 2000) IAHS Publ. No 272. pp 305 – 310.

Alkema, D. Mosselman, M. and Paulussen, I. (1994): Earthquake triggered landslides at the Brunssumerheide, Limburg, the Netherlands: Preliminary studies following the 1992 Roermond earthquake. Geologie en mijnbouw 73. Kluwer Academic Publishers. Pp. 387 – 391.

Abstract

Over the last decades, river floods in Europe seem to occur more frequently and are causing more and more economic and emotional damage. Understanding the processes causing flooding and the development of simulation models to evaluate countermeasures to control that damage are important issues. This study deals with the application of a 2D hydraulic flood propagation model for flood hazard and risk assessment. It focuses on two components: 1) how well does it predict the spatial-dynamic characteristics of floods and 2) how can the model results be transformed into a flood-risk assessment.

Flood-risk results from the interaction of flood water with human activities. This makes flood-risk assessment a multi-disciplinary endeavour: on one hand it requires good understanding of fluvial processes and flood behaviour; on the other hand a methodology is needed to quantify its impact on the socio-economic environment. In this study it is argued that in low-land areas with near-flat terrain and complex topography, traditional definitions of flood hazard and risk, based on magnitude-frequency relations, are not useful and that additional information is needed to differentiate the hazard using multiple parameters, for instance flood propagation, maximum water depths and flow velocities, duration, etc. Two-dimensional flood models are the appropriate tools for simulating flow of water to assess the consequences of terrain modifications on the flood characteristics. This is useful when flood consideration need to be included in the decision-making process and Environmental Impact Assessment studies.

This study presents three case-studies. The inundation of the Ziltendorfer Niederung (Germany) during the 1997 Oder floods is used to test the 2D hydraulic model Delft-FLS. It is shown that the model yielded good results in reconstructing this flood event and that differences between predicted and observed water depths can largely be attributed to errors in the input data. In the second case-study, the model is applied to the Adige floodplain near Trento (Italy) to assess the flood consequences of a planned new embanked motorway. It is concluded that such developments in flood-prone areas can have a significant effect on the flood characteristics and will result in a redistribution of the flood-risk in the area. The third case-study, the "Land van Maas en Waal" in the Netherlands, studies the effect of sub-compartments in a polder. It is concluded that compartmentalizing

structures have a significant effect on the propagation of the flood through the area, the speed of water level rising and on the duration of the inundation. It is demonstrated that Spatial Multi-Criteria Evaluation (SMCE) can be used for multi-parameter flood-risk assessment to generate flood-risk maps that can be used in the decision making process.

It is concluded that Delft-FLS is a powerful tool to simulate flood behaviour over complex topography and that "what-if" scenarios can help to assess the consequences of decisions and actions regarding flood characteristics. It is also concluded that for the incorporation of flood considerations in the decision-making process, the model results need to be transformed to risk. For this, SMCE could be a helpful tool.

Samenvatting

De laatste decennia is West Europa getroffen door een aantal grote overstromingen, veroorzaakt door rivieren, die in toenemende mate grote materiële en immateriële schade veroorzaken. Het is van groot belang om de oorzaken van deze ontwikkeling te onderzoeken. Het gebruik van simulatiemodellen is onderdeel hiervan. Dit proefschrift gaat over het toepassen van een tweedimensionaal overstromingsmodel voor het bepalen van overstromingsrisico's waarbij de volgende twee vragen centraal staan: 1) hoe goed voorspelt een dergelijk model een overstroming in zowel ruimte als tijd, en 2) hoe kunnen de modelresultaten worden vertaald naar overstromingsrisico.

Er is sprake van overstromingsrisico wanneer water gebieden binnendringt waar menselijke activiteiten plaatsvinden. Dit maakt het bepalen van overstromingsrisico's tot een multidisciplinaire aangelegenheid: het vereist aan de ene kant kennis over fluviatiele processen en het verloop van overstromingen, aan de andere kant moeten de sociaaleconomische gevolgen ervan worden vastgesteld. In deze studie wordt gesteld dat in nagenoeg vlakke gebieden met een complexe topografie de traditionele definitie van risico, die gebaseerd is op "*magnitude-frequency*" relaties, tekortschiet en dat aanvullende informatie nodig is om de risico's te differentiëren, bijvoorbeeld door te kijken naar de voortgang van de overstroming, de maximum waterdieptes en stroomsnelheden, de duur van de overstroming, etc. Om deze parameters te verkrijgen, is een tweedimensionaal overstromingsmodel nodig waarmee tevens kan worden geanalyseerd wat de gevolgen zijn van bepaalde ingrepen in de topografie op het gedrag van de overstroming. Dit is vooral van belang wanneer overstromingsrisico's meegewogen dienen te worden bij besluitvorming en milieueffect rapportages.

Deze studie omvat drie "*case-studies*". De overstroming van de Ziltendorfer Niederung (Duitsland) in 1997, is gebruikt om het overstromingsmodel – Delft-FLS – te testen. Uit deze studie blijkt dat Delft-FLS zeer goed in staat is om de overstroming te reconstrueren en dat de verschillen tussen gemodelleerde en gemeten waterdieptes voor een groot deel te wijten zijn aan fouten in de invoergegevens. In de tweede "*case-study*" wordt het model gebruikt om de gevolgen te bestuderen van de aanleg van een verhoogde autoweg in het dal van de Adige, nabij Trento (Italië). Uit deze studie kan worden geconcludeerd dat dit soort

grootschalige ingrepen in overstromingsgevoelige gebieden kunnen leiden to een herverdeling van de risico's. De derde "*case study*" betreft het Land van Maas en Waal waarin het effect van compartimentering in een polder wordt bekeken. De conclusie is dat de compartimentering niet alleen consequenties heeft voor de manier waarop de polder volloopt, maar ook op de stijgsnelheden van het water en de duur van de overstroming. Door middel van een voorbeeld is aangetoond dat Ruimtelijke Multi-Criteria Evaluatie (RMCE) toegepast kan worden om *multi-parameter* risicokaarten te genereren die gebruikt kunnen ter ondersteuning van besluitvorming.

De conclusie is dat Delft-FLS zeer geschikt is voor het simuleren van overstromingen in nagenoeg vlakke gebieden met een complexe topografie en dat het gebruikt kan worden voor scenariostudies om de gevolgen te bepalen van bepaalde ingrepen en beslissingen op het gedrag van overstromingen. Tevens is de conclusie getrokken dat wanneer overstromingen meegenomen dienen te worden in een besluitvormingsprocedure, de modelresultaten vertaald dienen te worden naar de sociaaleconomische gevolgen, de risico's. RMCE kan hierbij een rol spelen.

ITC Dissertation list

1. **Akinyede** (1990), Highway cost modelling and route selection using a geotechnical information system
2. **Pan He Ping** (1990), 90-9003-757-8, Spatial structure theory in machine vision and applications to structural and textural analysis of remotely sensed images
3. **Bocco Verdinelli, G.** (1990), Gully erosion analysis using remote sensing and geographic information systems: a case study in Central Mexico
4. **Sharif, M**. (1991), Composite sampling optimization for DTM in the context of GIS
5. **Drummond, J.** (1991), Determining and processing quality parameters in geographic information systems
6. **Groten, S.** (1991), Satellite monitoring of agro-ecosystems in the Sahel
7. **Sharifi, A.** (1991), 90-6164-074-1, Development of an appropriate resource information system to support agricultural management at farm enterprise level
8. **Zee, D. van der** (1991), 90-6164-075-X, Recreation studied from above: Air photo interpretation as input into land evaluation for recreation
9. **Mannaerts, C.** (1991), 90-6164-085-7, Assessment of the transferability of laboratory rainfall-runoff and rainfall - soil loss relationships to field and catchment scales: a study in the Cape Verde Islands
10. **Ze Shen Wang** (1991), 90-393-0333-9, An expert system for cartographic symbol design
11. **Zhou Yunxian** (1991), 90-6164-081-4, Application of Radon transforms to the processing of airborne geophysical data
12. **Zuviria, M. de** (1992), 90-6164-077-6, Mapping agro-topoclimates by integrating topographic, meteorological and land ecological data in a geographic information system: a case study of the Lom Sak area, North Central Thailand
13. **Westen, C. van** (1993), 90-6164-078-4, Application of Geographic Information Systems to landslide hazard zonation
14. **Shi Wenzhong** (1994), 90-6164-099-7, Modelling positional and thematic uncertainties in integration of remote sensing and geographic information systems
15. **Javelosa, R.** (1994), 90-6164-086-5, Active Quaternary environments in the Philippine mobile belt
16. **Lo King-Chang** (1994), 90-9006526-1, High Quality Automatic DEM, Digital Elevation Model Generation from Multiple Imagery
17. **Wokabi, S.** (1994), 90-6164-102-0, Quantified land evaluation for maize yield gap analysis at three sites on the eastern slope of Mt. Kenya
18. **Rodriguez, O.** (1995), Land Use conflicts and planning strategies in urban fringes: a case study of Western Caracas, Venezuela
19. **Meer, F. van der** (1995), 90-5485-385-9, Imaging spectrometry & the Ronda peridotites
20. **Kufoniyi, O.** (1995), 90-6164-105-5, Spatial coincidence: automated database updating and data consistency in vector GIS
21. **Zambezi, P.** (1995), Geochemistry of the Nkombwa Hill carbonatite complex of Isoka District, north-east Zambia, with special emphasis on economic minerals
22. **Woldai, T.** (1995), The application of remote sensing to the study of the geology and structure of the Carboniferous in the Calañas area, pyrite belt, SW Spain

23. **Verweij, P.** (1995), 90-6164-109-8, Spatial and temporal modelling of vegetation patterns: burning and grazing in the Paramo of Los Nevados National Park, Colombia
24. **Pohl, C.** (1996), 90-6164-121-7, Geometric Aspects of Multisensor Image Fusion for Topographic Map Updating in the Humid Tropics
25. **Jiang Bin** (1996), 90-6266-128-9, Fuzzy overlay analysis and visualization in GIS
26. **Metternicht, G.** (1996), 90-6164-118-7, Detecting and monitoring land degradation features and processes in the Cochabamba Valleys, Bolivia. A synergistic approach
27. **Hoanh Chu Thai** (1996), 90-6164-120-9, Development of a Computerized Aid to Integrated Land Use Planning (CAILUP) at regional level in irrigated areas: a case study for the Quan Lo Phung Hiep region in the Mekong Delta, Vietnam
28. **Roshannejad, A.** (1996), 90-9009-284-6, The management of spatio-temporal data in a national geographic information system
29. **Terlien, M.** (1996), 90-6164-115-2, Modelling Spatial and Temporal Variations in Rainfall-Triggered Landslides: the integration of hydrologic models, slope stability models and GIS for the hazard zonation of rainfall-triggered landslides with examples from Manizales, Colombia
30. **Mahavir, J.** (1996), 90-6164-117-9, Modelling settlement patterns for metropolitan regions: inputs from remote sensing
31. **Al-Amir, S.** (1996), 90-6164-116-0, Modern spatial planning practice as supported by the multi-applicable tools of remote sensing and GIS: the Syrian case
32. **Pilouk, M.** (1996), 90-6164-122-5, Integrated modelling for 3D GIS
33. **Duan Zengshan** (1996), 90-6164-123-3, Optimization modelling of a river-aquifer system with technical interventions: a case study for the Huangshui river and the coastal aquifer, Shandong, China
34. **Man, W.H. de** (1996), 90-9009-775-9, Surveys: informatie als norm: een verkenning van de institutionalisering van dorp - surveys in Thailand en op de Filippijnen
35. **Vekerdy, Z.** (1996), 90-6164-119-5, GIS-based hydrological modelling of alluvial regions: using the example of the Kisaföld, Hungary
36. **Pereira, Luisa** (1996), 90-407-1385-5, A Robust and Adaptive Matching Procedure for Automatic Modelling of Terrain Relief
37. **Fandino Lozano, M.** (1996), 90-6164-129-2, A Framework of Ecological Evaluation oriented at the Establishment and Management of Protected Areas: a case study of the Santuario de Iguaque, Colombia
38. **Toxopeus, B.** (1996), 90-6164-126-8, ISM: an Interactive Spatial and temporal Modelling system as a tool in ecosystem management: with two case studies: Cibodas biosphere reserve, West Java Indonesia: Amboseli biosphere reserve, Kajiado district, Central Southern Kenya
39. **Wang Yiman** (1997), 90-6164-131-4, Satellite SAR imagery for topographic mapping of tidal flat areas in the Dutch Wadden Sea
40. **Saldana-Lopez, Asunción** (1997), 90-6164-133-0, Complexity of soils and Soilscape patterns on the southern slopes of the Ayllon Range, central Spain: a GIS assisted modelling approach
41. **Ceccarelli, T.** (1997), 90-6164-135-7, Towards a planning support system for communal areas in the Zambezi valley, Zimbabwe; a multi-criteria evaluation linking farm household analysis, land evaluation and geographic information systems
42. **Peng Wanning** (1997), 90-6164-134-9, Automated generalization in GIS

43. **Lawas, C.** (1997), 90-6164-137-3, The Resource Users' Knowledge, the neglected input in Land resource management: the case of the Kankanaey farmers in Benguet, Philippines
44. **Bijker, W.** (1997), 90-6164-139-X, Radar for rain forest: A monitoring system for land cover Change in the Colombian Amazon
45. **Farshad, A.** (1997), 90-6164-142-X, Analysis of integrated land and water management practices within different agricultural systems under semi-arid conditions of Iran and evaluation of their sustainability
46. **Orlic, B.** (1997), 90-6164-140-3, Predicting subsurface conditions for geotechnical modelling
47. **Bishr, Y.** (1997), 90-6164-141-1, Semantic Aspects of Interoperable GIS
48. **Zhang Xiangmin** (1998), 90-6164-144-6, Coal fires in Northwest China: detection, monitoring and prediction using remote sensing data
49. **Gens, R.** (1998), 90-6164-155-1, Quality assessment of SAR interferometric data
50. **Turkstra, J.** (1998), 90-6164-147-0, Urban development and geographical information: spatial and temporal patterns of urban development and land values using integrated geo-data, Villaviciencia, Colombia
51. **Cassells, C.** (1998), 90-6164-234-5, Thermal modelling of underground coal fires in northern China
52. **Naseri, M.** (1998), 90-6164-195-0, Characterization of Salt-affected Soils for Modelling Sustainable Land Management in Semi-arid Environment: a case study in the Gorgan Region, Northeast, Iran
53. **Gorte B.G.H.** (1998), 90-6164-157-8, Probabilistic Segmentation of Remotely Sensed Images
54. **Tegaye, Tenalem Ayenew** (1998), 90-6164-158-6, The hydrological system of the lake district basin, central main Ethiopian rift
55. **Wang Donggen** (1998), 90-6864-551-7, Conjoint approaches to developing activity-based models
56. **Bastidas de Calderon, M.** (1998), 90-6164-193-4, Environmental fragility and vulnerability of Amazonian landscapes and ecosystems in the middle Orinoco river basin, Venezuela
57. **Moameni, A.** (1999), Soil quality changes under long-term wheat cultivation in the Marvdasht plain, South-Central Iran
58. **Groenigen, J.W. van** (1999), 90-6164-156-X, Constrained optimisation of spatial sampling: a geostatistical approach
59. **Cheng Tao** (1999), 90-6164-164-0, A process-oriented data model for fuzzy spatial objects
60. **Wolski, Piotr** (1999), 90-6164-165-9, Application of reservoir modelling to hydrotopes identified by remote sensing
61. **Acharya, B.** (1999), 90-6164-168-3, Forest biodiversity assessment: A spatial analysis of tree species diversity in Nepal
62. **Akbar Abkar, Ali** (1999), 90-6164-169-1, Likelihood-based segmentation and classification of remotely sensed images
63. **Yanuariadi, T.** (1999), 90-5808-082-X, Sustainable Land Allocation: GIS-based decision support for industrial forest plantation development in Indonesia
64. **Abu Bakr, Mohamed** (1999), 90-6164-170-5, An Integrated Agro-Economic and Agro-Ecological Framework for Land Use Planning and Policy Analysis

65. **Eleveld, M.** (1999), 90-6461-166-7, Exploring coastal morphodynamics of Ameland (The Netherlands) with remote sensing monitoring techniques and dynamic modelling in GIS
66. **Yang Hong** (1999), 90-6164-172-1, Imaging Spectrometry for Hydrocarbon Microseepage
67. **Mainam, Félix** (1999), 90-6164-179-9, Modelling soil erodibility in the semiarid zone of Cameroon
68. **Bakr, Mahmoud** (2000), 90-6164-176-4, A Stochastic Inverse-Management Approach to Groundwater Quality
69. **Zlatanova, Z.** (2000), 90-6164-178-0, 3D GIS for Urban Development
70. **Ottichilo, Wilber K.** (2000), 90-5808-197-4, Wildlife Dynamics: An Analysis of Change in the Masai Mara Ecosystem
71. **Kaymakci, Nuri** (2000), 90-6164-181-0, Tectono-stratigraphical Evolution of the Cankori Basin (Central Anatolia, Turkey)
72. **Gonzalez, Rhodora** (2000), 90-5808-246-6, Platforms and Terraces: Bridging participation and GIS in joint-learning for watershed management with the Ifugaos of the Philippines
73. **Schetselaar, Ernst** (2000), 90-6164-180-2, Integrated analyses of granite-gneiss terrain from field and multisource remotely sensed data. A case study from the Canadian Shield
74. **Mesgari, Saadi** (2000), 90-3651-511-4, Topological Cell-Tuple Structure for Three-Dimensional Spatial Data
75. **Bie, Cees A.J.M. de** (2000), 90-5808-253-9, Comparative Performance Analysis of Agro-Ecosystems
76. **Khaemba, Wilson M**. (2000), 90-5808-280-6, Spatial Statistics for Natural Resource Management
77. **Shrestha, Dhruba** (2000), 90-6164-189-6, Aspects of erosion and sedimentation in the Nepalese Himalaya: highland-lowland relations
78. **Asadi Haroni, Hooshang** (2000), 90-6164-185-3, The Zarshuran Gold Deposit Model Applied in a Mineral Exploration GIS in Iran
79. **Raza, Ale** (2001), 90-3651-540-8, Object-oriented Temporal GIS for Urban Applications
80. **Farah, Hussein** (2001), 90-5808-331-4, Estimation of regional evaporation under different weather conditions from satellite and meteorological data. A case study in the Naivasha Basin, Kenya
81. **Zheng**, **Ding** (2001), 90-6164-190-X, A Neural - Fuzzy Approach to Linguistic Knowledge Acquisition and Assessment in Spatial Decision Making
82. **Sahu, B.K.** (2001), Aeromagnetics of continental areas flanking the Indian Ocean; with implications for geological correlation and reassembly of Central Gondwana
83. **Alfestawi, Y.** (2001), 90-6164-198-5, The structural, paleogeographical and hydrocarbon systems analysis of the Ghadamis and Murzuq Basins, West Libya, with emphasis on their relation to the intervening Al Qarqaf Arch
84. **Liu, Xuehua** (2001), 90-5808-496-5, Mapping and Modelling the Habitat of Giant Pandas in Foping Nature Reserve, China
85. **Oindo, Boniface Oluoch** (2001), 90-5808-495-7, Spatial Patterns of Species Diversity in Kenya
86. **Carranza, Emmanuel John** (2002), 90-6164-203-5, Geologically-constrained Mineral Potential Mapping

87. **Rugege, Denis** (2002), 90-5808-584-8, Regional Analysis of Maize-Based Land Use Systems for Early Warning Applications
88. **Liu, Yaolin** (2002), 90-5808-648-8, Categorical Database Generalization in GIS
89. **Ogao, Patrick** (2002), 90-6164-206-X, Exploratory Visualization of Temporal Geospatial Data using Animation
90. **Abadi, Abdulbaset M.** (2002), 90-6164-205-1, Tectonics of the Sirt Basin – Inferences from tectonic subsidence analysis, stress inversion and gravity modelling
91. **Geneletti, Davide** (2002), 90-5383-831-7, Ecological Evaluation for Environmental Impact Assessment
92. **Sedogo, Laurent G.** (2002), 90-5808-751-4, Integration of Participatory Local and Regional Planning for Resources Management using Remote Sensing and GIS
93. **Montoya, Lorena** (2002), 90-6164-208-6, Urban Disaster Management: a case study of earthquake risk assessment in Carthago, Costa Rica
94. **Ahmad, Mobin-ud-Din** (2002), 90-5808-761-1, Estimation of Net Groundwater Use in Irrigated River Basins using Geo-information Techniques: A case study in Rechna Doab, Pakistan
95. **Said, Mohammed Yahya** (2003), 90-5808-794-8, Multiscale perspectives of species richness in East Africa
96. **Schmidt, Karin** (2003), 90-5808-830-8, Hyperspectral Remote Sensing of Vegetation Species Distribution in a Saltmarsh
97. **Lopez Binnquist, Citlalli** (2003), 90-3651-900-4, The Endurance of Mexican Amate Paper: Exploring Additional Dimensions to the Sustainable Development Concept
98. **Huang, Zhengdong** (2003), 90-6164-211-6, Data Integration for Urban Transport Planning
99. **Cheng, Jianquan** (2003), 90-6164-212-4, Modelling Spatial and Temporal Urban Growth
100. **Campos dos Santos, Jose Laurindo** (2003), 90-6164-214-0, A Biodiversity Information System in an Open Data/Metadatabase Architecture
101. **Hengl, Tomislav** (2003), 90-5808-896-0, PEDOMETRIC MAPPING, Bridging the gaps between conventional and pedometric approaches
102. **Barrera Bassols, Narciso (**2003), 90-6164-217-5, Symbolism, Knowledge and management of Soil and Land Resources in Indigenous Communities: Ethnopedology at Global, Regional and Local Scales
103. **Zhan, Qingming** (2003), 90-5808-917-7, A Hierarchical Object-Based Approach for Urban Land-Use Classification from Remote Sensing Data
104. **Daag, Arturo S.** (2003), 90-6164-218-3, Modelling the Erosion of Pyroclastic Flow Deposits and the Occurrences of Lahars at Mt. Pinatubo, Philippines
105. **Bacic, Ivan** (2003), 90-5808-902-9, Demand-driven Land Evaluation with case studies in Santa Catarina, Brazil
106. **Murwira, Amon** (2003), 90-5808-951-7, Scale matters! A new approach to quantify spatial heterogeneity for predicting the distribution of wildlife
107. **Mazvimavi, Dominic** (2003), 90-5808-950-9, Estimation of Flow Characteristics of Ungauged Catchments. A case study in Zimbabwe
108. **Tang, Xinming** (2004), 90-6164-220-5, Spatial Object Modelling in Fuzzy Topological Spaces with Applications to Land Cover Change
109. **Kariuki, Patrick** (2004), 90-6164-221-3, Spectroscopy and Swelling Soils; an integrated approach

110. **Morales, Javier** (2004), 90-6164-222-1, Model Driven Methodology for the Design of Geo-information Services
111. **Mutanga, Onisimo** (2004), 90-5808-981-9, Hyperspectral Remote Sensing of Tropical Grass Quality and Quantity
112. **Šliužas, Ričardas V.** (2004), 90-6164-223-X, Managing Informal Settlements: a study using geo-information in Dar es Salaam, Tanzania
113. **Lucieer, Arko** (2004), 90-6164-225-6, Uncertainties in Segmentation and their Visualisation
114. **Corsi, Fabio** (2004), 90-8504-090-6, Applications of existing biodiversity information: Capacity to support decision-making
115. **Tuladhar, Arbind** (2004), 90-6164-224-8, Parcel-based Geo-information System: Concepts and Guidelines
116. **Elzakker, Corné van** (2004), 90-6809-365-7, The use of maps in the exploration of geographic data
117. **Nidumolu, Uday Bhaskar** (2004), 90-8504-138-4, Integrating Geo-information models with participatory approaches: applications in land use analysis
118. **Koua, Etien L.** (2005), 90-6164-229-9, Computational and Visual Support for Exploratory Geovisualization and Knowledge Construction
119. **Blok, Connie A.** (2005), Dynamic visualization variables in animation to support monitoring of spatial phenomena
120. **Meratnia, Nirvana** (2005), 90-365-2152-1, Towards Database Support for Moving Object Data
121. **Yemefack, Martin** (2005), 90-6164-233-7, Modelling and monitoring Soil and Land Use Dynamics within Shifting Agricultural Landscape Mosaic Systems
122. **Kheirkhah, Masoud** (2005), 90-8504-256-9, Decision support system for floodwater spreading site selection in Iran
123. **Nangendo, Grace** (2005), 90-8504-200-3, Changing forest-woodland-savanna mosaics in Uganda: with implications for conservation
124. **Mohamed, Yasir Abbas** (2005), 04-15-38483-4, The Nile Hydroclimatology: impact of the Sudd wetland (Distinction)
125. **Duker, Alfred, A.** (2005), 90-8504-243-7, Spatial analysis of factors implicated in *mycobacterium ulcerans* infection in Ghana
126. **Ferwerda, Jelle, G.** (2005), 90-8504-209-7, Charting the Quality of Forage: Measuring and mapping the variation of chemical components in foliage with hyperspectral remote sensing
127. **Martinez, Javier** (2005), 90-6164-235-3, Monitoring intra-urban inequalities with GIS-based indicators. With a case study in Rosario, Argentina
128. **Saavedra, Carlos** (2005), 90-8504-289-5, Estimating spatial patterns of soil erosion and deposition in the Andean region using Geo-information techniques. A case study in Cochabamba, Bolivia
129. **Vaiphasa, Chaichoke** (2006), 90-8504-353-0, Remote Sensing Techniques for Mangrove Mapping
130. **Porwal, Alok** (2006), 90-6164-240-X, Mineral Potential Mapping with Mathematical Geological Models
131. **Werff, Harald van der** (2006), 90-6164-238-8, Knowledge-based remote sensing of complex objects: recognition of spectral and spatial patterns resulting from natural hydrocarbon seepages
132. **Vlag, Daniël van de** (2006), 90-8504-384-0, Modeling and visualizing dynamic landscape objects and their qualities

133. **Joshi, Chudamani** (2006), 90-8504-470-7, Mapping cryptic invaders and invisibility of tropical forest ecosystems: *Chromolaena odorata* in Nepal
134. **Bandara, K.M.P.S.** (2006), 90-8504-406-5, Assessing irrigation performance by using remote sensing
135. **Dilo, Areti** (2006), 90-8504-461-8, Representation of and Reasoning with Vagueness in Spatial Information. A system for handling vague objects
136. **Debba, Pravesh** (2006), 90-8504-462-6, Sampling scheme optimization from hyperspectral data
137. **Huisman, Marco** (2006), 90-6164-246-9, Assessment of rock mass decay in artificial slopes
138. **Lemmens, Rob** (2006), 90-6164-250-7, Semantic interoperability of distributed geo-services
139. **Chacón Moreno, Eulogio** (2007), 90-8504-559-2, Ecological and spatial modeling: Mapping ecosystems, landscape changes, and plant species distribution in Llanos del Orinoco, Venezuela
140. **Amer, Sherif** (2007), 90-6164-253-1, Towards Spatial Justice in Urban Health Services Planning
141. **Obakeng, Obolokile Thothi** (2007), 90-6164-254-X, Soil moisture dynamics and evapotranspiration at the fringe of the Botswana Kalahari, with emphasis on deep rooting vegetation
142. **Cho, Moses Azong** (2007), 978-90-8504-622-6, Hyperspectral remote sensing of biochemical and biophysical parameters
143. **Farifteh, Jamshid** (2007), 978-90-6164-259-6, Imaging Spectroscopy of salt-affected soils: Model-based integrated method
144. **Minang, Peter Akong**, (2007), 978-90-6164-260-2, Implementing global environmental policy at local level: community carbon forestry perspectives in Cameroon
145. **Noomen, Marleen F.** (2007), 978-90-8504-671-4, Hyperspectral reflectance of vegetation affected by underground hydrocarbon gas seepage
146. **Trias Aditya Kurniawan Muhammad**, (2007), 978-90-6164-261-9, The National Atlas as a Metaphor for Improved Use of a Geospatial Data Infrastructure

University of Utrecht

ITC INTERNATIONAL INSTITUTE FOR GEO-INFORMATION SCIENCE AND EARTH OBSERVATION

ISBN 978 90 6164 263 3
ITC Dissertation no 147
Cover designed by Dinand Alkema
© 2007 by Dinand Alkema